AFOSR-TR- 82-0987

(12)

UNIVERSITY OF SOUTHERN CALIFORNIA

SCHOOL OF ENGINEERING

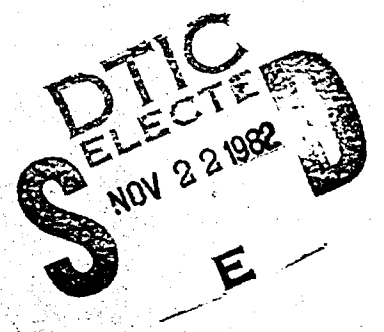

Approved for public release;
Distribution unlimited.

MECHANICAL ENGINEERING DEPARTMENT

Final

GAS INTERACTION AND LIQUID PHASE REACTIONS ASSOCIATED WITH SWIRL COMBUSTION AND COMBUSTION INSTABILITY

P. Roy Choudhury
Melvin Gerstein

University of Southern California

August 1982

Approved for public release; distribution unlimited

This work was supported by the Air Force Office of Scientific Research under Grant AFOSR 82-0222. Dr. B.T. Wolfson was the Technical Monitor.

12

UNCLASSIFIED
SECURITY CLASSIFICATION OF THIS PAGE (When Data Entered)

REPORT DOCUMENTATION PAGE	READ INSTRUCTIONS BEFORE COMPLETING FORM
1. REPORT NUMBER: AFOSR-TR- 82-0987	2. GOVT ACCESSION NO.: AD-A122 724
	3. RECIPIENT'S CATALOG NUMBER
4. TITLE (and Subtitle): GAS INTERACTION AND LIQUID PHASE REACTIONS ASSOCIATED WITH SWIRL COMBUSTION AND COMBUSTION INSTABILITY	5. TYPE OF REPORT & PERIOD COVERED: FINAL 1 June 77 - 30 June 82
	6. PERFORMING ORG. REPORT NUMBER
7. AUTHOR(s): P ROY CHOUDHURY, MELVIN GERSTEIN	8. CONTRACT OR GRANT NUMBER(s): AFOSR-82-0222
9. PERFORMING ORGANIZATION NAME AND ADDRESS: UNIVERSITY OF SOUTHERN CALIFORNIA, DEPARTMENT OF MECHANICAL ENGINEERING, LOS ANGELES, CA 90089-1453	10. PROGRAM ELEMENT, PROJECT, TASK AREA & WORK UNIT NUMBERS: 61102F, 2308/A2
11. CONTROLLING OFFICE NAME AND ADDRESS: AIR FORCE OFFICE OF SCIENTIFIC RESEARCH/NA, BOLLING AFB, DC 20332	12. REPORT DATE: August 1982
	13. NUMBER OF PAGES: 96
14. MONITORING AGENCY NAME & ADDRESS(if different from Controlling Office)	15. SECURITY CLASS. (of this report): UNCLASSIFIED
	15a. DECLASSIFICATION/DOWNGRADING SCHEDULE

16. DISTRIBUTION STATEMENT (of this Report)

Approved for Public Release; Distribution Unlimited.

17. DISTRIBUTION STATEMENT (of the abstract entered in Block 20, if different from Report)

18. SUPPLEMENTARY NOTES

19. KEY WORDS (Continue on reverse side if necessary and identify by block number)

RAMJETS	LIQUID PHASE DECOMPOSITION	COMBUSTION INSTABILITY
DUMP COMBUSTORS	FUEL SPRAY	
VOTEX AMPLIFIER	SLURRY FUELS	
SWIRL GENERATOR	DROPLET SHATTERING	
COMBUSTION EFFICIENCY	INLET PRESSURE OSCILLATION	

20. ABSTRACT (Continue on reverse side if necessary and identify by block number)

Three fundamental problems related to the combustion efficiency and smoother burning of an airbreathing propulsion system are studied. The first problem deals with the coupling of evaporation/decomposition of a liquid fuel and a novel technique of handling a slurry fuel. It has been found that at higher pressures liquid phase decomposition of a fuel is one of the primary sources of particulate formation and combustion inefficiency of an airbreathing combustor. Preliminary experiments and analysies of droplet shattering of a slurry

DD FORM 1 JAN 73 1473 EDITION OF 1 NOV 65 IS OBSOLETE

UNCLASSIFIED
SECURITY CLASSIFICATION OF THIS PAGE (When Data Entered)

fuel by pulsed low energy irradiation at selected frequencies show that this novel method of droplet break up might enable one to use slurry fuels without the usual problem of particle clustering. The second phase of the research dealing with vortex combustion and the use of gas jets in the role of vortex amplifier and swirl generator identifies fundamental methods of increasing combustion efficiency, promoting smoother burning and decreasing the characteristic length of a burner. Finally the study of the coupling between the inlet pressure oscillation and combustion instability has identified the role of frequency, amplitude, wave-form and phase angle leading to pressure magnification in the burner. Through vortex control and a feedback system it may be possible to eliminate combustion instability.

ABSTRACT

Three fundamental problems related to the combustion efficiency and smoother burning of an airbreathing propulsion system are studied. The first problem deals with the coupling of evaporation/decomposition of a liquid fuel and a novel technique of handling a slurry fuel. It has been found that at higher pressures liquid phase decomposition of a fuel is one of the primary sources of particulate formation and combustion inefficiency of an airbreathing combustor. Preliminary experiments and analyses of droplet shattering of a slurry fuel by pulsed low energy irradiation at selected frequencies show that this novel method of droplet break up might enable one to use slurry fuels without the usual problem of particle clustering.

The second phase of the research dealing with vortex combustion and the use of gas jets in the role of vortex amplifier and swirl generator identifies fundamental methods of increasing combustion efficiency, promoting smoother burning and decreasing the characteristic length of a burner.

Finally the study of the coupling between the inlet pressure oscillation and combustion instability has identified the role of frequency, amplitude, waveform and phase angle leading to pressure magnification in the burner. Through vortex control and a feedback system it may be possible to eliminate combustion instability.

CONTENTS

I INTRODUCTION

This report deals with progress on three related problems. Each of these represents an advance in basic science while, at the same time, allowing insight into the problems of providing stable, efficient combustion.

One phase of the work reported here is concerned with the role of liquid phase reactions in the evaporation and combustion of liquid fuel. There is a large amount of research reported in the literature concerning non-reactive evaporation and evaporation followed by gas phase reaction. The liquid phase has been largely ignored. This research has provided the fundamental aspects of the formation of solids during evaporation. It has been shown that these solids, which are non-volatile and difficult to burn, can produce a major effect on combustion time and, therefore, combustion efficiency.

The second phase of the work reported here deals with the control and stability of vortex combustion. Here, too, a new understanding of the role of fuel and an injection in a vortex structure have uncovered both stabilizing and destabilizing processes. This fundamental understanding can have a major influence on the design of side dump combustors and the use of gas jets in the role of vortex amplifier and swirl generator.

The third phase of the work deals with the problem of amplification of inlet pressure oscillations leading to combustion instability and eventual flame blow off. This work has just begun and the preliminary results show that a novel technique of feed back control can, in principle, eliminate combustion instability induced by the pressure oscillation in the inlet.

Several problems involving coupled evaporation and liquid phase decomposition of fuel droplets in flowing media are solved in Section 2. These involve single droplets as well as a distribution of droplets in a typical spray. Experimentally determined diameter reduction rate as well as a second order reaction have been assumed in selected problems to describe the liquid phase decomposition. Analyses show that in all cases liquid phase decomposition can have an important effect on combustor efficiency and particulate emission for air breathing systems operating at higher pressures. The slow burning residue particles can cause both IR and visible signatures in the exhaust.

Section 3 deals with a novel technique of droplet shattering by irradiation at discrete frequency bands. Preliminary experiments show that this method might enable one to use slurry fuels without the usual problem of particle clustering. Analytical effort is continuing to determine the fundamental causes of droplet shattering by this method.

Uses of gas jets in the role of vortex amplifier and swirl generator are discussed in Section 4. Interaction of multiple vortices in a side dump gas generator ramjet is also discussed and the single most important vortex which is crucial to the stable and smooth burning is identified.

The study of the amplification of the inlet pressure pulsation leading to rough burning and eventual flame blowoff is covered in Section 5. It is expected that through a better understanding of the magnification of the input disturbance in the combustor, a feed back control system can be developed which could eliminate the problem of combustion instability. The objective of the present research, however, is not to develop hardware but to provide fundamental knowledge which can be used by others for development purposes.

2. EFFECTS OF COUPLED EVAPORATION AND LIQUID PHASE DECOMPOSITION

2.1 Empirical diameter reduction rate:

Several examples of the effects of coupled fuel evaporation and liquid phase decomposition on the burner performance at higher pressures are illustrated here. Both experimentally determined rate of decrease of diameter and an assumed second order one-step decomposition rate are used in the following analysis.

Using the data of the diameter reduction rate of fuel droplets at higher pressures in the vicinity of a hot plate it is possible to introduce an empirical parameter α to describe the departure of the usual linear D^2-t relationship. Thus, experimentally observed rate of change of diameter of an evaporating fuel droplet at an elevated pressure can be expressed by the following semiempirical equation.

$$\frac{dD^2}{dt} = -\beta_o (1 - \alpha t^2) \quad ; \quad 1 \geq \alpha t^2 \tag{1}$$

where D = droplet diameter

β_o = initial shape of D^2-t curve

α = empiricial paramter

t = time.

Equation (1) can be expressed in a non-dimensional form in the following way

$$\frac{dD^{*2}}{d\tau} = -(1 - 3\eta\tau^2) \qquad 1 \geq 3\eta\tau^2 \tag{2}$$

where D^* = D/D_o (D_o = initial diameter)

τ = $\beta_o t / D_o^2$, nondimensional time

η = $\alpha D_o^4 / (3\beta_o^2)$, a constant inefficiency parameter.

Figure 1 is a non-dimensional form of eqn.(1) calculated from Ref. 1. It clearly shows that with increasing ambient pressure, the inefficiency parameter η progressively increases and the rate of change of diameter also decreases with time. Although data for pure 1 octene has been shown in Fig. 1, similar behavior of progressively decreasing rate of change of diameter is observed for various other pure fuels and commercial blends. At this time it is not clear exactly how η is related to the decomposition rate, pressure, fuel type and perhaps the initial diameter of the droplet. Also neither the chemical composition of the product species nor the possible nucleation rate is known. Nevertheless, equation (1) appears to be a convenient semiempirical means of presenting the coupled phenomenon of evaporation and liquid phase decomposition. Figure 2 shows the experimental results for n-heptane. The nonlinearity caused by the liquid phase decomposition is clearly evident in Figures 1 and 2.

2.2 History of a distribution function f(D,t):

Since the experiments were conducted in a stagnant atmosphere without any flow, a distribution function for droplet size in a functional form f(D,t) was selected for analysis. For such a distribution function, the conservation of number in the absence of flow, droplet shattering and coalescence is given by

$$\frac{\partial f}{\partial t} + \frac{\partial}{\partial D}(fR) = 0 \qquad (3)$$

where R = the rate of reduction of droplet diamater

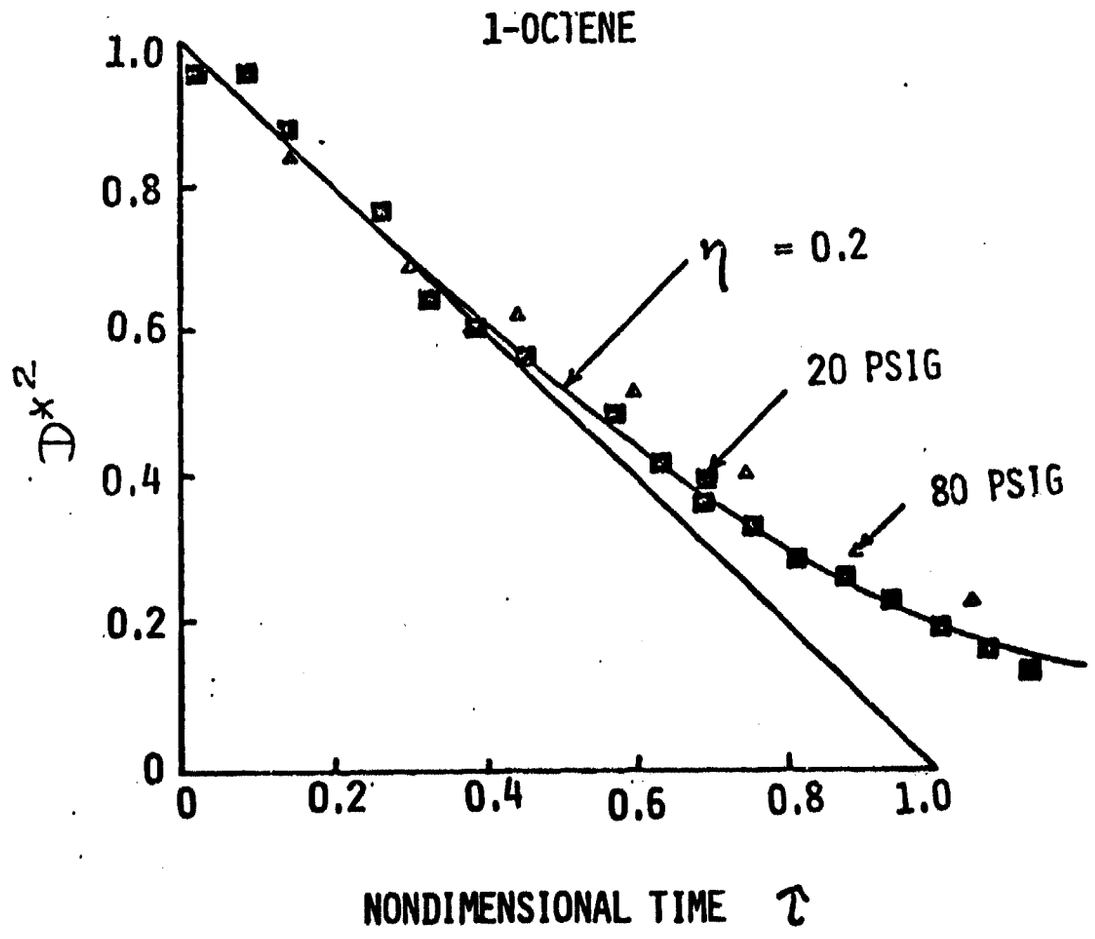

Figure 1. Comparison of semiempirical rate equation and experimental data for a 3.5 mm droplet suspended over a 450 C plate.

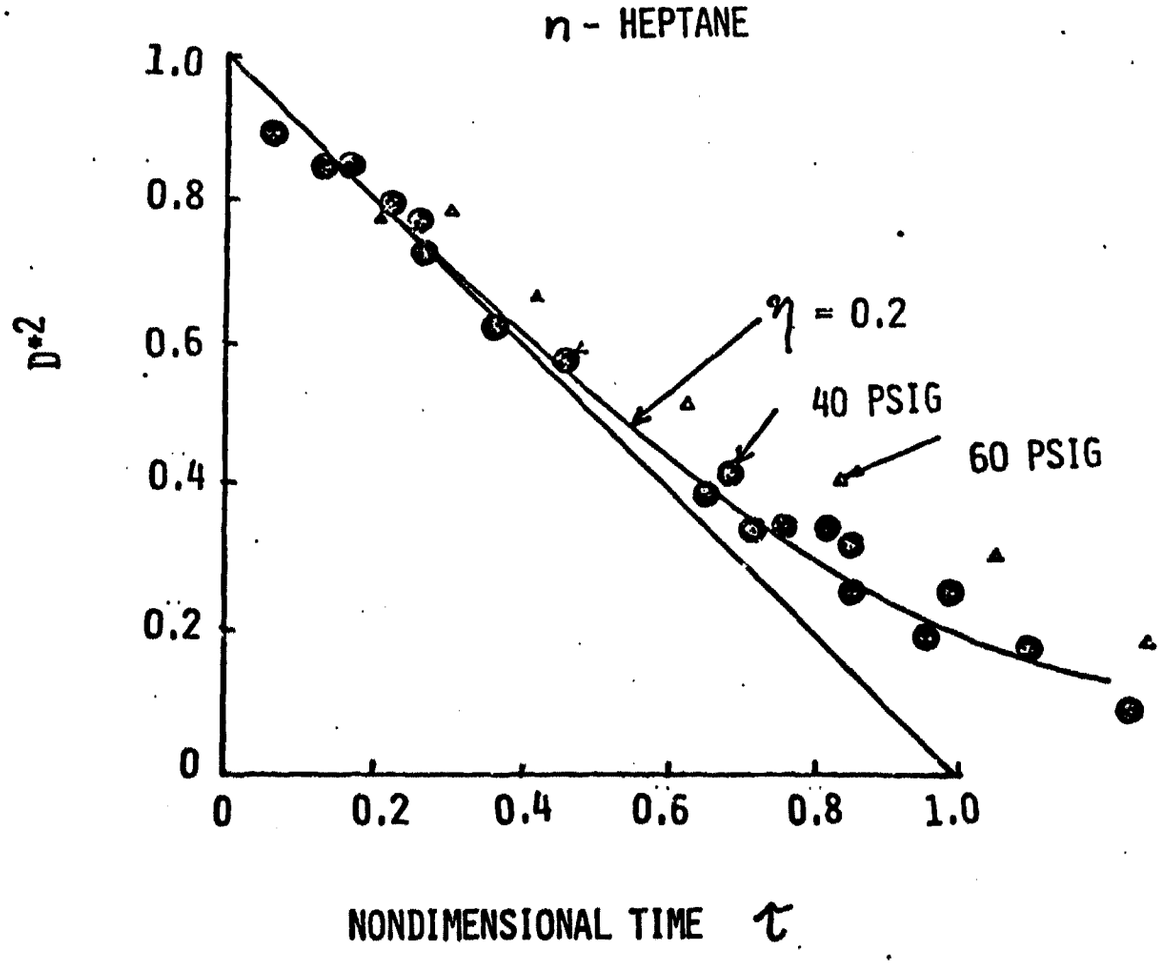

Figure 2. Comparison of semiempirical rate equation and experimental data for a 2.4 mm droplet suspended over a 450 C plate.

Calculating R from equation (1), the conservation of number, eqn. (3) can be simplified in the following form.

$$\frac{\partial f}{\partial t} - \frac{\beta_0}{2D}(1 - \alpha t^2)\frac{\partial f}{\partial D} = -\frac{\beta_0}{2D^2}(1 - \alpha t^2) f \qquad (4)$$

A general solution of this equation (Ref. 2,3) in a functional form is as follows.

$$U\left[\frac{f}{D}, \{\beta_0 t\left(1 - \alpha\frac{t^2}{3}\right) + D^2\}\right] = 0 \qquad (5)$$

A particular solution for the present physical problem can be written in the following manner

$$f(D,t) = AD\left[\beta_0 t\left(1 - \frac{\alpha t^2}{3}\right) + D^2\right]^n e^{-B\left[\beta_0 t\left(1 - \alpha\frac{t^2}{3}\right) + D^2\right]^m} \qquad (6)$$

where n and m are determined from the initial distribution function at t = o.

A and B are constants to be determined from the physical problem.

If an initial distribution function $f(D,O) = f_o = AD^3 e^{-BD^2}$ is assumed then m = 1 and n = 1.

In a dimensionless form, eqn. (6) with m = 1 and n = 1 is as follows:

$$f(D^*,\tau) = A\bar{D}_o^3 D^*\left[\tau(1 - \eta\tau^2) + D^{*2}\right] e^{-B\bar{D}_o^2\left[\tau(1-\eta\tau^2) + D^{*2}\right]} \qquad (7)$$

where $\bar{D}_o$ = initial number averaged diameter of the spray

$D^* = D/\bar{D}_o$, nondimensional diameter

$\tau = \beta_0 t/\bar{D}_o^2$, nondimensional time

$\eta = \frac{\alpha}{3}\frac{\bar{D}_o^4}{\beta_o^2}$, a constant inefficiency parameter.

Defining fdD^* as the fraction of droplets in the diameter range D^* and $D^* + dD^*$, and recognizing that the initial number averaged D^* is 1, the values of A and B can be calculated easily.

$$A = \frac{81}{128} \frac{\pi^2}{\bar{D}_o^3} \tag{8a}$$

$$B = \frac{9}{16} \frac{\pi}{\bar{D}_o^2} \tag{8b}$$

Equations (7), (8a) and (8b) allow one to calculate all the important properties of the size distribution of the droplets as a function of the non-dimensional time. Although the number averaged diameter of the spray as a function of time can be calculated for both simple evaporation and coupled evaporation/decomposition, it will not provide any information on the size of the particulate matter. The products of decomposition appear to be formed by nucleation and their size and number can not be determined from the average droplet size. Each droplet at a given time may contain numerous particulate matters of different size.

Figure 3 is a plot of eqn. (7) with $\eta = 0$ at various values of τ. Figure 4 is a similar plot with $\eta = 0.2$. For the value of η chosen, the distribution function remains unchanged after $\tau \sim 1.3$. There will be no more evaporation after that time and f will represent the particulate matter which is formed during decomposition. Since particles appear to be formed by nucleation, $f(D^*, 1.3)$ does not describe the size distribution of the particulate matter.

The fraction of total mass of the liquid fuel in the spray at a given time is given by

$$M(t) = \int_0^\infty \frac{\rho_\ell \pi D^3}{6} f(D,t)\, dD \tag{9}$$

where M(t) = fraction of total mass of the spray

ρ_ℓ = density of the fuel

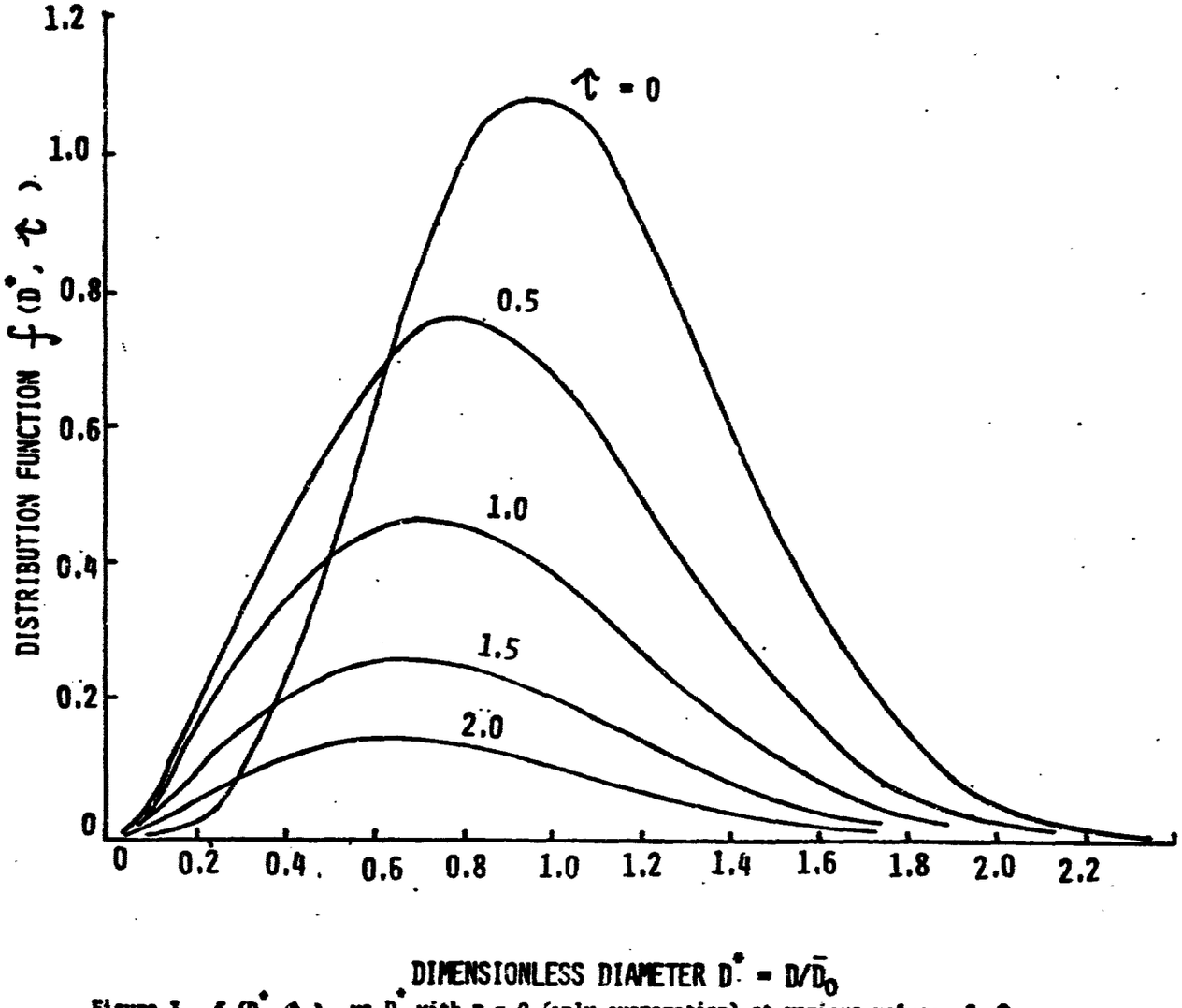

Figure 3. $f(D^*, \tau)$ vs D^* with $\eta = 0$ (only evaporation) at various values of τ.

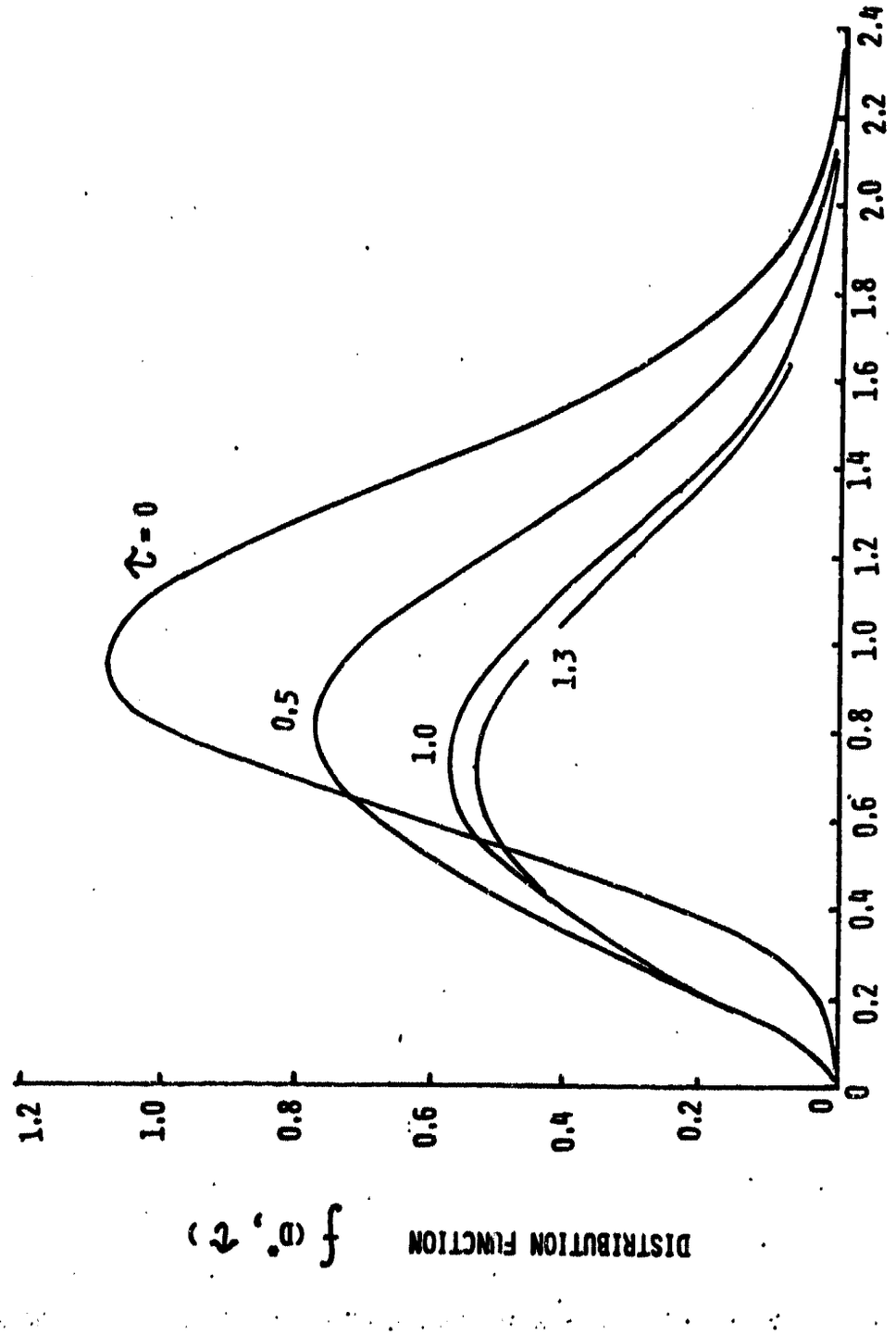

Figure 4. $f(D^*, \tau)$ vs. D^* with n=0.2 (coupled decomposition and evaporation) at various values of $\tau \leq 1.3$.

Assuming that the inefficiency parameter η is independent of the droplet diameter D, the fraction of initial mass evaporated is given by the following equation.

$$1 - e^{\frac{-9}{16}\pi\tau(1-\eta\tau^2)} \left[1 + \frac{9\pi}{40}\tau(1-\eta\tau^2)\right] \qquad (10)$$

Equation (9) represents the fraction of mass evaporated with both evaporation and decomposition continuing simultaneously. For the case of only evaporation, $\eta = 0$, and eqn. (9) reduces to a simpler form. Figure 5 is a plot of eqn. (10) with $\eta = 0.2$ and $\eta = 0$. As before, for $\eta = 0.2$ evaporation from the spray ceases at $\tau \sim 1.3$. The results of Fig. 5 are indications of the maximum combustion efficiency obtainable in a combustor. When all the fuel evaporates, in principle, it will be possible to obtain a 100% combustion efficiency. However, because of decomposition, the maximum possible combustion efficiency will be much less than 100% and will depend upon the value of η. The value of $\eta = 0.2$ was chosen here for illustration. Larger values of η where the decomposition reaction is very fast will lead to a lower combustion efficiency characterized by a smaller amount of fuel evaporated from the spray.

This simplified analysis shows that liquid phase decomposition can become a serious problem in a system where the fuel is sprayed in a high pressure environment. Advanced airbreathing propulsion system and fuel spray in a Diesel Engine are cases in point. At higher pressures the decomposition rate seems to increase and the evaporation rate decreases. Experiments show that the products of decomposition tend to nucleate and eventually form nonvolatile particulate matter which is more difficult to burn. Although the details of both the decomposition rate and the mechanism of nucleation are not understood at this time, the

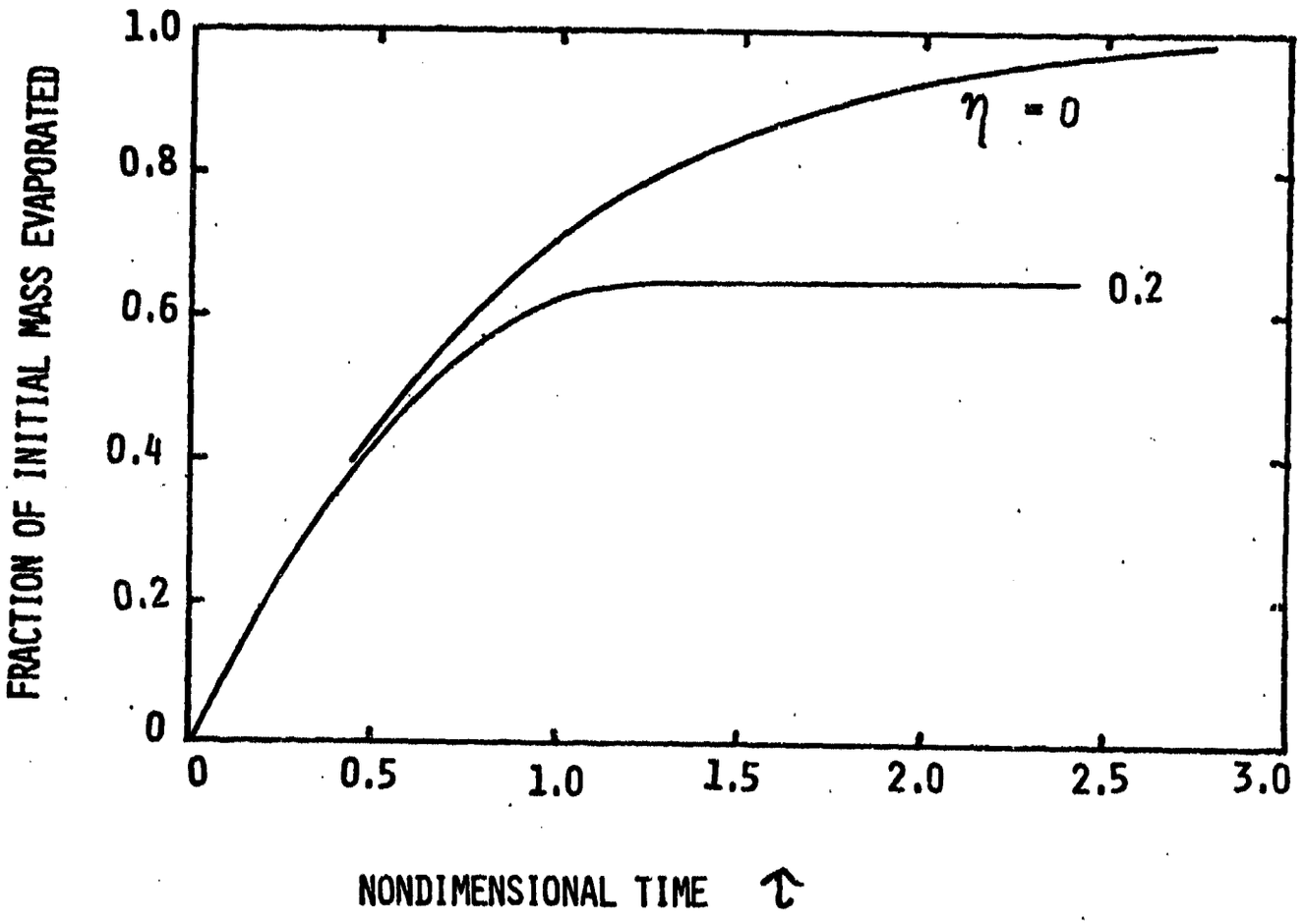

Figure 5. Fraction of initial mass evaporated for $\eta = 0$ and $\eta = 0.2$ at various values of τ.

experimental data can be used to illustrate the potential problem with decomposition. Decomposition in the liquid phase can cause a large reduction in combustion efficiency and an increase in emission of particulate matter in the exhaust. The pressure level at which $\eta = 0.2$ applies varies with the type of fuel. For 1-octene, a gage pressure of 20 psig seems to cause the same degree of inefficiency as 40 psig in the case of n-heptane (Figs. 1 and 2). Therefore, the results shown in the figures are applicable to either a n-heptane spray at 40 psig or 1-octene spray at 20 psig.

As the inefficiency parameter η increases, because of liquid phase decomposition the amount of nonvolatile residue also increases. Figure 6 is a plot of the fraction of initial mass in spray remaining as residue, as a function of η. It also shows the maximum degree of evaporation in a system, no matter how long the residence time or the characteristic length of the burner are.

More study is necessary to identify the products of decomposition, ascertain the global reaction rate and to characterize the inefficiency paramter η.

2.3 Decomposition Chemistry:

It has generally been assumed that liquid phase decomposition is not likely to occur during evaporation and combustion of drops since the liquid temperature is restricted by the boiling point of the liquid. The formation of deposits formed in the liquid phase has been demonstrated in Ref. 4 for commercial fuel oils and for "pure" fuels (Ref. 1) at elevated pressure. Increased pressure, of course, serves to increase the boiling temperature of the liquid and, exponentially, the reaction rates in the liquid phase. Some nominally "pure" liquids may contain dissolved oxygen and traces of metallic impurities. A comparison of single drop burning in air and in nitrogen (Fig. 7 Ref. 4) shows that there is a pronounced difference. Since rapid

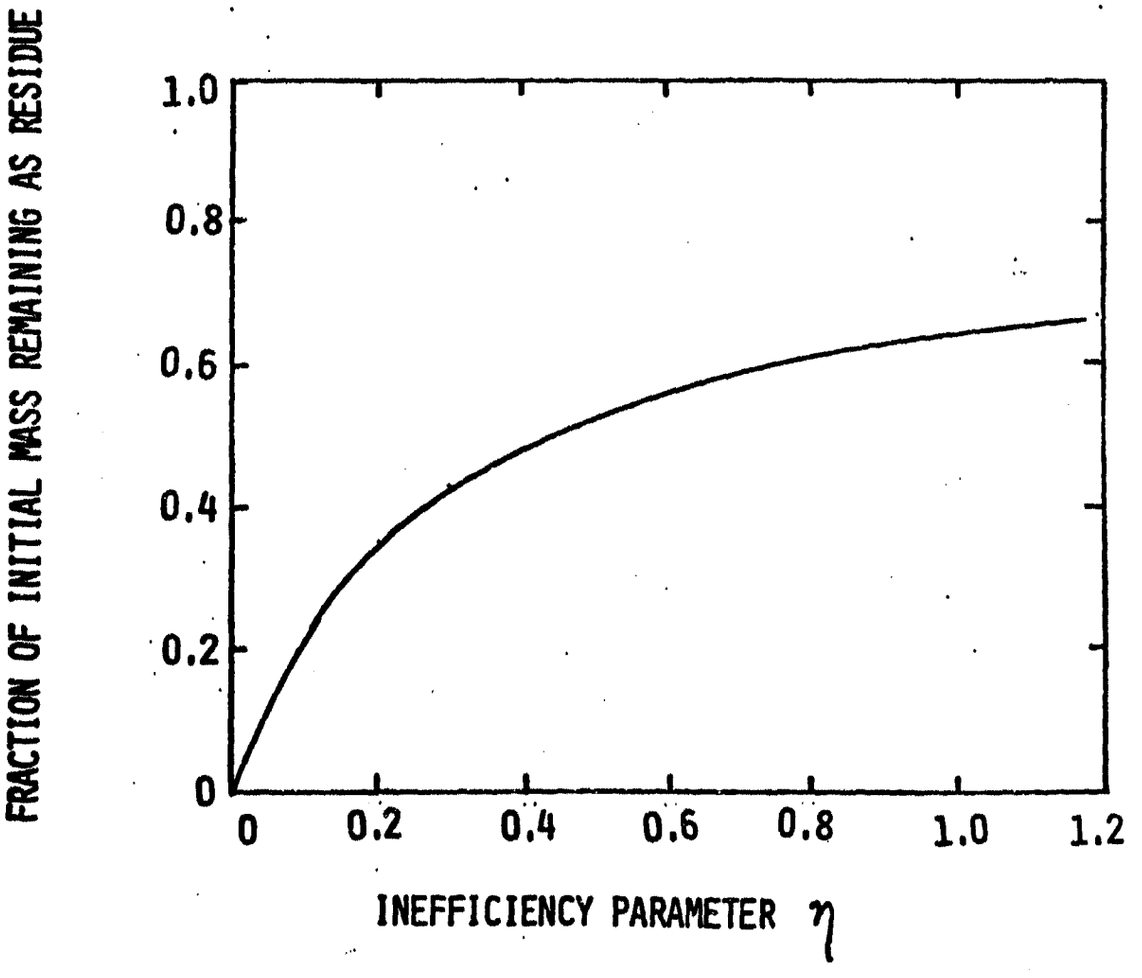

Figure 6. Fraction of initial mass remaining as residue for various values of η.

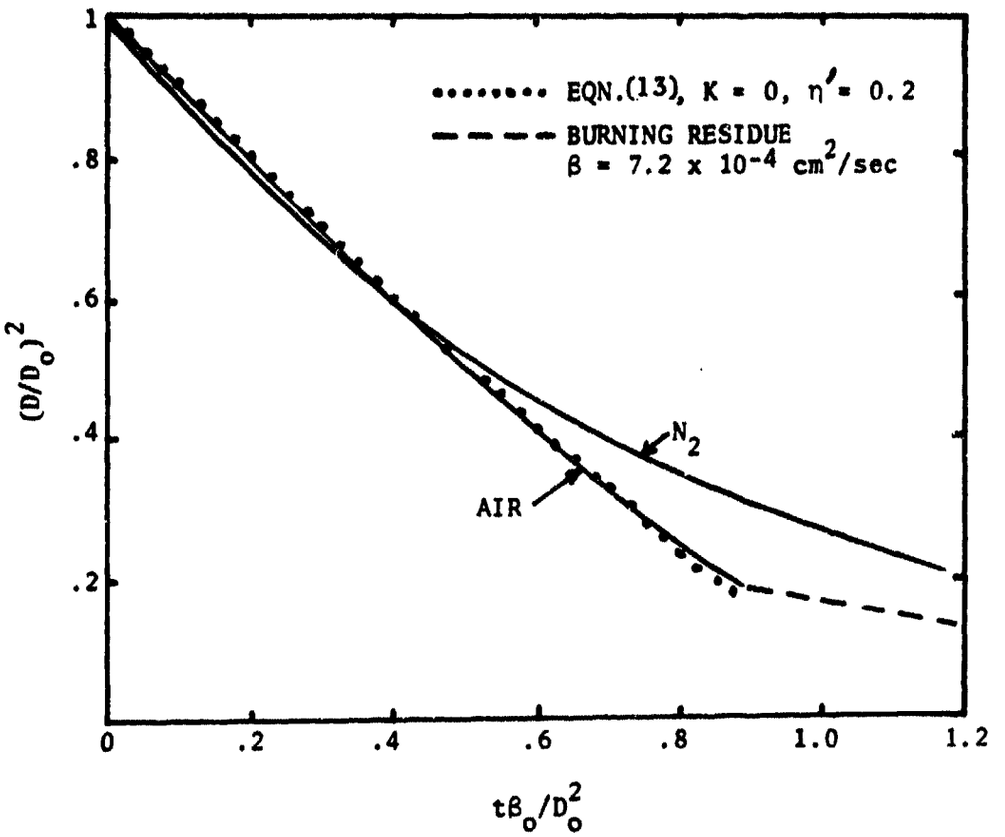

Figure 7. Data from Ref. 4 in a dimensionless form, D_o = 502 micron, Type A Residual Fuel Oil.

mixing in the liquid phase is observed during our experiments and was probably present in the work of Ref. 4, it is likely that dissolved oxygen in the original fuel and absorbed during reaction may contribute to the liquid phase process. Other species including radicals may also be absorbed at the surface and rapidly mixed with the rest of the liquid, producing more rapid decomposition. Some of these factors have yet to be studied. Benson, in developing a mechanism for cool flame reactions has proposed a series of reactions which occur at temperatures of the order of the boiling point of typical fuels (Ref. 5).

Several oxidation mechanisms are discussed by Benson. One of them leads to olefin formation about 250°C from hydrocarbon radical produced by removal of a hydrogen atom or by absorption of a free radical from the gas phase. The high density of the liquid phase compared to the gas phase leads to about a factor of 1000 in the increase of reaction rate.

At temperatures of the order of 200-250°C, one can postulate the following ractions:

$$RH + O_2 \rightarrow RO_2H + 18\text{-}24 \text{ kcal} \quad .$$

$$RO_2H \rightleftarrows \dot{R} + HO_2$$

$$RO_2H + \dot{R} \rightleftarrows \dot{R}O_2 + RH$$

$$\dot{R} + O_2 \rightleftarrows \dot{R}O_2$$

$$R\dot{C}HCH_3 + O_2 \rightarrow RCH = CH_2 + HO_2$$

$$HO_2 + RCH_2CH_3 \rightarrow H_2O_2 + R\dot{C}HCH_3$$

The net reaction would be:

$$O_2 + RCH_2CH_3 \rightarrow RCH = CH_2 + H_2O_2 + 2 \text{ kcal}$$

Benson has also proposed an ionic mechanism which may provide an even more likely mechanism at temperatures of the order of 240-320°C where 5 to 43% conversion of n-alkanes to cyclic oxides was observed in the vapor phase. This mechanism which is initiated by an adduct of the form

$$R_2CH + O_2 \rightleftarrows (R_2\dot{C}H...O_2^-H)$$

can produce hydroperoxides as well as cyclic oxides and various free radicals which can produce olefins.

If olefins, diolefins, aromatics, etc., are already present in the fuel, the process of carbon formation does not require these reactions. Once the unsaturated products are formed, condensation reactions such as the Diels-Alder reaction can produce various ring compounds and ultimately aromatics. (Ref. 6)

All of these reactions are catalyzed by oxygen and by transition metals. No claim is made that the liquid phase chemistry is known. It is an experimental observation that liquid phase reactions occur during drop combustion and that known reactions can account for this observation. Drop tower experiments are now being set up involving the interrupted evaporation and burning of single drops to isolate possible reaction products and provide a better understanding of the mechanism.

While a detailed knowledge of the decomposition chemistry is essential for understanding the fundamental mechanism, the experimental results can now be used in a semiempirical manner for studying the two-phase flow problem with coupled evaporation, decomposition, and finally burning of the products of decomposition. The performance of a burner, for example, depends upon the entire history of the injected fuel droplet in the flowing primary air stream. The behavior of the fuel droplets not only determines the

combustion efficiency of the burner, but also the possible formation of pollutants and particulate matter in the exhaust gases. The collision of either droplets or the residue particles might cause carbon buildup on the walls of the combustion chamber.

The decomposition reaction has been observed to be significant at higher pressures for both pure and commercial fuel blends. Synthetic fuels (e.g., fuel derived from shale) are especially susceptible to decomposition process during evaporation.

2.4 Droplet behavior in a flowing System:

The coupling between droplet evaporation and liquid phase decomposition observed experimentally applies to an essentially stagnant medium (Ref. 1) at higher pressures. In a realistic environment the rates of both evaporation and decomposition are expected to increase significantly due to forced convection. When a droplet is injected in a flowing medium, in addition to the thermodynamic states of the droplet and its surroundings, the relative velocity between the droplet and the flowing gas has a large influence on the behavior of the droplet.

The history of a single 100 micron diameter 1 octene droplet which is injected into a flowing air stream at 4 atm has been analyzed in this section. In particular, the droplet trajectory and the time variation of the droplet diameter, axial and transverse velocities are investigated for determining the overall effect of the droplet decomposition. It is assumed that the evaporation/decomposition of a single injected droplet does not perturb the properties of the flowing gas. Thus, the gas velocity, density, and the temperature are assumed to be constant and are not affected by the presence of the droplet. The other assumptions are as follows:

a) Stokes' drag, $C_D = 24/Re$ is applicable, (Re = Reynolds number is based upon the relative velocity and the instantaneous diameter of the droplet). The range of Re is between a maximum value of about 540 to a minimum value of 0.

b) The increase in the rates of both evaporation and final burning of the nonvolatile residue are given by the Ranz-Marshall correlation equation, $Nu = 2 + 0.6\ Re^{0.5} Pr^{0.3}$ (Nu = Nusselt number based upon the droplet diameter, Pr = Prandtl number). In a stagnant case, the Nusselt number approaches 2. However, in a flowing system, depending upon the Re, Nu can be significantly higher than the limiting value of 2.

c) The decomposition reaction of the liquid fuel is described by a second order, single step reaction $2F \rightarrow S$ (S = nonvolatile residue) with an activation energy of 40 kcal/mole. Different values of frequency factor are assumed for describing the limiting cases where i) reaction is dominating and ii) evaporation is the primary process by which the diameter decreases.

d) Evaporation and decomposition reaction take place at the saturation temperature of the mixture consisting of an ideal solution of the liquid fuel and the assumed soluble residue which is the product of reaction. Even though the residue has been observed experimentally, its chemical composition and thermodynamic properties are not known at this time. In subsequent calculations, the density of the residue is assumed to be equal to the density of the liquid fuel.

The analytical model is for a two-dimensional motion of a droplet in a one-dimensional flow field of air with constant properties which are unaffected by the presence of the single droplet. The governing equations are as follows:

$$\text{x-momentum:}\quad \frac{d\xi}{d\tau} = B\,\frac{1-\xi}{\mathcal{D}^2} \tag{1}$$

$$\text{y-momentum:}\quad \frac{d\zeta}{d\tau} = -B\,\frac{\zeta}{\mathcal{D}^2} \tag{2}$$

$$\text{Droplet evaporation:}\quad \frac{d\mathcal{D}^2}{d\tau} = -(1-\eta'\tau^2)\left(1 + K\sqrt{\mathcal{D}\sqrt{(1-\xi)^2+\zeta^2}}\right) \tag{3}$$

Residue concentration due to combined evaporation and decomposition:

$$\frac{dC}{d\tau} = \frac{4F D_o^2}{\beta_o} C_{S_o} (1-C)^2 e^{-E/RT} - \frac{3}{2}\,\frac{C}{\mathcal{D}^2}\cdot\frac{d\mathcal{D}^2}{d\tau} \tag{4}$$

Mixture saturation temperature:

$$\frac{1}{T} = \frac{R}{\lambda}\ln\frac{2(1-C)}{(2-C)} + \frac{1}{T_S} \tag{5}$$

where:

β = $(18\,\mu_g)/(\rho_\ell \beta_o)$, μ_g = gas viscosity, ρ_ℓ = density of the liquid, β_o = initial slope of D^2-t

ξ = u/u_g, (u = x component of droplet velocity, u_g = gas velocity

$\mathcal{D}$ = D/D_o (D = droplet diameter, D_o = initial diameter)

τ = nondimensional time $t\beta_o/D_o^2$, essentially t/t_{evap}

ζ = v/u_g, (v = y component of droplet velocity)

η' = $\alpha D_o^4/\beta_o^2$, α = a parameter describing the nonlinear D^2-t curve, $\frac{dD^2}{dt} = -\beta_o(1-\alpha t^2)$

K = $0.3\,Re_o^{0.5}\,Pr^{0.3}$, ($Re_o$ = Reynolds number based upon the initial diameter = $(\rho_g|V_R|D_o)/\mu_g$, V_R = $\sqrt{(u_g-u)^2+(v_g-v)^2}$, v_g = 0 here
Pr = Prandtl number)

C = nondimensional concentration, C_S/C_{S_o}, (C_S = concentration of the solid residue, C_{S_o} = concentration of the residue in the pure phase, 0.0032 gmole/cc)

A = frequency factor in the rate equation

E = activation energy (40 kcal/mole)

T = mixture saturation temperature

R = gas constant

λ = enthalpy of evaporation

T_S = saturation temperature of the pure liquid

Equations (1) through (5) are solved with the following initial conditions:

$$\xi(0) = 0; \quad \zeta(0) = \zeta_o; \quad D(0) = 1 \text{ and } C(0) = 0$$

A 100 micron, 1 octene droplet was selected as an example. It was assumed to be injected with $\zeta_o = 0.4$ in an air stream at 4 atm with a gas velocity $u_g = 91$ m/sec and temperature $T_g = 722$ K. The initial value of the evaporation constant β_o for 1 octene droplet was chosen to be 4×10^{-2} cm^2/sec.

Figure 8 shows the diameter history of the droplet for several cases of interest. When the frequency factor F is 10^{20}, the evaporation rate is much faster than the decomposition rate and the droplet nearly evaporates completely before the formation of residue causes the evaporation process to stop. For a gas velocity of 91 m/sec, the evaporation ceases at $\tau = 0.192$. An increase in the gas velocity would increase the evaporation rate and would further diminish the role of liquid phase decomposition. When F is increased to a value of 10^{25}, the decomposition becomes extremely important and evaporation ceases at $\tau = 0.027$. Only a very small amount of liquid can evaporate during this time and the diameter of nonvolatile residue becomes 91 microns. If the residue does not react after this point, the diameter remains constant. Even though the properties of the residue are not known at this time, it is

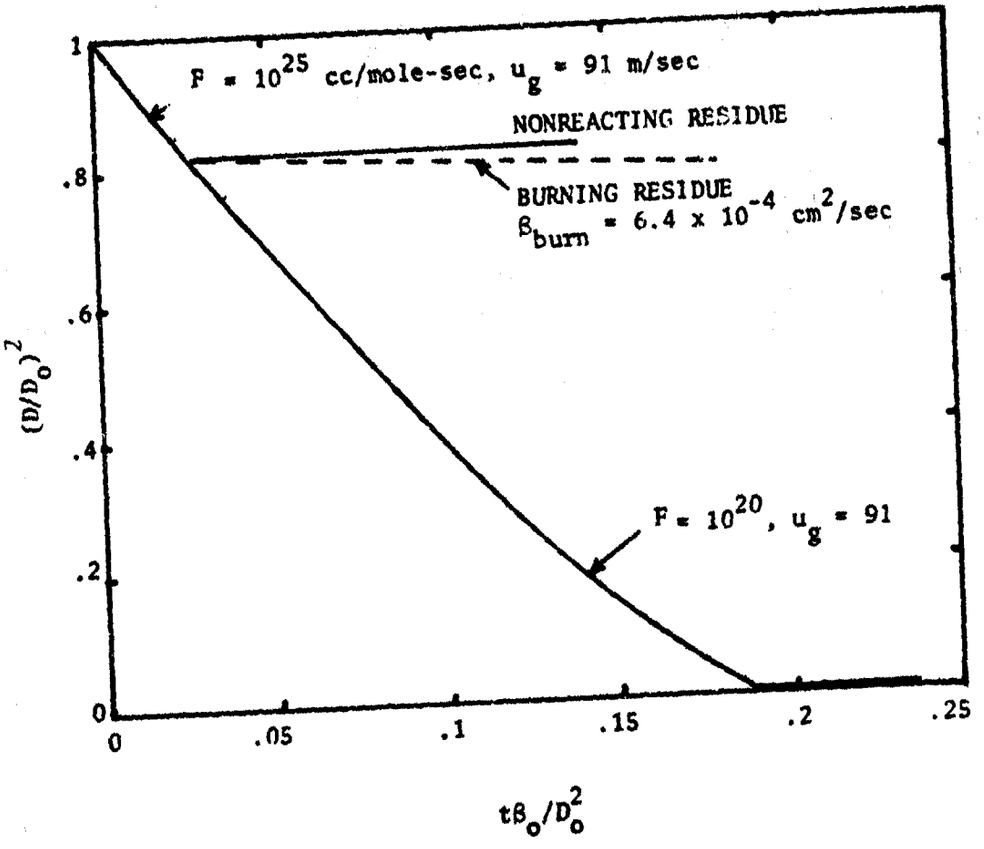

Figure 8. 100 micron 1 octene droplet diameter history. $u_o = 0$, $v_o/u_g = 0.4$, $T_g = 722$ K, p = 4 atm.

conceivable that the residue would actually burn. Assuming that the burning rate of the residue is comparable to that of carbon particles, the value of β_{burn} for burning carbon (6.4×10^{-4} cm^2/sec, Ref. 7) has been used to show the diameter reduction of the residue as a function of time. Even though the Ranz and Marshall correlation is incorporated with β_{burn} the overall burning rate of the residue is very small compared to the other rates considered here.

Since the details of the liquid phase decomposition are not known at this time, two limiting values of the frequency factor were chosen to indicate the possibilities of incomplete evaporation and residue formation.

Figure 9 shows the time variation of the transverse velocity for various cases described earlier. For $F = 10^{20}$, rapid evaporation causes the droplet to attain the gas velocity rather quickly. On the other hand, when $F = 10^{25}$, large nonvolatile residue particle remains in the flow field and it takes a long time to attain a zero relative velocity. Two other cases, one of burning residue and the other of nearly all decomposition are also shown in the Figure for $F = 10^{26}$.

The x-components of droplet velocity are shown in Figure 10 as a function of time. Decomposition process, on the whole, causes a delay in attaining a zero relative velocity between the droplet and the gas.

Droplet trajectories on a nondimensional plane are shown in Figure 11. With faster decomposition rate, larger residue particles penetrate deeper in the transverse direction. In a burner these particles might hit the wall, shatter, and possibly form nucleii for soot and other particulate matter. Carbon deposits might also be formed in this manner on the walls of the chamber. Particles which do not collide on the wall, travel in the axial direction possibly burn and finally add to the total population of particulate matter.

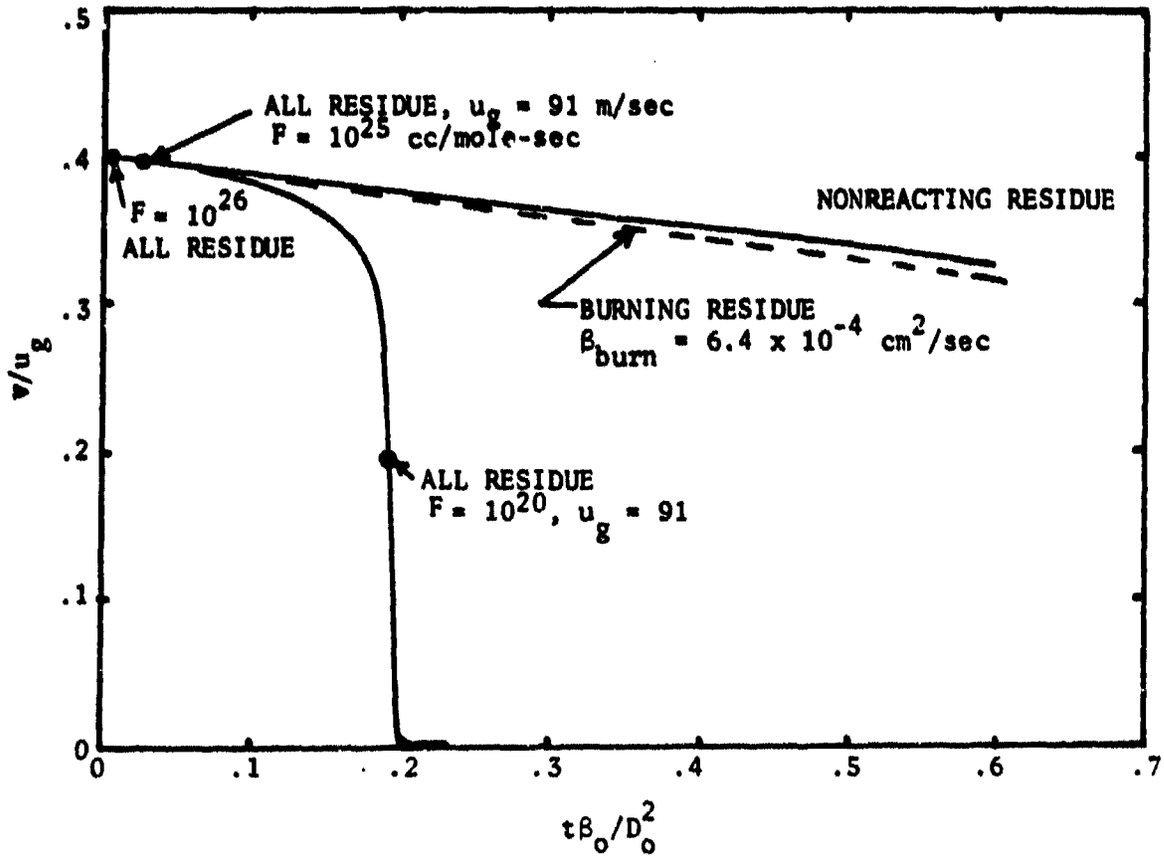

Figure 9. y-component of 100 micron 1 octene droplet velocity. u_g = 91 m/sec, T_g = 722 K, p = 4 atm.

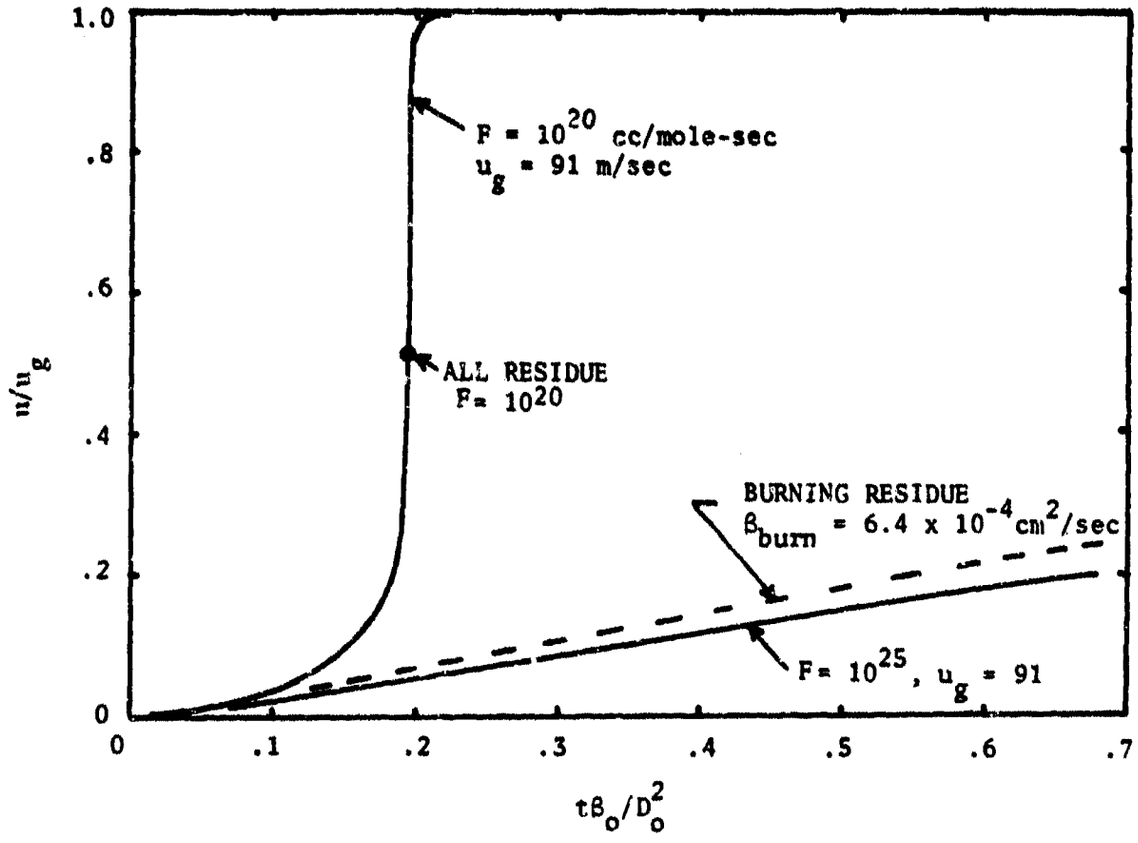

Figure 10. x-component of 100 micron 1 octene droplet velocity u_g = 91 m/sec, T_g = K,p = 4 atm.

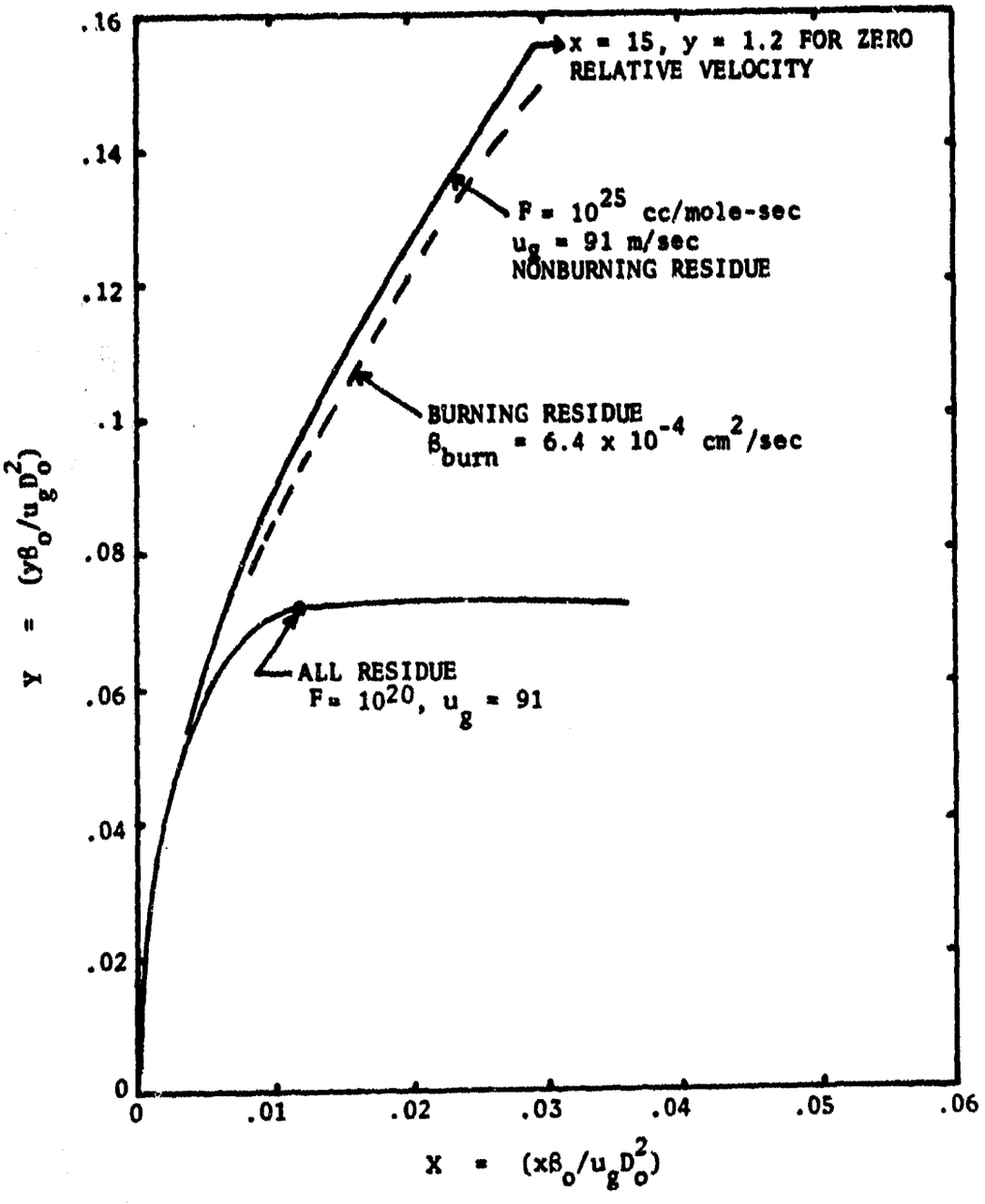

Figure 11. Trajectories of 100 micron 1 octene droplet, $u = 0$, $v_o/u_g = 0.4$, $u_g = 91$ m/sec, $T_g = 722$ K, $p = 4$ atm.

In order to give a proper perspective of the distances travelled by the droplet and the residue, the trajectories of Figure 11, are redrawn on Figure 12. The influence of liquid phase decomposition on the system is clearly shown in the Figure. When very little decomposition is present, the droplet attains the gas velocity within a very short distance. The remaining residue (2.3 micron diameter) does not penetrate too far in the transverse direction. However, with faster decomposition reaction, the residue travels over large distances both in the axial and transverse directions. Under such a condition, the droplet residue is more likely to hit the wall.

The coupling between evaporation and liquid phase decomposition can become a serious problem in a burner using liquid fuel and operating at a high pressure. A reduction in the combustion efficiency and an increase in the population of particulate matter in the exhaust are possible when the decomposition rate becomes dominant. Even though only a single droplet was used in the analysis, the results indicate that when a large number of decomposing particles are present, the flow field might undergo radical changes.

An examination of Equation 14 shows that for extremely small droplets (small values of D_o), the effect of the decomposition reaction can be minimized. Thus, finer atomization during spray and/or additives which help shatter the droplets would be useful. Finally, additives to increase volatility and a larger relative velocity for accelerating the evaporation rate would tend to alleviate the problem of unwanted liquid phase decomposition. Figure 13 shows the effect of the initial relative velocity on the onset of decomposition of a 20 micron droplet.

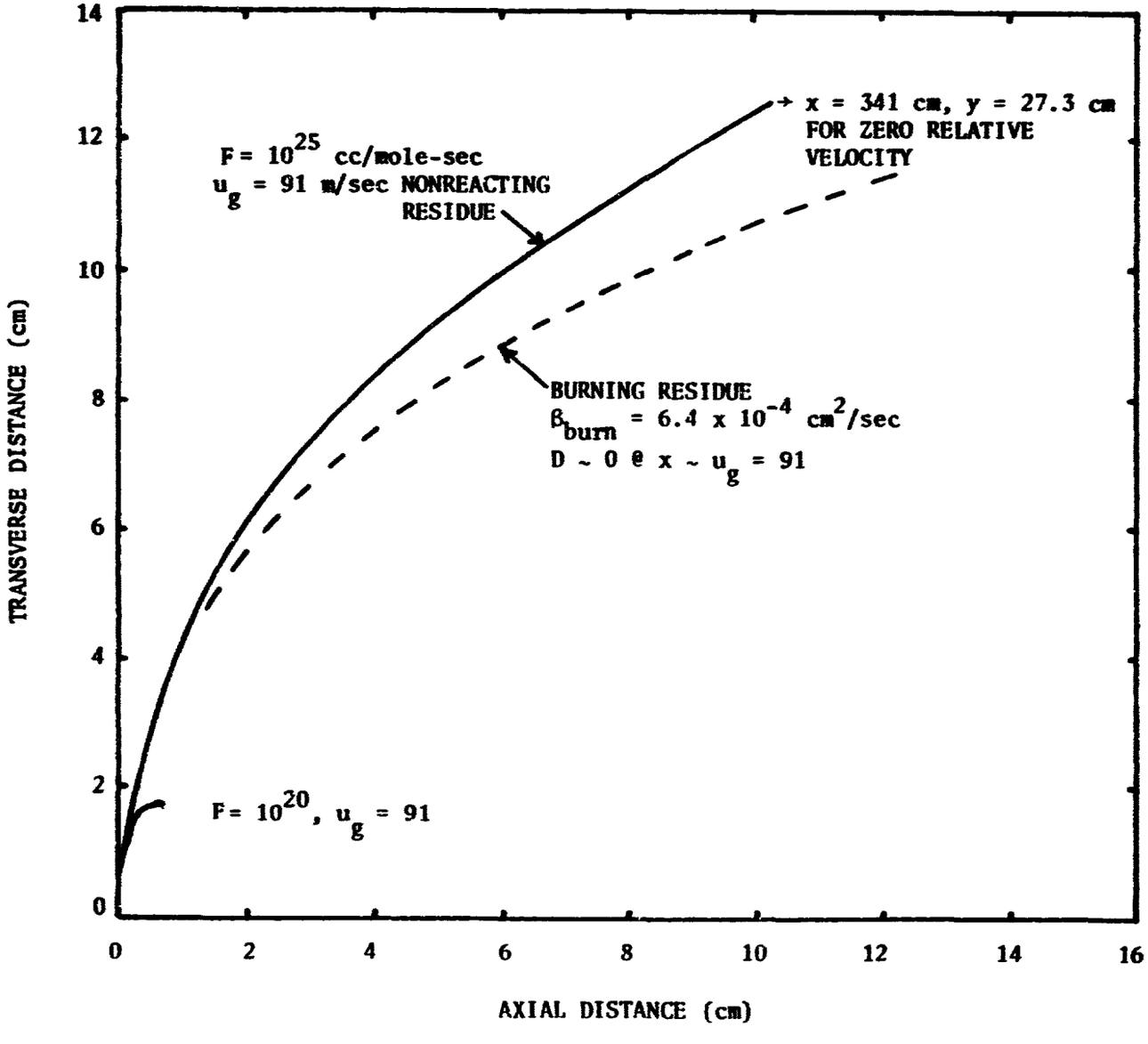

Figure 12. Actual distance travelled by 100 micron 1 octene droplet.

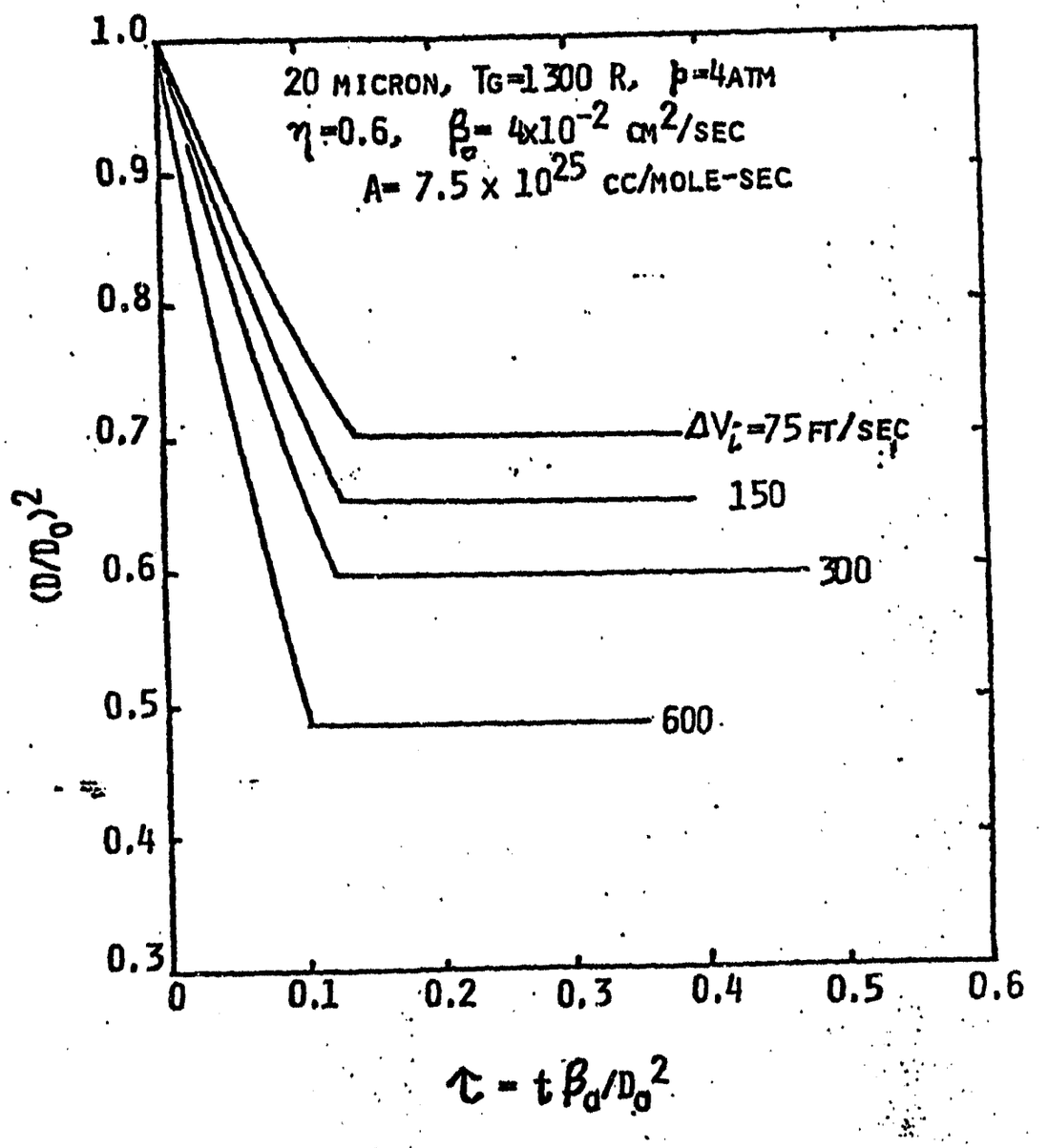

Figure 13, Calculated diameter variation of a droplet with time.

2.5 Evaporation Decomposition of a hexadecane spray:

The coupled effect of evaporation and decomposition (eqns. (14) and (15)) of a hexadecane spray with a realistic drop size distribution in a one dimensional flow field is reported in this section. Results show again that liquid phase decomposition at higher pressures might cause a substantial reduction of combustion efficiency of an advanced air breathing propulsion system.

In order to determine the effect of droplet decomposition and residue formation on the overall performance of a combustor the history of a hexadecane spray with a realistic drop size distribution has been chosen as an example. The fuel is assumed to be sprayed in a 600K, 4 atm. air stream travelling with a velocity of 50 m/s. The gas flow is assumed to be steady and one-dimensional with constant thermochemical properties. The distribution of drop size typical of an airblast atomizer was assumed to follow the data shown in Reference (8). The percent of the total population occupied by each subgroup with a given mean subgroup diameter is listed in Table 1. Hexadecane spray was assumed to follow this distribution.

TABLE 1

DISTRIBUTION OF MEAN SUBGROUP DIAMETERS

Percent Population	Mean Diameter of Subgroup (micron)	Percent Population	Mean Diameter of Subgroup (micron)
15	20	17	60
24	30	12	80
27	40	5	100

Coupled phenomena of evaporation/decomposition of the mean diameter of each subgroup were analyzed neglecting interparticular interaction between different subgroups. In other words, collision between droplets, shattering and their coalescence were ignored.

Using the simplifying assumptions of the earlier problem, eqns. (11), (13), (14) and (15), in their dimensional form, are solved with the following initial conditions.

$$D(0) = D_o;\ u(0) = 0;\ C(0) = 0;\ T(0) = T_s$$

When C approaches 1 the droplet consists only of nonvolatile residue and practically no liquid. At this point, evaporation ceases and $\frac{dD^2}{dt}$ approaches 0.

Since the residue burns extremely slowly, very little reduction in diameter is expected even when it enters the combustor.

These equations with the initial conditions given above are solved using a Fourth-Order Runge-Kutta scheme for coupled nonlinear ordinary differential equations (Ref. 9). Thermochemical properties of pure hexadecane were obtained from Ref. 10 and the value of evaporation constant $\beta_o = 3.5 \times 10^{-3}$ cm^2/sec was estimated from the data of Ref. 11.

Figure 14 shows the behavior of the mean diameter of each subgroup with time when the frequency factor F is assumed to be 10^{18} cm^3/gmole-sec. At this value of F there is a strong coupling between evaporation and liquid-phase decomposition. The evaporation of the spray ceases 2 millisec after injection and the form of the initial distribution, now with smaller subgroup diameters remains virtually unchanged after that time. Figure 14 is basically the history of the distribution of droplet diameters if the same group of droplets are followed. Since droplets of different size are accelerated at different rates, the diameter distribution at a given geometric location will not be the same as that for the corresponding time. Figure 15 shows the distribution of the mean diameters of each subgroup at various physical locations. The spray ceases to evaporate only 1.5 cm downstream of the injection point. Once again, the strong coupling for $F = 10^{18}$ is responsible for the behavior of the diameter distribution.

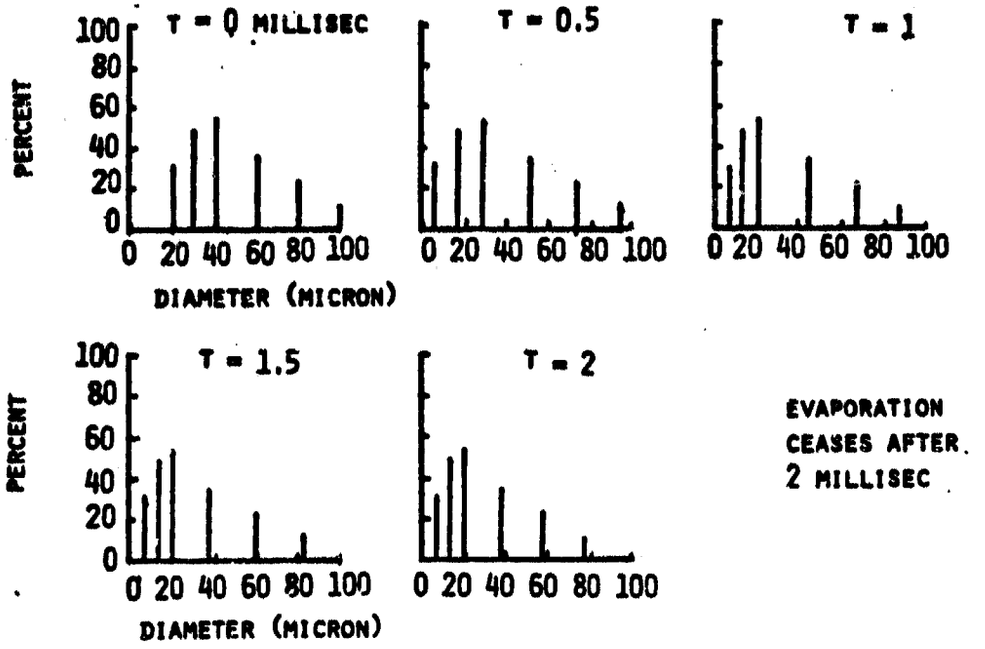

Figure 14. History of droplet distribution. Hexadecane spray 50 m/s, 600°K, 4 atm. air stream. $F=10^{19}$ cm^3/gmole-sec.

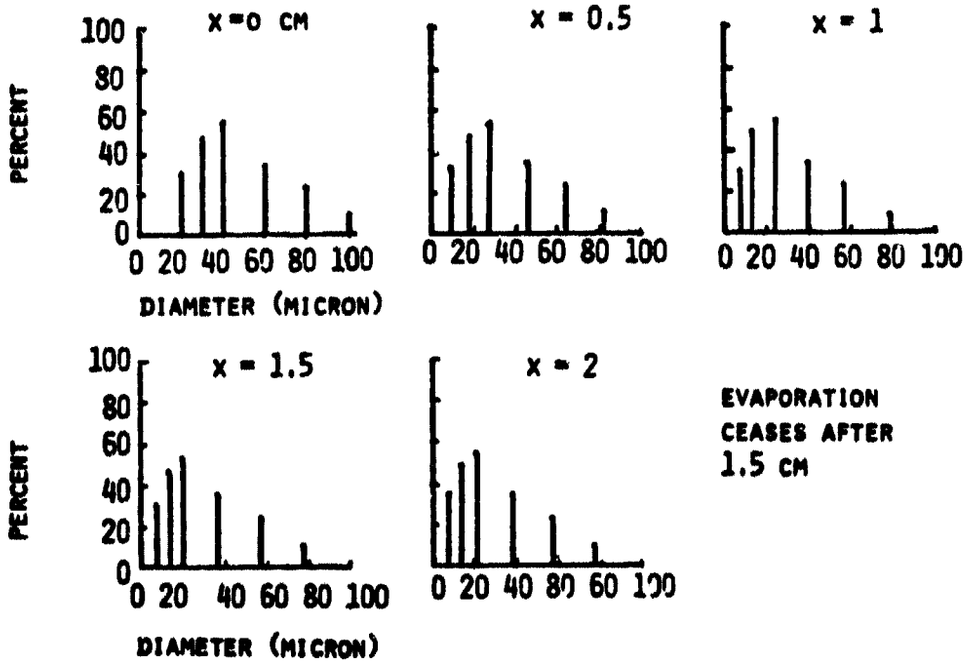

Figure 15. Behavior of hexadecane spray with distance 50 m/s, 600K, 4 atm air stream. $F=10^{18}$ cm^3/gmole-sec.

The details and the mechanism of the liquid-phase decomposition reaction are not known. But the importance of the process of decomposition is illustrated here by choosing two values of F. One causes a strong coupling between evaporation and decomposition and the other allows only a weaker coupling. A value of F = 10^{15} cm^3/gmole-sec is chosen for illustrating the second case. As mentioned previously, the decomposition chemistry is not known although pyrolysis studies of hydrocarbons have been the subject of research for many years. It is likely that the liquid phase decomposition processes leading to a char residue may resemble some of the gas phase reactions leading to smoke. The higher liquid density would tend to favor reactions depending on the fuel concentration. On the other hand, the relatively low liquid temperature compared to flame temperature would tend to rule out reactions of high activation energy. It is likely that atomized fuels contain dissolved air so that the influence of oxygen and the existence of oxidative cracking cannot be ignored.

In the work reported in Reference 1, a simple second order reaction was assumed to account for the formation of a solid residue.

$$\frac{dC_s}{dt} = k\, C_F^{\,2} \qquad (16)$$

where $k = F \exp(-E/RT)$

C_F = fuel concentration

C_s = concentration of solid residue

It was further assumed that the solid was soluble in the fuel. Under these circumstances the vapor pressure of the fuel decreases with time as more and more solid is dissolved. The drop temperature increases leading to accelerated decomposition.

More recent work suggests that insoluble solids may form during the decomposition. Under these circumstances, the liquid temperature remains constant at T_s and the exponential nonlinearity of equation (14) does not exist.

Figure 16 shows the behavior of a 100 micron droplet for three different limited cases. For the case of soluble residue, the residue formation is accelerated by the increase of mixture temperature indicated by eqn. (15). Because of the lower temperature the rate of formation of residue is smaller when the residue does not dissolve in the liquid fuel.

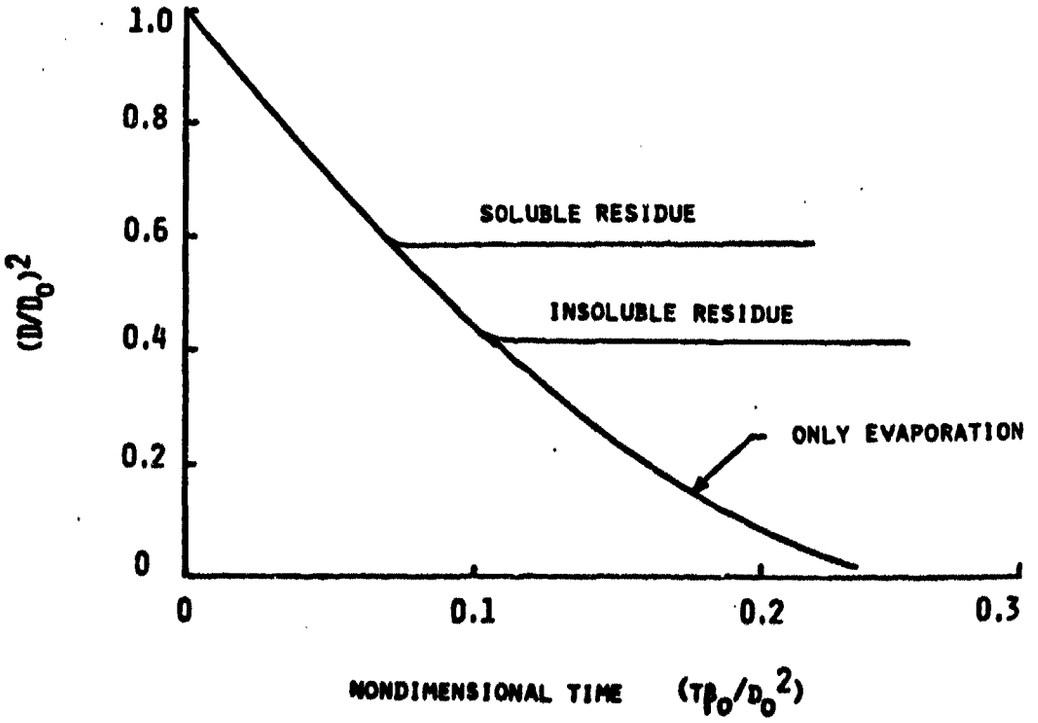

Figure 16. The effect of solubility of residue. 100 micron hexadecane droplet. 50 m/s, 600 K, 4 atm air stream. P-10^{18} cm^3/gmole-sec.

For smaller characteristic times, the process of evaporation in the presence of forced convection is responsible for the reduction of droplet diameter. The overall behavior of the evaporating drop remains qualitatively the same but the particle growth would be slower for the insoluble char. Since the kinetics are not known, the break in the curve from liquid evaporation to char could still occur at roughly the same time period by adjusting the value of the reaction rate constrat, k. The behavior of the products of decomposition are now under study to evaluate the nature of the product by interrupting the evaporation process to look for soluble and insoluble products and to estimate a global reaction rate. The remainder of calculations in this section have been made assuming a soluble product according to Ref. 1.

Figures 17 and 18 show the distribution of diameters at various locations downstream of the injection point. These calculations are performed for $F=10^{15}$. At a distance of 5 cm, half of the original six subgroups has completely evaporated. Only one subgroup remains at 12 cm. Evaporation still continues at this point. Finally, the evaporation ceases completely at 14 cm and residues with a mean diameter of 6.7 micron remain in the flow field. Since most of the spray has already evaporated at this location, such a weak coupling is not expected to have a major impact on the performance of a ramjet combustor.

Although ramjets do not use pure hexadecane as fuel it is used here to illustrate a potential problem area which can have a major impact on the combustion efficiency, carbon deposit and particulate emission. Particulate emission as a source of pollution is not important in ramjets but depending upon the amount of emission it can reduce the combustion efficiency of a burner. Commercial fuel blends and future synthetic fuels such as shale oil are more susceptible to liquid-phase decomposition than pure fuels. Thus, the example of hexadecane shows a conservative estimate of the nature of the problem.

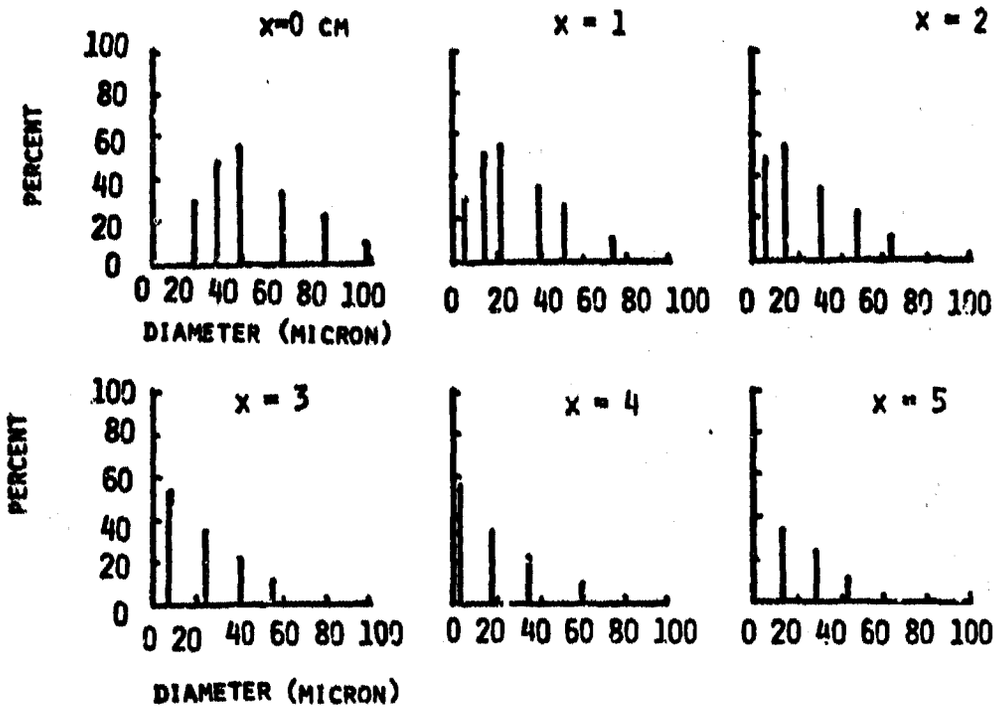

Figure 17. Diameter distribution of hexadecane spray at various locations. 50 m/s, 600 K, 4 atm air stream. $F=10^{15}$ cm^3/gmole-sec.

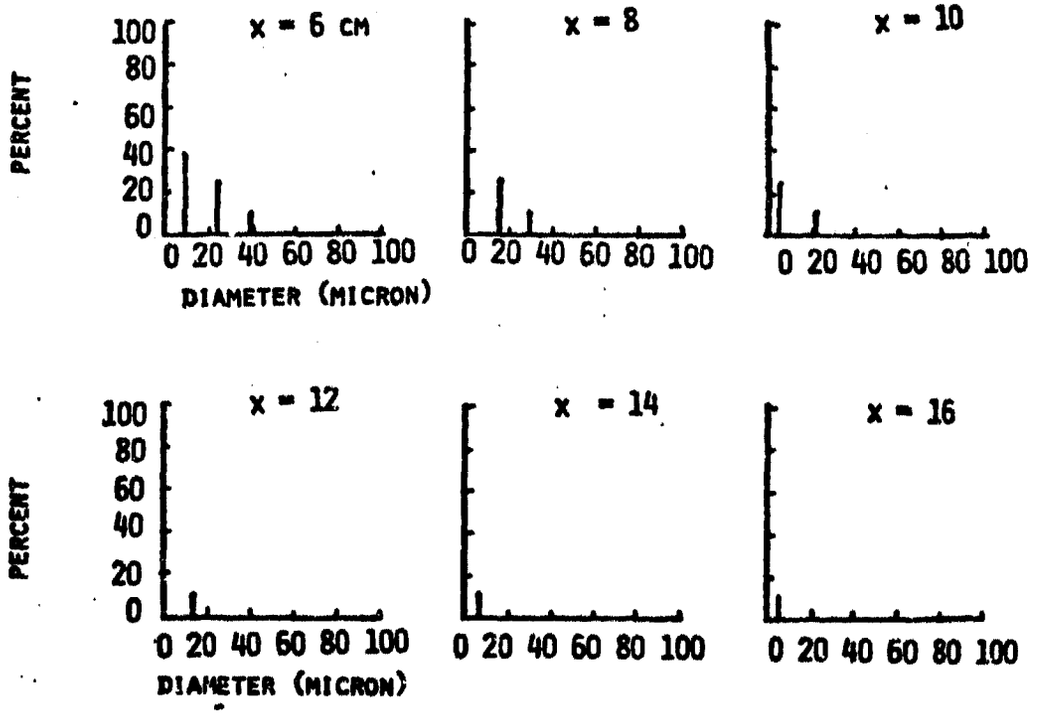

Figure 18. Diameter distribution of hexadecane spray at varous locations. 50 m/s, 600 K, 4 atm air stream. $F=10^{15}$ cm^3/gmole-sec.

The fluid mechanics has been simplified here by assuming a one-dimensional flow with constant gas properties. While this is not entirely correct in a ramjet environment, problems associated with liquid-phase decomposition are just as critical in a one-dimensional flow as in multidimensional flow systems. In a two-dimensional flow field and also with swirl the nonvolatile residue is expected to impinge on the walls of the chamber and cause deposits (Ref. 12). Residue particles which shatter at the wall on impact might contribute to the population of smaller particulate matter in the exhaust.

Figure 19 shows the percent of original mass of the spray that remains unevaporated at any given location downstream of the injection point. For the case of a strong coupling ($F=10^{18}$ cm^3/gmole-sec) roughly 34% of the original mass remains unevaporated. Thus, for this particular case the combustion efficiency might not exceed 66% because only 66% of the original mass of fuel is able to evaporate. The non-volatile residue particles burn very slowly. Reference 12 shows that for a typical burner with a given characteristic length, the reduction of diameter of these particles due to burning is not very significant.

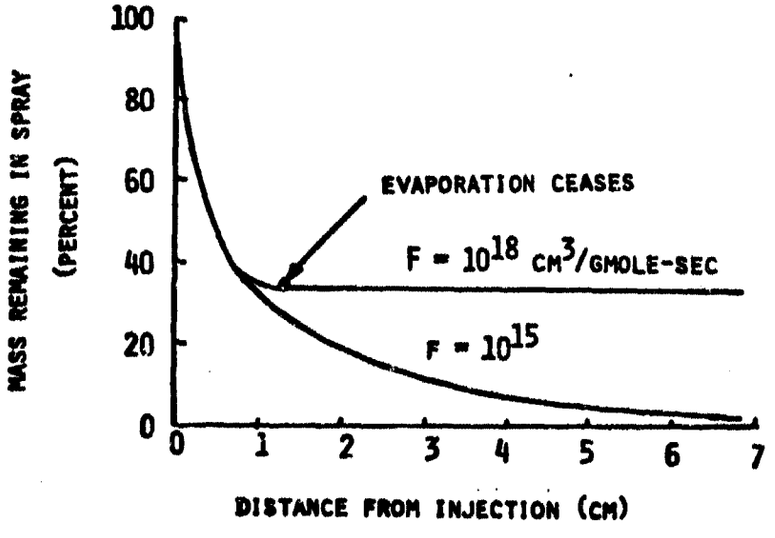

Figure 19. Mass remaining in hexadecane spray. 50 m/s, 600 K, 4 atm air stream.

For the case of $F=10^{15}$ $cm^3/gmole\text{-}sec$, the coupling between evaporation and decomposition is rather weak. The entire spray evaporates nearly completely before residues are formed. For this case, an ideal combustion efficiency of nearly 100% might be expected. Figure 20 is a plot of the possible ideal combustion efficiency based upon the amount of fuel actually evaporated. It is plotted from Fig. 19 and shows the combustion efficiency as a function of the characteristic length available for evaporation. When decomposition rate is faster than the evaporation rate, as in the case of $F=10^{18}$, an increase in the characteristic length would not change the burner performance significantly. The maximum possible combustion efficiency as a function of the frequency factor is shown in Fig. 21. It focuses attention on the importance of liquid phase decomposition in a burner with no restriction on the allowable characteristic length.

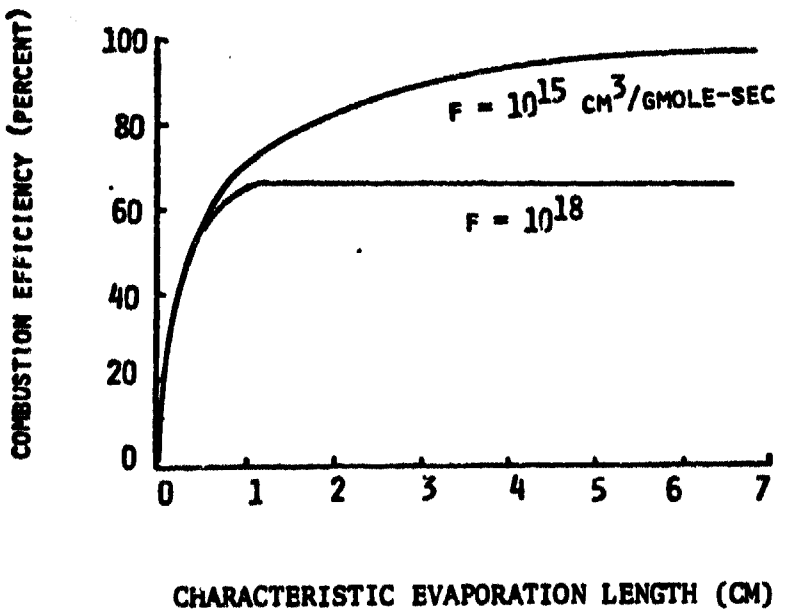

Figure 20. Combustion efficiency as a function of the characteristic evaporation length.

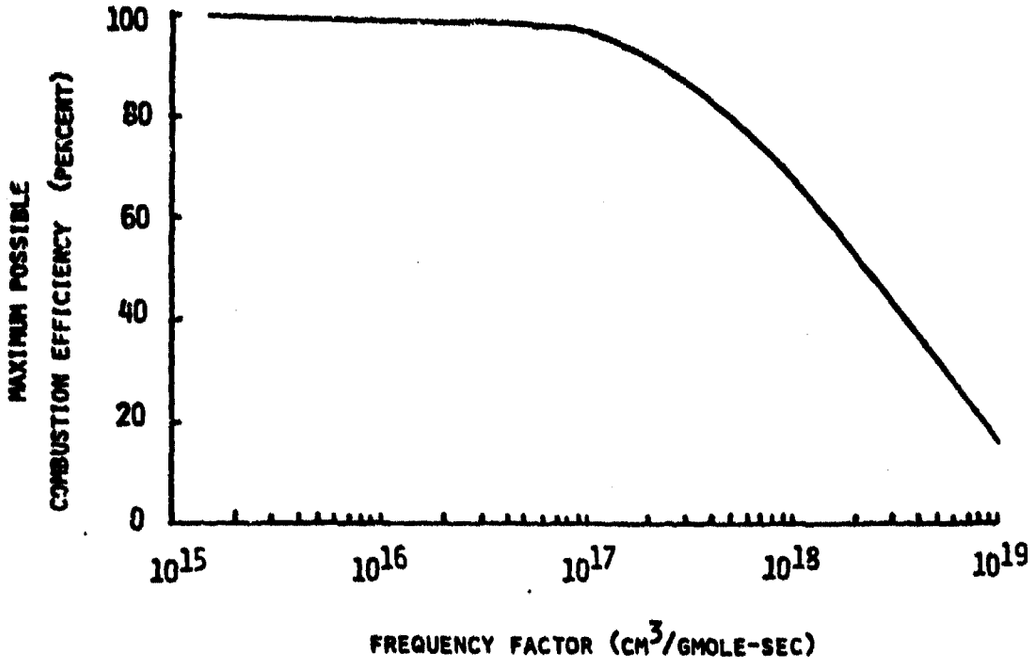

Figure 21. Maximum possible combustion efficiency with liquid phase decomposition.

2.6 Future work on liquid phase decomposition

The most important missing link in these analyses is the decomposition rate which includes the frequency factor and activation energy. Unless these are known with some degree of accuracy the problem associated with droplet decomposition can only be described in a parametric manner with the activation energy and frequency factor as missing parameters. Therefore, it is absolutely essential that the products of decomposition be identified. In the future attempts will be made to filter out the nucleii and analyze them. From the known products the overall, global reaction rate can be postulated. The role of nucleation on the system behavior will also be investigated.

3.0 DROPLET SHATTERING BY IRRADIATION AT DISCRETE FREQUENCY BANDS

3.1 Introduction

A novel technique of droplet shattering by means of irradiation at selected frequencies has been investigated as a part of the AFOSR project. This method would enable one to use slurry fuels without the usual problem of particle clustering. Preliminary experiments with pulsed irradiation at 1.06 micron show that the proposed technique of droplet breakup might be a major breakthrough and would allow effective use of slurry fuels for both military and civilian applications.

A systematic study plan which would lead to a better understanding of the droplet breakup mechanism by irradiation at selected frequencies has been proposed for the future which will include slurry fuels and other synthetic fuels such as, for example, shale oil. Although this preliminary study addresses the potential of droplet breakup by irradiation, the practical uses of this technique or the cost effectiveness are beyond the scope of this research project. Thus, the size, weight and the cost of the source of radiation have not been considered. The possibility of this method and the results of a simplified analysis are given in this section. More analyses are necessary for understanding the mechanism by which the droplet breaks up when pulsed by an extremely small energy source (on the order of 20 mJ).

In view of the trend toward obtaining fuels with larger volumetric heating values (Btu/gallon, for example), there has been a renewed interest in developing slurry fuels. Volumetric enthalpy of reaction can be increased by simply increasing the mass of the fuel per unit volume. This can be accomplished in a two-phase system by adding particles of solid fuel (e.g. carbon, boron etc) to a primary liquid fuel which can be either of petroleum base or synthetic as in shale oil. The size of the particles of solid fuel depends upon the particular application and may range from submicron size to hundreds of micron. Gasoline or diesel-type fuel has a volumetric enthalpy of reaction of approximately 116,000 Btu/gallon. A carbon slurry fuel with roughly a 50% mass loading can, at this time, increase this value to 180,000 Btu/gallon. With research and better understanding of the characteristics and handling of slurry fuels, this figure is expected to increase significantly in the near future.

In addition to providing a large volumetric enthalpy of reaction, the slurry fuels are really "fuel extenders" in the sense that less petroleum-base fuel and more plentiful coal can be used. Thus, the less plentiful petroleum-base fuel consumption can be immediately reduced if slurry fuels are used efficiently.

Although, slurry fuels appear very attractive, there remain many unsolved problems associated with the spray, evaporation and burning characteristics of a droplet of such a fuel.

Preliminary work at Exxon (Ref. 13) on the behavior of carbon slurry fuels shows the existence of undesirable large clusters of particles during the evaporation of the fuel. Because of these clusters unsatisfactory carbon burnout

was observed in a stirred homogeneous reactor. Experiments are continuing at Exxon with a variety of catalysts in the slurry to accelerate the combustion of larger particle clusters. The problem of particle clustering and deposit on the combustor wall have been reported during the 50's by NACA. Formation of particle clusters either during evaporation or burning is very undesirable and must be avoided. Clusters of slow burning particles can cause a substantial reduction in combustion efficiency of a burner. At the present time clustering appears to be one of the major problem areas in the use of slurry fuels.

Preliminary work on a carbon slurry fuel for cruise missile application at the Air Force Aero Propulsion Laboratory (Ref.14) shows a good potential. The slurry is produced by suspending submicron carbon particles in JP-10 and RJ-6 liquid fuels. This work is currently being extended in scope to include boron particles.

Reference 15 lists general, overall observations of the thrust efficiency of a dump combustor with carbon and aluminum slurry fuels. The carbon slurry consisted of a mixture of carbon and TH Dimer. The aluminum slurry was a mixture of aluminum and decalin. No information on the evaporation, particle clustering or the burning characteristics of these two slurries were given.

In addition to being an important future fuel source for the Department of Defense (Ref.16), the slurry fuels in the role of "fuel extenders" can be used in stationary powerplants and other non-defense applications. However, unlimited use of slurry fuels must await satisfactory resolution of problems associated with spray, evaporation, clustering, particle deposition and burning of these fuels. Discussion of some of these problems based upon selected recent experiments in a furnace environment appears in Reference 17.

These critical problem areas are discussed and a novel method of irradiation at selected frequency bands which could virtually eliminate the problem of particle clustering is suggested. It can be used also for a heavy crude oil which is not properly atomized in a spray. The irradiation technique proposed here requires very little energy and helps break up large droplets into many smaller ones. Although the exact mechanism of droplet shattering by this irradiation method has not been investigated thoroughly, preliminary observation indicates that the droplets tend to break up due to localized thermal effects associated with pulsed irradiation.

In addition to studying the conditions under which droplets of a variety of slurry fuels and unrefined heavy crude oil can be shattered, evaporation and burning characteristics of these unconventional fuels will also be investigated in the future. Once the evaporation and burning rates of the shattered droplets are known, it will be possible to consider analytically the behavior of a two-phase mixture of fuel and oxidizer in a burner. The results of such an analytical study is expected to provide valuable guidelines for the design of a burner either for civilian or for military application.

3.2 Technical discussion: Background

If the slurry fuel is directly injected in a hot air stream of a burner, the liquid portion of the slurry would tend to evaporate first leaving behind a cluster of particles which is more difficult to burn. Since the burning rate of particles like carbon is much slower than the reaction rate of gaseous fuels, the characteristic length of a burner using a slurry fuel has to be much greater. As larger clusters are formed, the problem with the characteristic length becomes more severe. It is essential, therefore, to make sure that large clusters are not formed when a droplet of slurry fuel evaporates. One method of avoiding large particle clusters would be to start with finely atomized droplets.

Following this line of reasoning, preliminary experiments are performed at the University of Southern California where slurry droplets are shattered by pulsed irradiation at selected frequencies.

Laser Experiment: ARCO graphite and ARCO clear multi-viscosity oils were chosen as samples for irradiation at a selected wavelength by means of a pulsed laser. Although ARCO graphite oil is used for lubrication and not as a fuel, it was chosen for easy availability of a sample of homogeneous slurry system. The graphite oil consists of submicron graphite particles which remain in suspension indefinitely without any visible settling or stratification. It will be possible to prepare a slurry fuel with a mixture of submicron carbon particles and a liquid hydrocarbon fuel. However, commercially available lubricating oil was used for determining the feasibility of droplet breakup by subjecting it to irradiation over a specific frequency range.

In order to determine the absorption/transmission characteristics of the sample of oil slurry, IR spectrophotometric experiments were performed on several samples of clear and graphite oils. Specifically, the objective of these experiments were to determine the frequency range in which the clear oil is transparent to the incident radiation and the graphite oil absorbs most of the incident energy. Figures 22 & 23 show typical results of the IR spectrophotometric studies. The clear oil appears to transmit all the incident energy over a large range of frequencies. The graphite oil, on the other hand, behaves nearly as a black body and appears to absorb most of the incident radiation over a large range of frequencies. Further experiments showed that at a wavelength of 1.06 micron (the available laser frequency) the clear oil is practically transparent and the graphite oil behaves nearly as a black body.

Small oil droplets (between 2 and 3 mm in diameter) were suspended from a hollow quartz tube and exposed to a pulsed laser beam with a wavelength of 1.06 micron. Beams with energies between 25 and 50 milli J and a pulse duration of approximately 15 nanosec were able to break up the suspended droplet into many smaller droplets. The breakup phenomenon was not what one might call "explosive shattering". The droplets appeared to splatter gently and deposit themselves on the walls of the test chamber. Figure 24 shows a portion of the deposits superimposed on a grid with 1 mm spacing. Figure 25 shows the size of the original droplet of graphite oil which was irradiated by the laser beam. Since the sample of clear oil transmitted most of the energy at a wavelength of 1.06 micron, a droplet of clear oil remained unaffected when exposed to the pulsed laser beam.

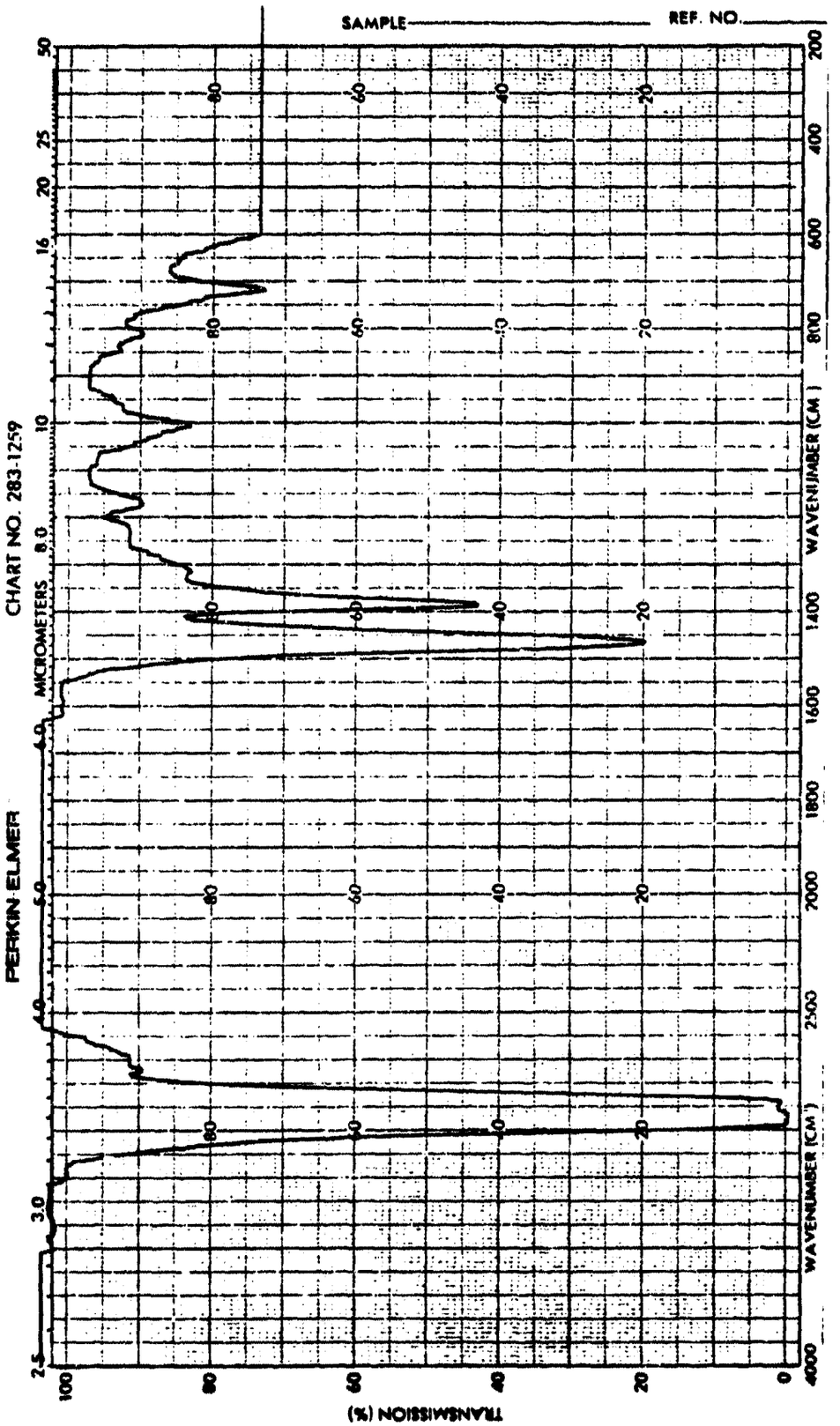

Figure 22. IR Spectrophotometric Scan of ARCO Clear 10-40 Oil

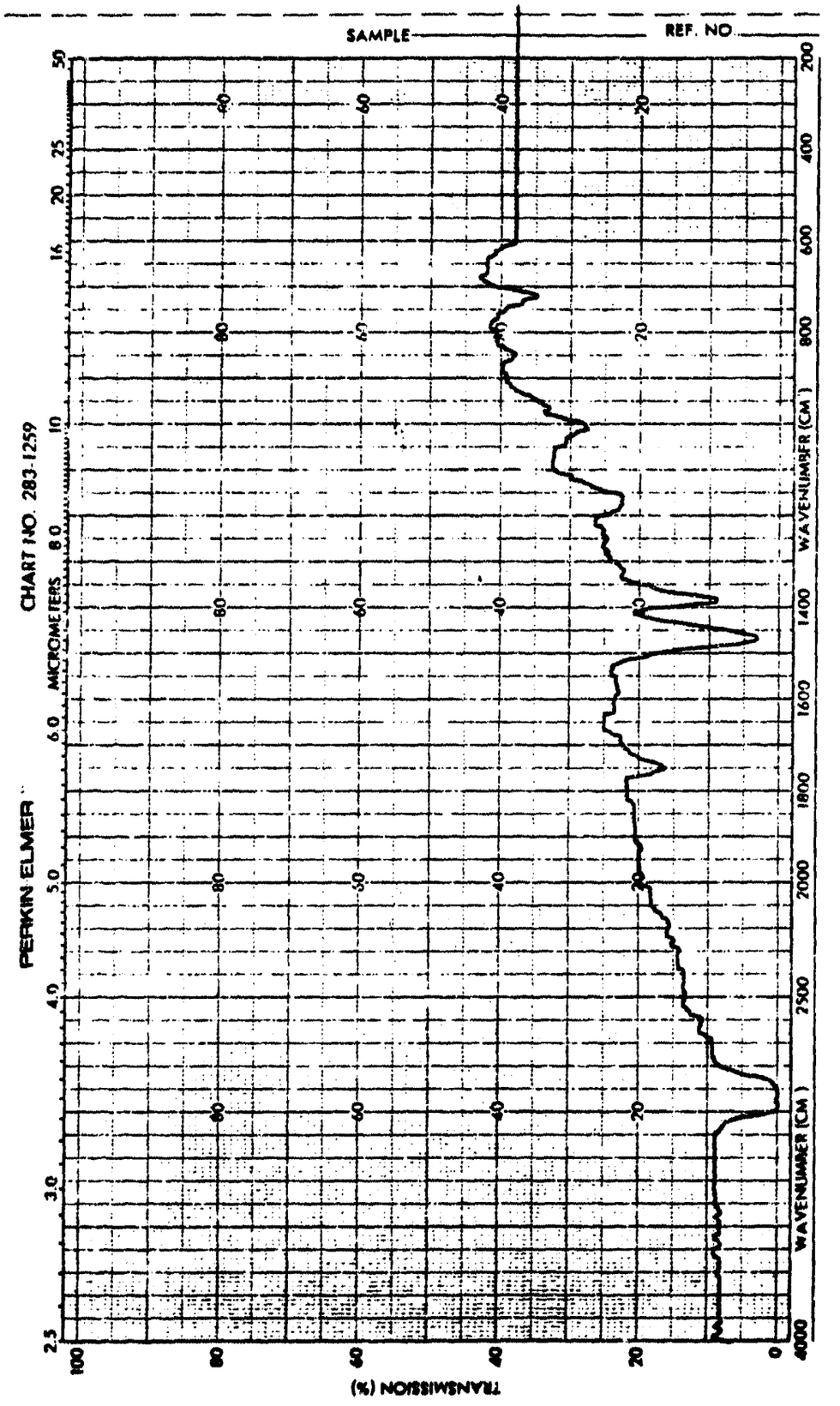

Figure 23. IR spectrophotometric scan of ARCO graphite 10-40 oil

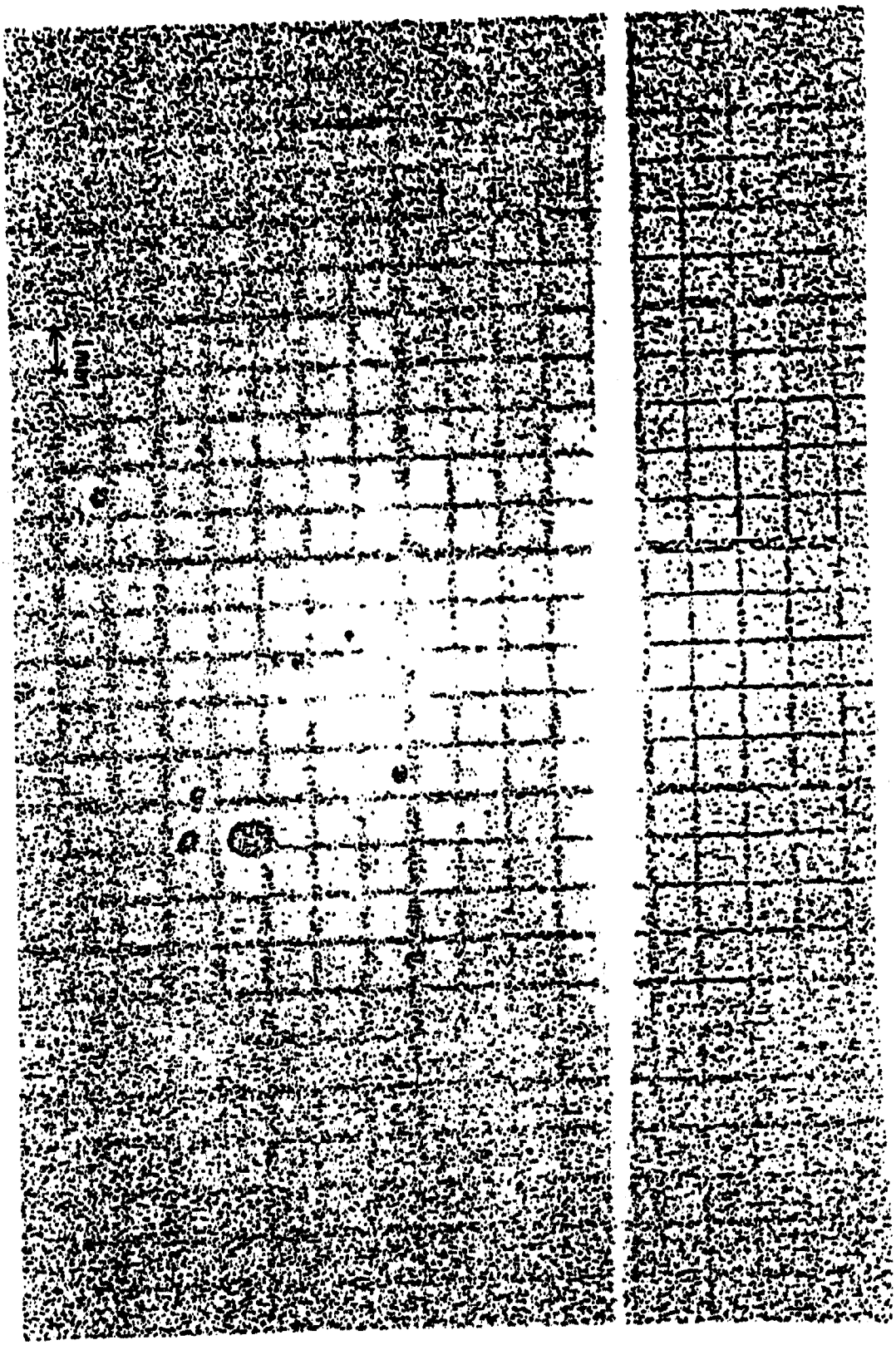

Figure 24. Traces of droplets on the wall of the test section (approximately 1 cm from the droplet).

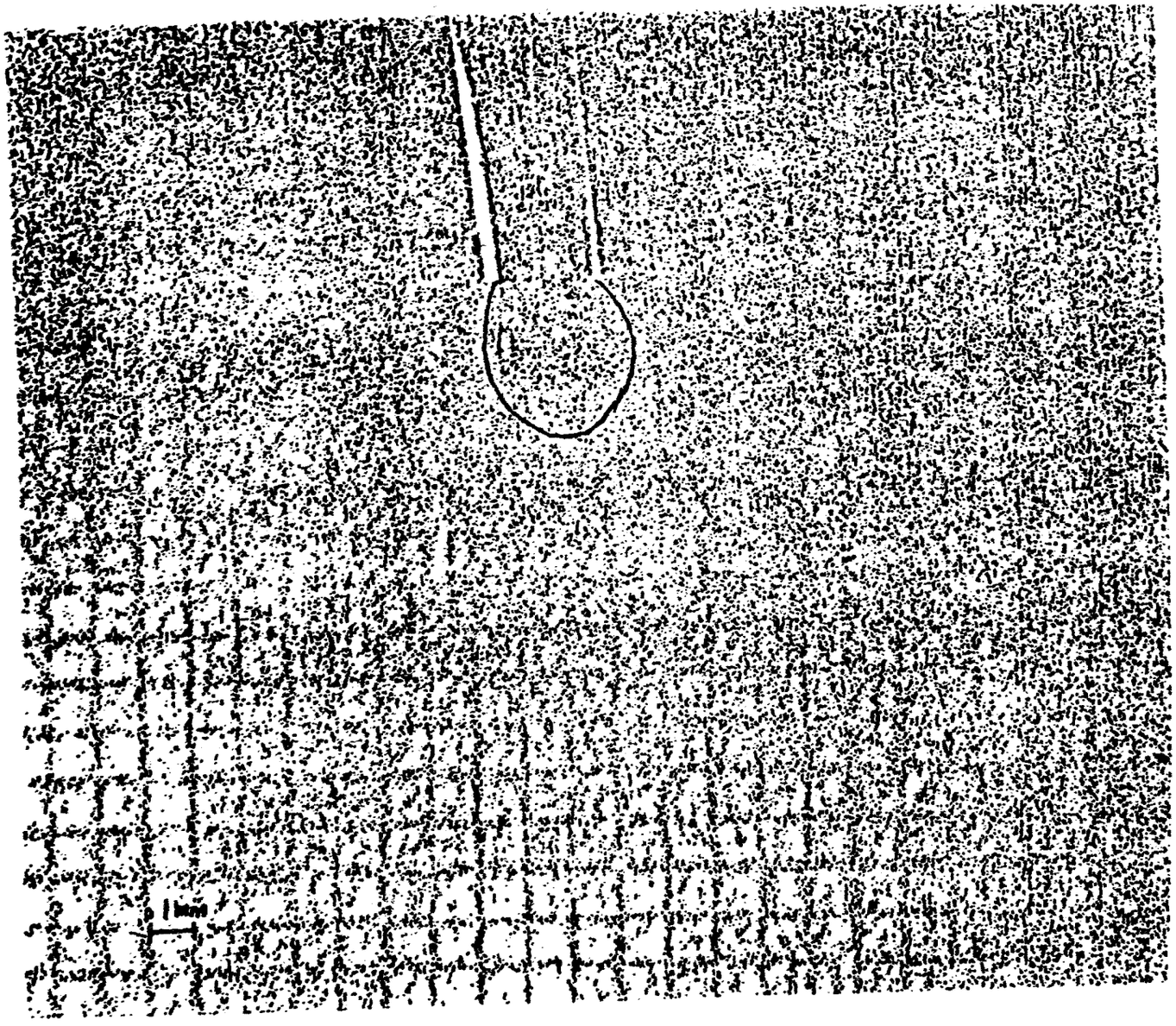

Figure 25. Size of the original drop before irradiation.

An energy level of 25 to 50 milli J, on the whole, is too small to cause droplet shattering due to uniform heating. With the addition of such a small energy the increase of temperature of the droplet is practically negligible except perhaps for local areas at the point of incidence. It is quite possible that the local temperature on a spherical shell just below the droplet surface is rather high even though the average temperature of the droplet is practically unchanged. This local hot surface might cause local evaporation and hence shattering of the liquid droplet. The physical model described here can actually take place in a pulsed system when the rate of energy absorption decays radially toward the center of the droplet and heat is transferred to the surroundings from the droplet surface. As a consequence, the local temperature just below the surface might reach a maximum value; high enough to cause local evaporation and droplet shattering. Although this sequence of events is feasible, it is not quite clear if actually the local evaporation is responsible for the traces of very small droplets shown in Fig. 24. Another probable explanation of the droplet breakup is that the absorbed energy is of the same order as the energy required to overcome the surface tension and generate "new surface areas". Preliminary experiments with both continuous irradiation and irradiation with longer pulse duration indicate that perhaps the surface tension model is not responsible for droplet breakup. The minimum pulse duration in these experiments were of the order of 20 millisec with peak powers of the order of several watts. The steep temperature gradient induced by a short duration pulse of high power (low total energy) may be responsible for the drop breakup. An investigation of the mechanism of the shattering of drops containing suspended solids is an important aspect of this research. More work will be necessary to understand thephenomenon of droplet breakup in this manner. In the

meantime, however, the technique of droplet breakup described in this report can become a major breakthrough which could facilitate the use of slurry fuels without the problem of particle clustering. As mentioned earlier, one of the reasons for the formation of clusters is that the liquid part of the slurry fuel evaporates first leaving behind the remaining particulate matter contained in the droplet. If bigger slurry droplets can be broken up into many smaller ones, the possibility of the formation of bigger particle clusters will be diminished drastically.

The preliminary experiments on the feasibility of droplet breakup utilized a pulsed laser beam at a wavelength of 1.06 micron. Other wavelengths can be equally effective and selected from the IR spectrophotometric traces shown in Figs. 22 and 23. Because of the ease of availability, a pulsed laser at a wavelength of 1.06 micron was used to prove the feasibility of slurry droplet breakup by the technique of irradiation at a selected wavelength.

In addition to the regions of 100% transmission, the IR spectrophotometric scan of Fig. 22 for a sample of clear 10-40 oil shows frequency bands where the entire incident energy is absorbed. For example, between a wavelength range of 3.35 to 3.45 micron, practically all the energy will be absorbed (i.e. 0 transmission coefficient). Pulsed radiation at this band of wavelength is expected to break up a droplet of clear oil.

Similar frequency bands for other oils including shale and heavy crude oils can be identified. Incident radiation at these frequences would help break up larger droplets and would make this technique applicable to both slurry and single phase liquid fuels. For the case of crude oil, for example, it will no longer be necessary to preheat the fuel and reduce its viscosity before injection. Droplet atomization will be possible simply by pulsed irradiation at an appropriate wavelength.

Figure 24 shows the effect of a pulsed laser beam on a small droplet. Although the energy level of the beam is rather small, the peak power level is of the order of a MW. It is not clear what kind of power level will be required in a continuous beam to produce similar droplet breakup. Also it is not known if there exists an optimum combination of beam energy and pulse duration. The answer to these critical questions depends upon the mechanism of droplet breakup. Therefore, the probable droplet breakup model described earlier must be investigated during the early phase of this research effort.

A simplified preliminary thermal model is used to determine the possible temperature rise at the droplet surface immediately after being subjected to a heat flux over a given time period. Assuming a spherical symmetry for simplicity, the following equation, initial and boundary conditions are used for obtaining the temperature distribution in a droplet.

Energy:
$$\frac{\partial T}{\partial t} = \alpha_t \frac{1}{r^2} \frac{\partial}{\partial r}\left(r^2 \frac{\partial T}{\partial r}\right) \tag{17}$$

Initial condition:
$$T(r,o) = T_o \tag{18}$$

Boundary condition:
$$-k \frac{\partial T(a,t)}{\partial r} = -\frac{q_o}{\Delta t_o} + h\left[T(a,t) - T_o\right], \quad o < t < \Delta t_o \tag{19a}$$

$$= h\left[T(a,t) - T_o\right] \quad \Delta t_o < t \tag{19b}$$

where a = drop radius

c = specific heat

h = heat transfer coefficient

k = thermal conductivity

q_o = energy/area

r = radial distance

t = time

T = temperature

The solution* of eqn. (17) for small t is as follows:

$$T(r,t) - T_o = \frac{Q}{4\pi k \Delta t_o} \frac{1}{1-\frac{ah}{k}} \frac{1}{r} \left\{ -\operatorname{erfc}\left(\frac{a-r}{2\sqrt{\alpha_t t}}\right) \right.$$

$$+ \exp\left[-\left(1-\frac{ah}{k}\right)\left(1-\frac{r}{a}\right) + \alpha_t \left(\frac{1}{a}-\frac{h}{k}\right)^2 t\right]$$

$$\operatorname{erfc}\left[\frac{a-r}{2\sqrt{\alpha_t t}} - \left(\frac{1}{a}-\frac{h}{k}\right)\sqrt{\alpha_t t}\right] + \operatorname{erfc}\frac{a-r}{2\sqrt{\alpha_t (t-\Delta t_o)}}$$

$$- \exp\left[-\left(1-\frac{ah}{k}\right)\left(1-\frac{r}{a}\right) + \alpha_t \left(\frac{1}{a}-\frac{h}{k}\right)^2 (t-\Delta t_o)\right]$$

$$\left. \operatorname{erfc}\left[\frac{a-r}{2\sqrt{\alpha_t (t-\Delta t_o)}} - \left(\frac{1}{a}-\frac{h}{k}\right)\sqrt{\alpha_t (t-\Delta t_o)}\right] \right\}$$

where α_t = thermal diffusivity

erfc = complimentary error function

Q = energy of incident beam

*This is worked out by Dr. H.T. Yang of USC.

Using the following approximate values for a typical lubricating oil the maximum surface temperature for various pulse durations are shown in Figure 26.

$k = 0.14$ J/m sec K

$c = 2.0$ kJ/kg K

$\alpha_t = 8 \times 10^{-8}$ m^2/sec

$h = 7.3 \times 10^{3}$ J/m^2 sec K

$a = 0.254 \times 10^{-2}$ m

$Q = 20$ mJ

An average lubricating oil boils at around 400°C. Thus, Fig. 26 indicates that a minimum pulse duration of the order of a microsec will be needed to cause local boiling. Earlier experiments show that pulse duration of the order of millisec is not able to break up a droplet. More experiments are planned to ascertain if the droplet break up is indeed due to local boiling.

3.3 Future work on droplet shattering

In the future the following tasks would be attempted:

(1) Investigation of the fundamental mechanism by which larger droplets are broken up into many smaller ones.

(2) IR spectrophotometric studies of selected single phase and slurry fuels would be conducted to ascertain the available windows where nearly all the incident radiation can be transmitted.

(3) In the case of slurry fuels, the size of carbon particles and their mass loading would be the main variables in the study.

(4) For a given laser beam, the beam energy level as well as the duration of pulse at a selected frequency would be the major variables at the beginning.

(5) From the analysis of (1) and photographs of the splattered drops, optimum values of beam energy and its duration would be identified.

(6) Feasibility of slurries other than carbon slurries (e.g. boron slurry) would be investigated.

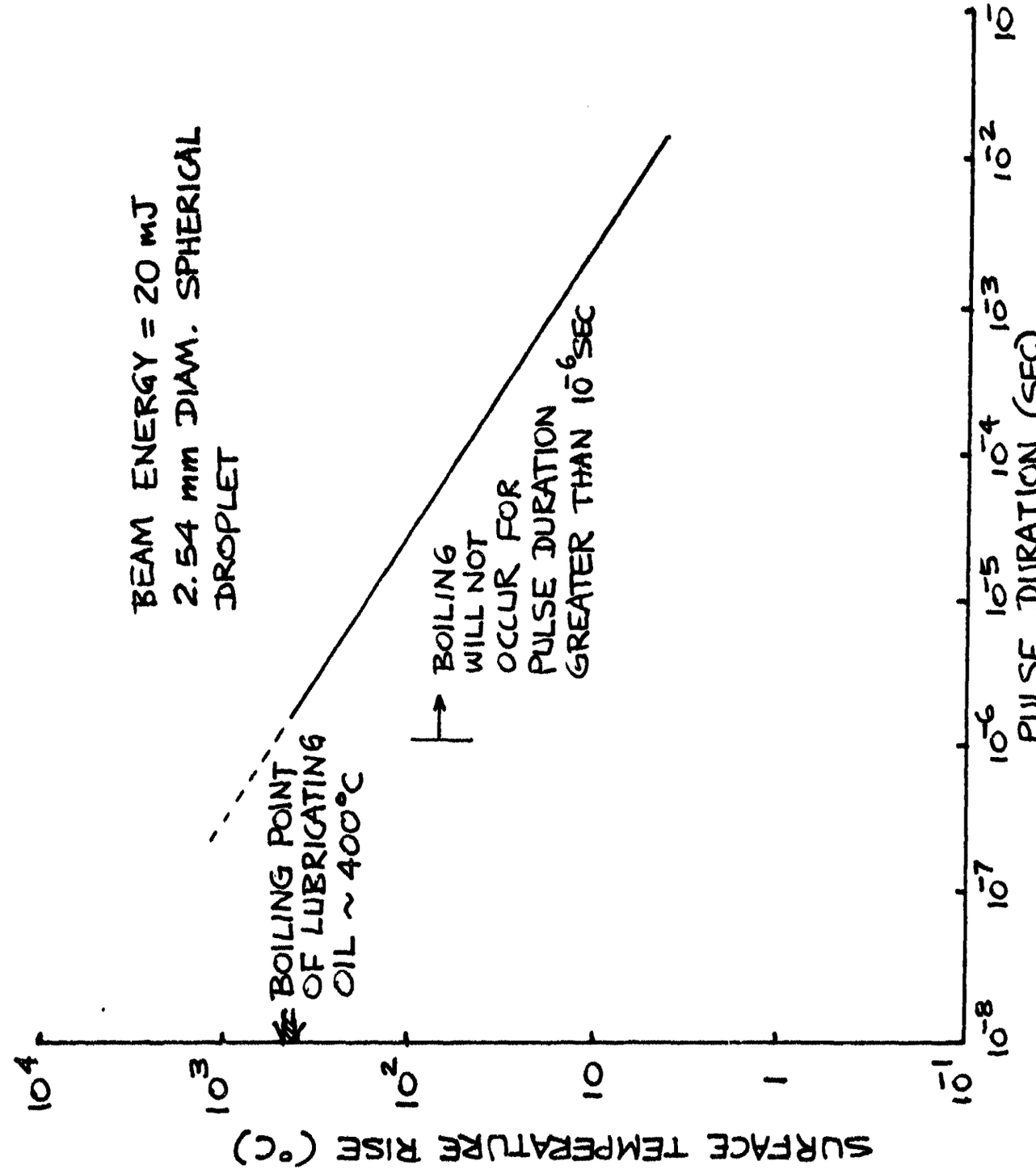

Figure 26. Maximum surface temperature as a function of pulse duration.

4. VORTEX AMPLIFICATION AND SWIRL GENERATION BY INTERACTING GAS JETS

4.1 Introduction

Sudden expansion burners (dump combustors) are being investigated as possible candidates for advanced air-breathing propulsion systems which are compact, smooth burning and highly efficient[18]. Unfortunately, except for the side dump concept, most sudden expansion burners have rather low flame spreading rates. Also, when the characteristic length of the burner is reduced, the combustible mixture becomes stratified due to an insufficient time for evaporation of the fuel droplets. In many instances, fuel stratification and geometric constraint in a compact, volume-limited dump burner cause rough burning[19].

In order to remove some of the deficiencies of the basic dump burner concept, a slight modification has been proposed[19]. In the modified burner, small gas jets located upstream of the dump plane are used for vortex amplification. The vortices induced by the gas jets and the sudden expansion step interact and, thereby, amplify the size of the recirculation zone. If the location and the momentum flux of the jet system are chosen properly, a significant increase in the size of the recirculation zone downstream of the sudden expansion step can be achieved. On the whole, the jet system helps increase the flame spreading and the characteristic residence time,[20] and decrease the effect of fuel stratification. Thus, the use of gas jets gives rise to a variable strength flame holder[21] where the strength of flame holding could be modulated over the entire flight path as the need arose. In addition to the gas jets in the radial direction, swirl can be induced in the burner by means of proper orientation of the jets.[22]

Most of the studies of the interaction of gas jets in a dump burner were conducted in both two-dimensional and axisymmetric laboratory burners with low inlet stagnation pressure and temperature. Unlike realistic ramjet burners, premixed propane-air mixtures were used in the laboratory burners and the nozzles were not choked. Because of these operating differences questions can be raised regarding the usefulness of the jet systems in a liquid fuel injected burner operating at higher pressures and temperatures with choked nozzles.

This section describes a series of experiments at higher pressures and temperatures in a 15.2 cm-diam burner with a 2.5 cm step conducted at the Air Force Aero Propulsion Laboratory (AFAPL), Dayton, Ohio. The ranges of pressure and temperature were consistent with a typical ramjet application, and the burner nozzle was always choked. The first objective was to determine if the jet system could perform effectively in a high temperature, high pressure environment with a choked burner nozzle. The second objective was to ascertain if it would be possible to predict the performance of a larger burner operating at higher pressures and temperatures from known behavior of smaller laboratory scale burners at lower pressures and temperatures.

4.2 Experiments and Results

Premixed propane air mixtures at slightly over 1 atm of pressure and inlet temperature of 327 K were used both in two-dimensional and axisymmetric combustors. Three different sizes of two-dimensional channel burners (20.3 x 2.5 cm, 7.5 x 2.5 cm, and 51. x 3.8 cm) and two axisymmetric burners (10.2 and 7.6 cm diam) with unchoked nozzles were studied. Pressure, temperature, location, diameter, number of holes, and the momentum flux of the jet system as well as the step height were varied. A typical transverse jet system was located 1.3 cm upstream of the step and consisted of 36 equally spaced 1-2 mm-diam holes. The jet mass flow rate was approximately 3-4% of the primary air

flow rate. Figure 27 is a sketch of an axisymmetric dump combustor with a jet system upstream of the sudden expansion step. Figure 28 shows the plenum chamber of the jet system of a swirl jet with a swirl angle θ_j. When $\theta_j = 0$, the jet flows in the radial direction and no swirl is introduced in the burner. The angle θ_j has been varied parametrically from 0 to 60 deg. Shop air at room temperature was used in the jets both at USC and AFAPL. In order to reduce the number of variables no attempt was made to use heated air, oxygen, or fuel in the jet and thereby increase the performance of the burner.

Figure 29 is a sketch of the AFAPL combustion tunnel. A J85 air heater was used to heat the inlet air to two preselected temperatures in the neighborhood of 550 and 720K. Also, as shown in the figure, two different locations could be chosen for injecting fuel in the burner. When the fuel was injected far upstream (about 1.6 m) the mixture was assumed to be uniformly mixed and the term "premixed fuel injection" was used to describe this injection system. On the other hand, when the fuel was injected 12 cm upstream of the dump plane, the fuel air mixture was no longer homogeneous. This type of injection in the AFAPL test was referred to as "wall injection." Choked flow was maintained in the burner nozzle for all the tests by means of an exhaust system downstream of the burner It was possible to measure the engine thrust in the AFAPL facility. From the measured thrust, the average stagnation temperature in the burner and, thus, the increase in stagnation temperature across the burner could be calculated. The ratio of the temperature rise from thrust measurement to that calculated from equilibrium thermodynamics was defined as the combustion efficiency.

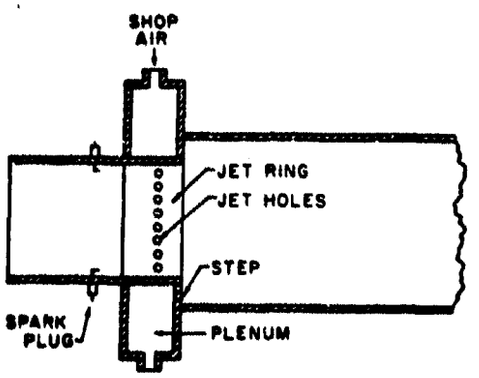

Figure 27. Sketch of an axisymmetric dump burner with a jet system (USC).

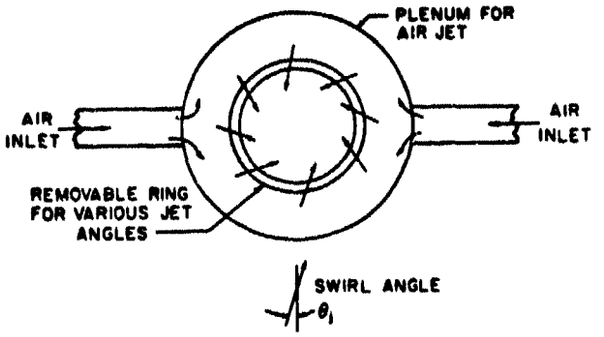

Figure 28. Plenum chamber of the jet system (USC).

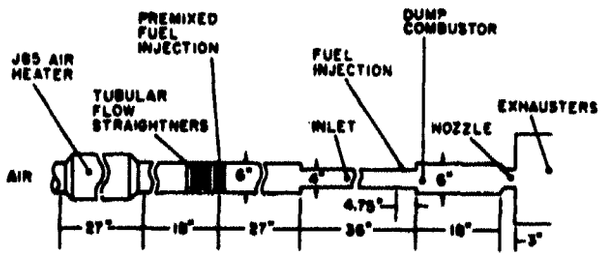

Figure 29. Sketch of the AFAPL combustion tunnel.

The AFAPL combustor was 15.2 cm in diameter with a 2.5 cm step. Oxygen was introduced in the flow system to counteract the vitiation due to the J85 burner. Therefore, the primary flow stream can be considered "air like." Table 2 lists the range of jet variables considered at AFAPL.

Except for the jet stagnation pressure, the selection of the variables was based upon the tests performed at USC. The shop air at AFAPL had to be maintained at a higher pressure so that enough flow of air could be established through the jet. Therefore, it was not possible to vary the jet pressure parametrically to determine its effect on the burner performance.

Lean blowoff limits for three different two-dimensional channel burners are shown in Fig. 30. Also shown are the rich blowoff limits for a 7.5 x 2.5 cm burner. Only a limited number of experiments were performed with rich mixtures. In spite of the differences in chamber size, all lean blowoff data points seem to follow a trend which is independent of the size of the system. Earlier observation, both in axisymmetric and two-dimensional systems with different step heights, indicated that flame blowoff in dump burners was a local phenomenon and was independent of the burner size as long as the step height was sufficiently large to provide an adequate recirculation zone volume.[23]

Table 2

Range of jet variables at AFAPL

Jet variables	Range
P_j	6.7-10 atm
$\dot{m}_j/\dot{m}_a$	0-6%
x_j	1.3 cm
N	36
d_j	1, 1.3, and 2 mm
θ_j	0, 20, and 45 deg

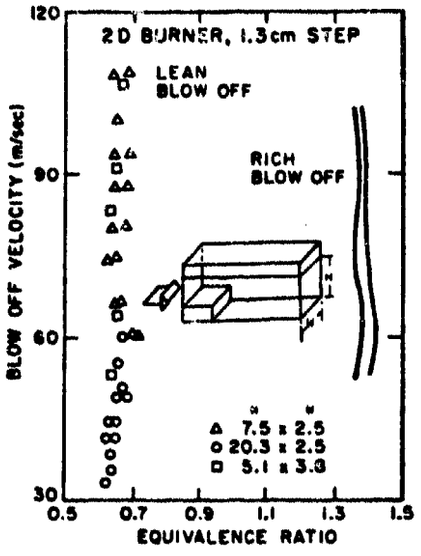

Figure 30. Blowoff limits for channel burners; propane-air mixtures, P_a = 1 atm, T = 327 K.

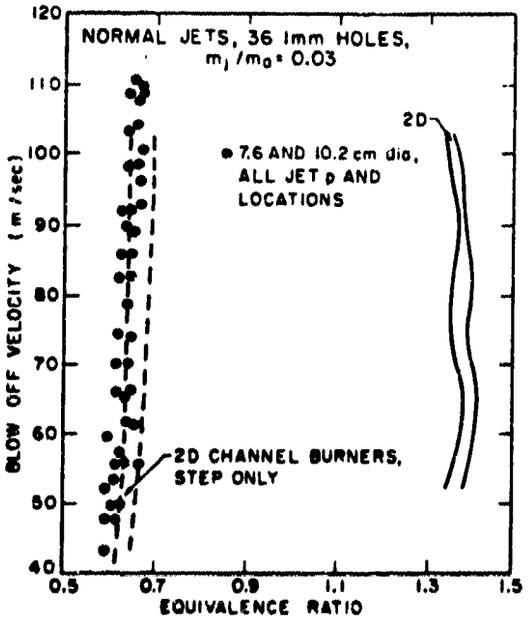

Figure 31. Blowoff limits of axisymmetric burners with air jets; P_j = 1.3-4 atm, x_j = 0.3-2.3 cm, h = 1.3 cm.

Figure 31 shows the lean blowoff data for both 10.2 and 7.6 cm diam burners with a 1.3 cm step. The data points represent jet pressures from 1.3 to 4 atm and jet locations from 0.3 to 2.3 cm upstream of the step. There were between 18 and 36 jets with diameters in the range of 0.76-1.3 mm. Additional experiments also showed that within the range of the jet variables, the blowoff limit was independent of the location, number of holes, hole diameter, and jet pressure as long as the jet mass flow rate relative to the primary flow rate was kept constant. The range of blowoff limits of the channel burners is also shown in the figure by means of lines. The difference in the equivalence ratio at lean blowoff between the axisymmetric and the two-dimensional burners can be attributed to the difference in size of the recirculation zone downstream of the step.

The insensitivity of lean blowoff to the variation of jet pressure, jet location, etc., applies also to the case of swirl jets. Figure 32 shows the lean blowoff points for 40 deg swirl jet system in a 7.6 cm burner with 1.3 cm step. Also shown are the data for normal jets in an axisymmetric chamber and a channel burner without any jet. The equivalence ratio at blowoff was larger for the 40-deg swirl angle than for the normal jets. Additional study showed that the difference was the largest for the 45-deg swirl angle and decreased for both smaller and larger angles. No perceptible difference in the equivalence ratio at lean blowoff was observed for swirl angles between 0 and 20 deg. The difference in equivalence ratio at blowoff with and without the jet system was probably caused by the local dilution of the combustible mixture by the cold air. Since the degree of penetration of the swirl jets can not be predicted, it was not possible to determine exactly why a 45-deg swirl jet would cause more local dilution than, for example, a 60 deg swirl jet. The burner

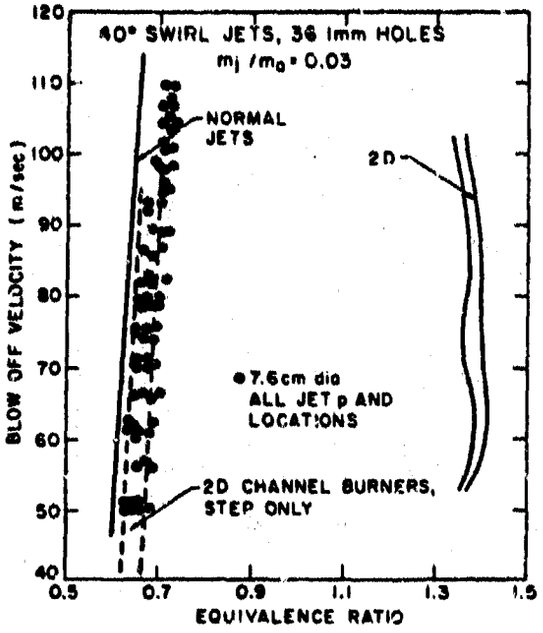

Figure 32. Blowoff limits with 40 deg swirl jets; P_j = 1.3-4 atm, x_j = 0.3-2.3 cm, h = 1.3 cm.

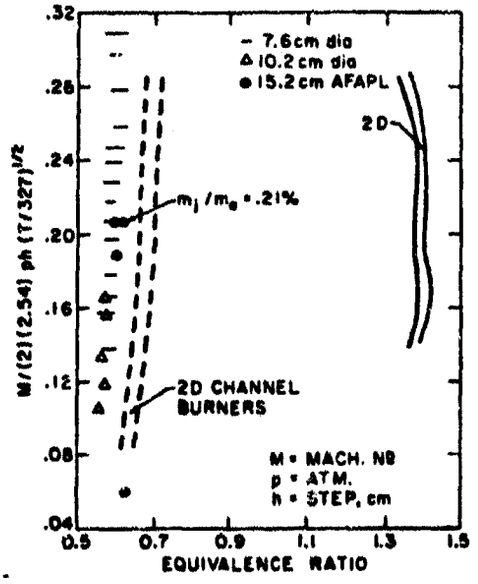

Figure 33. Comparison of lean blowoff data - USC: h = 1.3 cm AFAPL: h = 2.5 cm.

performance was degraded to some extent due to the quenching action and dilution of the combustible mixture by the cold air jets. It is possible to use heated air, oxygen, or even fuel in the jet system and improve the burner performance. No attempt was made to use any gas other than air at room temperature during the course of this investigation. It was felt that the feasibility of the concept of using gas jets for vortex amplification and swirl generation can be demonstrated adequately with the use of shop air at room temperature.

The lean blowoff performance of the USC system was correlated with that of the AFAPL burner using a homogeneous reactor parameter for a second-order reaction[24]. The homogeneous reactor parameter has been used successfully in the past for correlating flame blowoff in bluff body flame holders operating under different pressure and temperature environments. In the present work the reactor parameter is expressed in terms of Mach number and step height rather than the velocity and the dimension of the flame holder. Figure 33 shows that in spite of large differences in pressure and temperature the lean blowoff data of the test programs can be correlated for the case of "premixed fuel injection." It did not seem to make any difference whether the burner nozzle was choked or not. The blowoff limits of the USC channel burners are also shown in the figure for comparison. The blowoff performance was independent of burner size in the range of 7.6-15.2 cm. The constants used in the homogeneous reactor parameter were chosen for the convenience of data reduction. For example, the inlet temperature for the USC tests was 327 K and this value was used for normalizing the temperature. Also the use of inlet Mach number instead of the velocity made it possible to compare the two test results over a reasonable range of values of the reactor parameter. Figure 34 compares the lean blowoff limits

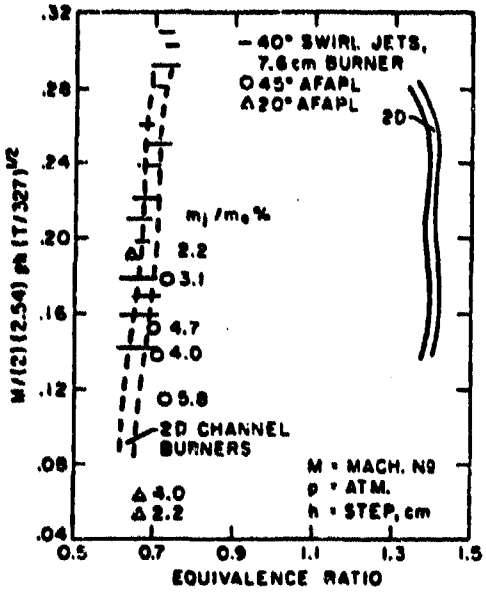

Figure 34. Comparison of lean blowoff data with jet systems
USC: m_j/m_a = 0.03, 40 deg swirl; AFAPL: 45 deg swirl

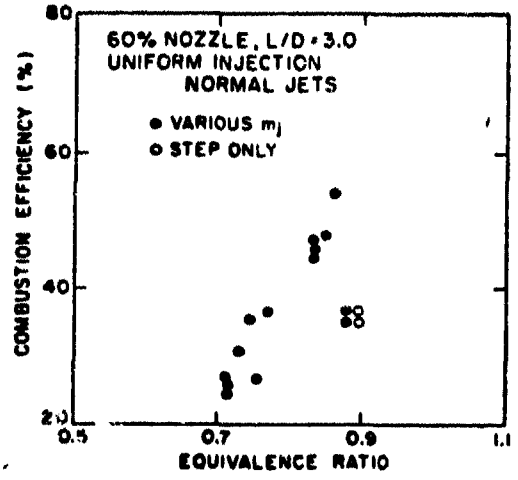

Figure 35. Combustion efficiency: 60% nozzle, uniform injection.
T = 556K, θ_j = 0 deg.

with both normal and swirl air jets. Since the inlet temperature in the AFAPL burners was rather high, quenching due to the jet air had a greater effect on the burner performance. The correlation of Fig. 33 and 34 shows that the lean blowoff performance of larger burners with choked nozzle can be predicted from the data of smaller laboratory scale burners at lower pressures and temperatures. This is true for the case of "premixed fuel injection." It was not possible to duplicate the condition of "wall injection" at USC. Therefore, flame blowoff with "wall injection" was not attempted at AFAPL during the course of this investigation.

Because of the low chamber pressure in the USC burner the nozzle was not choked and no attempt was made to measure the thrust. However, both thrust and combustion efficiency data were available for the AFAPL tests. At USC the improvement in burner performance with the jet system was ascertained in a qualitative manner from observation. The AFAPL tests showed quantitatively that the combustion efficiency can indeed increase for either the normal or the swirl jet system. Figures 35 and 36 show the variation of the combustion efficiency for a normal and a 45-deg swirl jet system. The fuel injection was "uniform" and the nozzle was large. With increasing jet momentum flux a large increase in combustion efficiency was observed particularly for relatively rich mixtures. For very lean mixtures the increase in combustion efficiency was not so spectacular. The chamber length to diameter ratio L/D for these and all of the tests conducted at AFAPL was 3. Generally, when larger nozzles ($A_{throat}/A_{chamber} = 0.6$) and "uniform" fuel injection (injection point 1.6 m upstream of the step) were used, the jet system helped increase the combustion efficiency. A combination of smaller nozzle (40%), leaner mixtures, and

"wall injection" (injection point 12 cm upstream of the step) can actually degrade the combustion efficiency when jet air is used. Figures 37 and 38 show such a trend when normal and swirl jets are used. Even though the cooling effect of the cold air jet was accounted for in the calculation of the equilibrium reaction temperature, its influence on the chemical kinetics was not considered in the calculation of the combustion efficiency. Also the effect of cold air jets on the evaporation rate of the droplets was not taken into account in calculating the equivalence ratio.

Figure 39 is a composite figure for the combustion efficiency of a burner with two different nozzles, gas jet system and "wall" and "uniform" injections. It shows the maximum value of combustion efficiency as a function of the swirl angle. The use of gas jets, even without the swirl, can increase the combustion efficiency of a dump burner with the larger nozzle. The performance can be further increased if, instead of using cold air, it is heated to the inlet condition. This would help eliminate the chemical and thermal penalties imposed upon the burner due to the quenching effect at regions of flame stabilization. Two extreme cases of fuel injection systems, equivalence ratios, and two nozzle sizes were used in Figure 39 to illustrate the ranges of combustion efficiency to be expected. In an actual case, the nozzle is not as small as 40% and the fuel injection is not as restrictive as "wall injection". Therefore, the data in Figures 37-39 show only the limiting behavior of the system. A realistic configuration is expected to have larger increases in combustion efficiences.

A series of tests with "wall injection" showed that the change in combustion efficiency with the gas jet system was sensitive to the mixture equivalence ratio for both the nozzles. For very lean mixtures the combustion efficiency was reduced with air jets for both nozzles. With air jets, the combustion efficiency increased when the equivalence ratio was between 0.7 and 0.9. The increase, however, was not as large with the smaller nozzle.

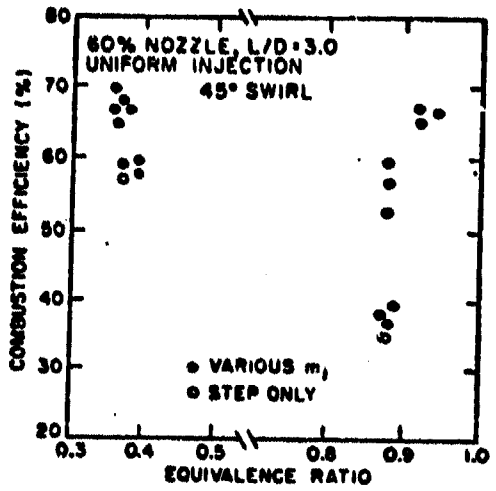

Figure 36. Combustion efficiency; 60% nozzle, uniform injection, T = 556 K, θ_j = 45° deg.

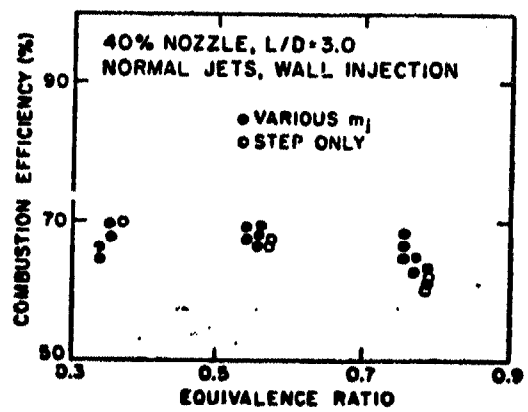

Figure 37. Combustion efficiency; 40% nozzle, wall injection, T = 556 K, θ_j = 0 deg.

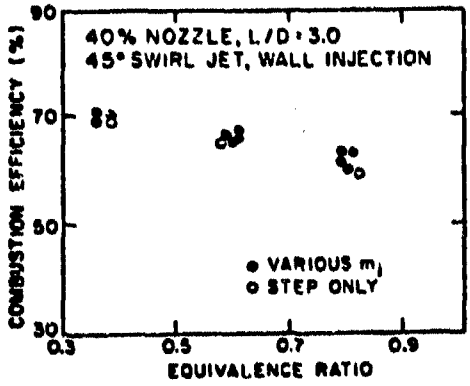

Figure 38. Combustion efficiency; 40% nozzle, wall injection, T= 556 K, θ_j = 45 deg.

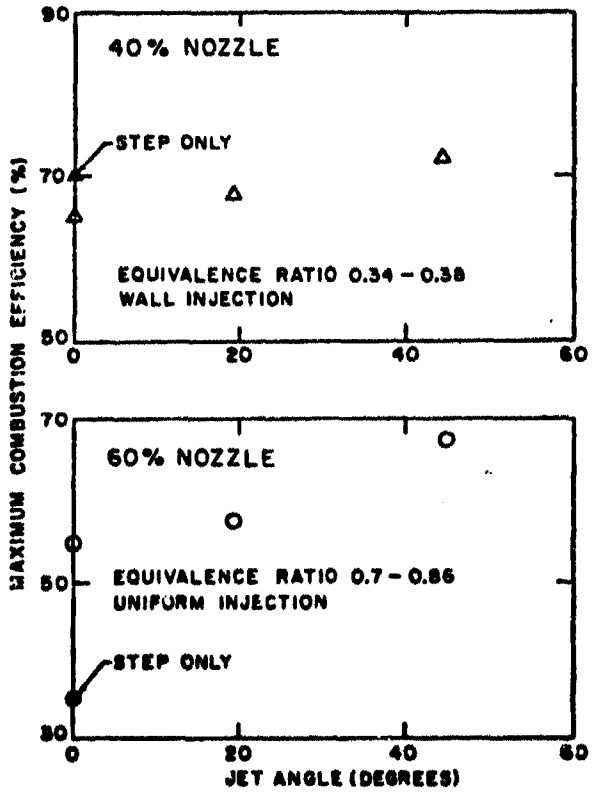

Figure 39. Maximum combustion efficiency vs swirl angle.

The overall effect of the gas jets on the flowfield is to increase the size of the recirculation zone. The amplification of the recirculation zone due to the interaction of the two flowfields is believed to be the primary cause of the increase in combustion efficiency.

Results of the two experimental programs show that:

1) Small scale tests at low temperature can be used to predict the blowoff performance of a larger burner operating in a more realistic environment. Thus, geometric scaling is possible for the case of uniform injection.

2) Swirl induced by gas jets is a convenient method of increasing the combustion efficiency of a burner.

3) Normal jets, even without the swirl, are able to increase the combustion efficiency.

4) A jet system with cold air can degrade the burner performance when lean mixtures and smaller nozzles are used.

4.3 Comparison of Airjets and Guide Vanes as Swirl Generators

The cooperative test program described in the previous section has shown that the fluid amplifier concept can be used in a realistic system for increasing combustion efficiency. Small gas jets in the dual role of vortex amplifier and swirl generator were found to be effective under certain operating conditions in increasing the combustion efficiency. It was also found that geometric scaling is possible when the combustible mixture is premixed. The beneficial effect of swirl generation and vortex amplification by gas jets has been adequately demonstrated for both the small laboratory scale and more realistic larger burners. The

increase in the size of the recirculation zone is the primary reason for the improvement of the burner performance[20]. Swirl can also be introduced in the flow field by means of mechanical guide vanes which are permanently located upstream of the dump plane. Because of the increase in flame spreading, the use of guide vanes can also increase the burning efficiency. Swirl induced by means of hub-mounted guide vanes show that the loss of stagnation pressure is higher with the guide vanes than with the airjets. Figure 40 is a sketch of the guide vanes whose angles were varied to obtain swirl numbers* characterizing a weak to moderate swirl intensity. For the case of a strong swirl (S = 0.67), the pressure loss was exorbitant and the burner was not operational.

Burning efficiencies were determined by measuring exhaust temperatures at three points whose radii correspond to one-third the area of the exit plane. These efficiences are qualitative at best and indicate the effectiveness of the flame spreading and do not include the effect of the pressure loss in the system. Thus, these are not the combustion efficiencies of a burner. Calculations from the temperature measurement indicate that both swirl generators, namely the guide vanes and the airjets, are fairly effective in spreading the flame. However, the pressure loss with the guide vanes is greater than that with the airjet system. Figure 41 compares the pressure loss in the system at various upstream velocities. Because of the design differences of the two systems, it was not possible to compare the swirl number defined in Figure 40. Comparisons are based upon approximately equal relative burning efficiencies determined

---

* See Figure 40 for the definition of the swirl number

by the ratio of the (actual temperature rise)/(ideal Temperature rise). The 20^{o} guide vanes are somewhat comparable to the 20^{o} swirl jets with a jet flow rate of around 3% of the primary flow. The pressure loss with the mechanical guide vanes is larger than that with the airjets. For comparison, the pressure drop in a dump combustor without any swirl is also shown in Figure 41 as a function of the upstream velocity.

Swirl Number S

$$S = \frac{\int_o^R Vr\rho u 2\pi r dr}{R \int_o^R \rho u^2 2\pi r dr}$$

R = DUCT RADIUS: V = TANGENTIAL VELOCITY: u = AXIAL VELOCITY

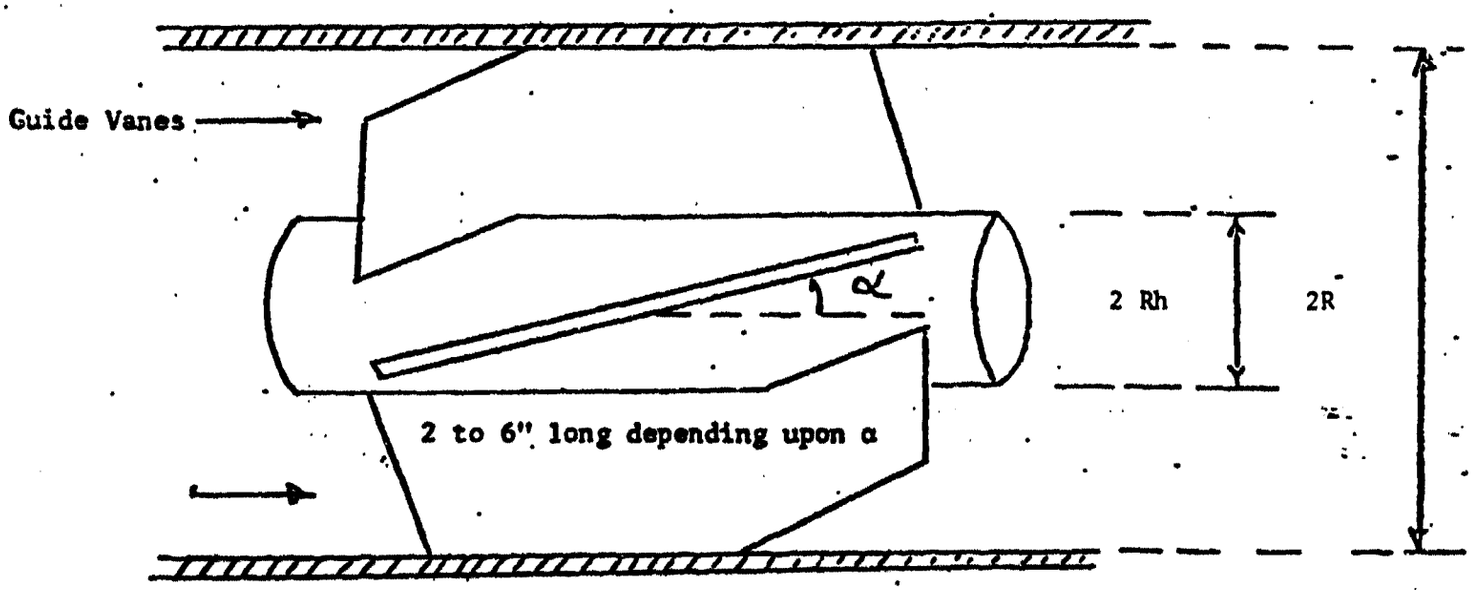

Swirl Number, S = 2/3 tan α when $R_h \to 0$

S < 0.4 WEAK SWIRL; S >0.6 STRONG SWIRL

Figure 40. Sketches of a typical swirl jet and typical hubmounted guide vanes.

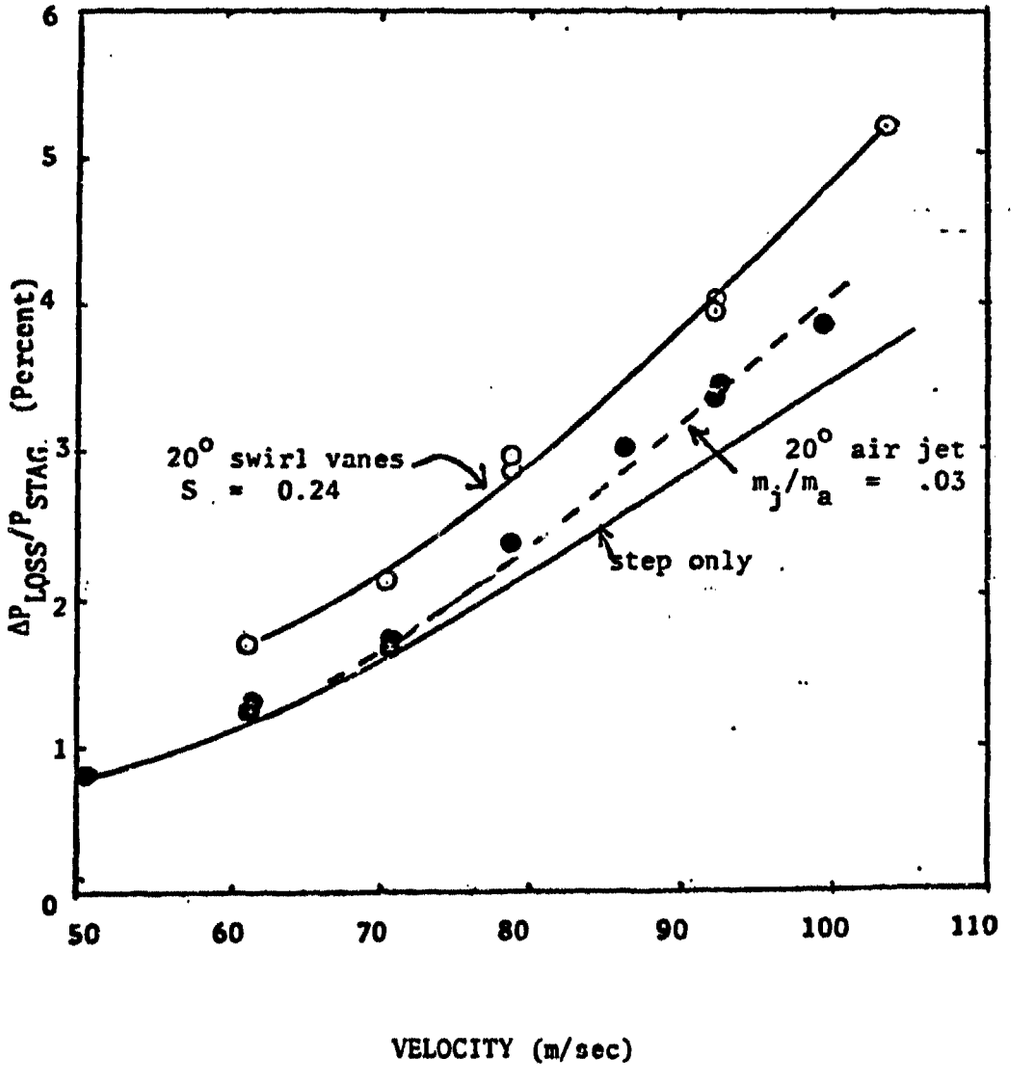

Figure 41. Pressure loss induced by two swirl generators of approximately equal performance.

Figure 42 shows that the lean blowoff performance of these two swirl generators is very similar. No rich blowoff was attempted during this phase of the program. Earlier data points are shown for comparison.

Even though both swirl generators appear to be similar in many respects because of the low pressure drop and versatility of operation, swirl jets are preferable.

4.4 Side dump gas generator combustor:

Unlike the usual dump combustor concept, where the main flow of the propulsion system is in the axial direction, in a side dump combustor the flow enters the combustion chamber from the side through multiple inlets. In these combustors the dump plan is the plane of the inlets and no other geometric sudden expansion is necessary for flame stabilization. In one of the concepts of a side dump combustor, gaseous fuel-rich exhaust from a gas generator serves as fuel and is injected at the head of the combustion chamber.

Side dump ramjets are being investigated both in this country and abroad as possible candidates for light weight, compact and efficient propulsion systems. Although most of these studies appear in the classified literature, results of many unclassified theoretical and experimental investigations are available in the open literature. Reference 25, for example, discusses design variables and applications of various ramjet and ramrocket concepts. Reference 26 is an analytical and experimental study of the flow field of a multiple inlet side dump combustor. Interaction of vortices induced by the multiple inlets in a small laboratory burner has been reported in Reference 27. Reference 28 discussed selected cold flow studies of the flow field of a side dump combustor with gas injection at the head.

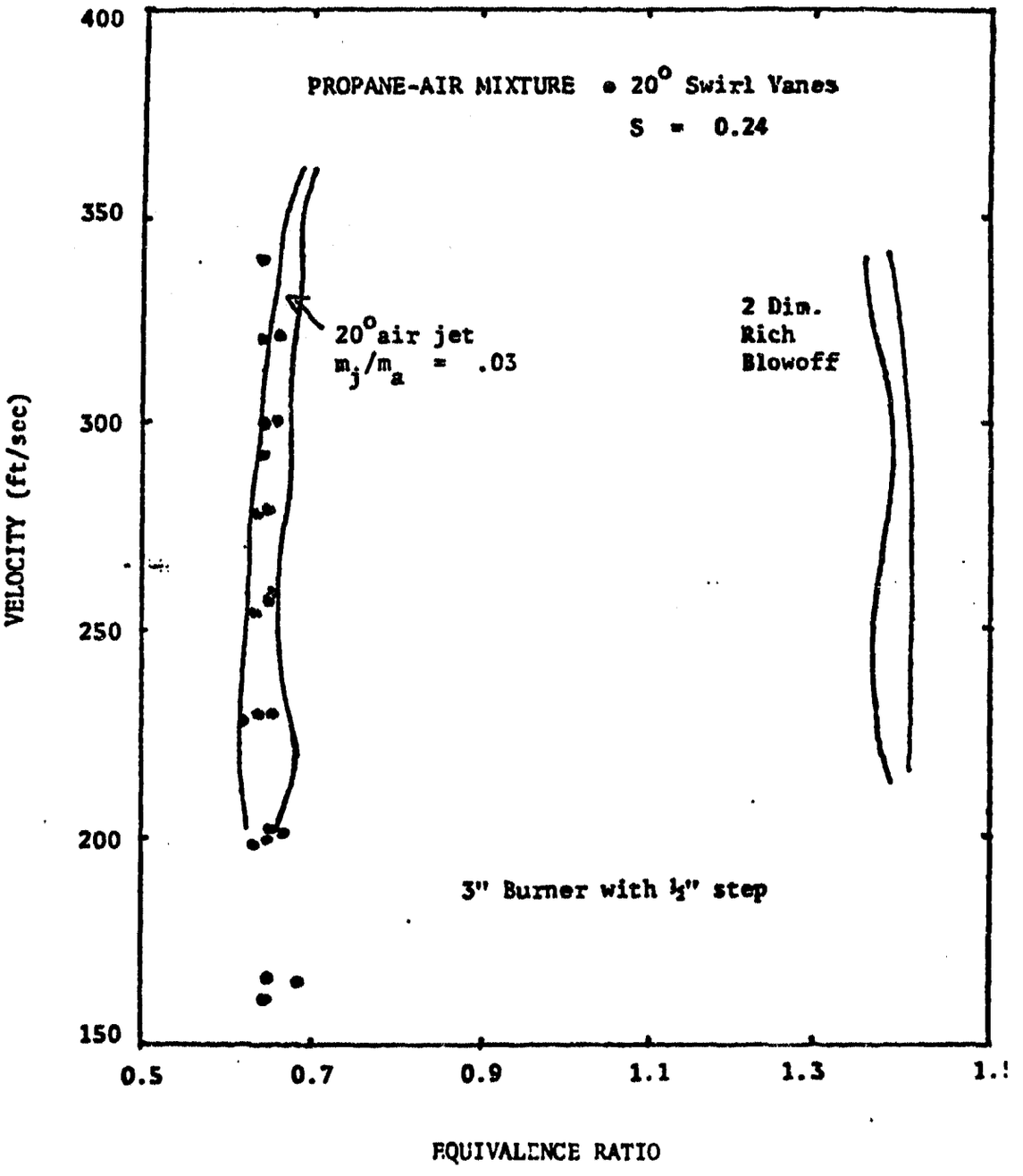

Figure 42. A comparison of flame blowoff performance of two swirl generators.

The present section describes an experimental study of the characteristics of a small laboratory scale side dump combustor with four inlets. The study includes the behavior of the burner as different system parameters are varied and recirculation zones perturbed. In addition, the effect of swirl (by canting and inlets) on the burner performance has been investigated. The results show that unless the vortices interact in an appropriate manner, the burner performance can degrade substantially.

An 38.9 mm diameter burner with four 31.8 mm diameter inlets equally spaced around the circumference was used. Rich propane-air mixtures at room temperature and pressures between 2 and 4.5 atm. and equivalence ratios between the range of 12 and 28 were used for simulating the fuel-rich exhaust of a gas generator. The air supply for the primary flow was approximately at 1 atm. and 330 K. It was possible to obtain inlet air velocities in excess of 150 m/s. Figure 43 is a sketch of the burner. Its design permitted one to change the inlet flow angle θ, the distance L from the inlet section to the head of the combustor and the injection pattern of the gaseous fuel at the head of the combustor. It was also possible to introduce swirl in the flow by canting the inlets as shown in the end view of Fig. 43. Swirl introduced in this manner does not require any add-on mechanical devices such as guide vanes and is expected to cause a relatively smaller pressure loss in the system.

Plastic models of several smaller axisymmetric and channel side dump burners were utilized for studying the vortex patterns qualitatively under cold flow conditions. These preliminary qualitative studies proved invaluable in the design, construction and the operation of the actual burner shown in

Fig. 43. Projections of the system of vortices at the inlet section and at the head of the combustor are shown. The vortices at the head are affected by swirl, the length L, flow angle and pattern of fuel injection at the head. Vortices at the inlet are also affected by the inlet angle and swirl. However, they appear to be too weak to strongly influence the operation of the burner.

In addition to the fuel injection at the head, fuel could be injected independently in the inlet pipe and the recirculation zones downstream of the inlet. Injection points are shown in Fig. 43 by means of arrows. A streamlined ring was inserted in the burner to interfere with the recirculation zones and reduce their size. This was done to ascertain if rough burning can be induced in a side dump burner in this manner. It was possible to induce rough burning by this means in a channel burner.[19]

mples of exhaust gases from three points were analyzed in a Hewlett-Packard 5730A Gas Chromatograph and a Hewlett-Packard 3390A Integrator. Sampling points were changed from run to run to determine if any unburned fuel remained in the exhaust. Similarly, the exhaust temperature at three points in the exhaust plane were measured by means of Platinum Rohdium thermocouples.

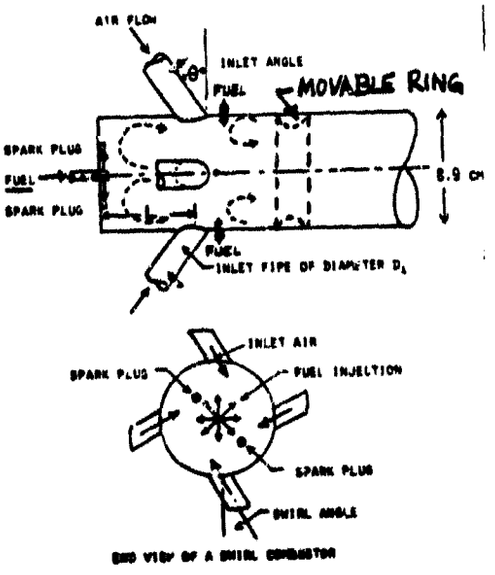

Figure 42. Sketch of a side dump burner with four inlets.

Table 3 summarizes the range of variables considered in this study.

TABLE 3

VARIABLE	RANGE
. Inlet Velocity	up to 150 m/s
. Equivalence ratio of fuel mixture	12 to 28
. Fuel injection pressure	2 to 4.5 atm
. Inlet angle	20, 45 degrees from vertical
. Swirl angle	0, 20, 45 degrees from radial direction
. Distance to head L/D_i	0.6 to 4.0

Flow visualization by means of traces of soap solution on the wall shows that for a given L, the system of vortices at the head is very stable and more or less qualitatively unaffected by the changes of flow angle. Further tests show that the system of vortices at the head can be virtually destroyed by means of gas injection in the axial direction at the head. This behavior was substantiated in the actual burner where the axial injection of fuel at the head caused erratic flame stabilization and narrower flame blowoff limits. Therefore, for all the tests, fuel was injected radially so as to strengthen the system of vortices at the head (Fig. 4.[illegible]). The recirculation zone at the head due to these vortices is crucial to the stable operation of the combustor. Since the fuel was added directly to the recirculation zone, only a small amount of fuel was necessary to stabilize the flame.

The size and the strength of the recirculation zone at the head, for a given operating condition, is a function of the length to the head L, swirl and finally the injection pattern of the fuel. Figure 44 shows the effect of changing L on the flame blowoff equivalence ratio at an inlet velocity of 100 m/s. Although the overall equivalence ratios of Figure 44 indicate a lean mixture, locally at the head the mixture is very rich. These blowoff limits are then the rich blowoff limits for the "flame holder" at the head. Satisfactory operation of the burner was possible with a very small overall equivalence ratio. The overall equivalence ratio at the lean blowoff was so small that it could not be measured very accurately. Figure 44 shows that at an inlet velocity of 100 m/s without any swirl the best flame blowoff performance (i.e., the widest limits) is obtained when L/D is 1.6 (D_i = inlet diameter). For both the smaller and the larger values of L/D, a degradation in the blowoff performance is evident. For smaller values of L/D, the size of the recirculation zone is too small and for larger values, possibly the strength of the vortex is reduced thereby adversely affecting the burner performance. The inlet flow angle θ does not have any influence on the vortex system at the head of the present burner. Flame blowoff data for both θ = 20 and 45 degrees are identical within the range of data scatter. Fuel injection pressure and the equivalence ratio of fuel mixture within the range shown in Table 3 had no influence on the flame blowoff. Although an inlet velocity of 100 m/s was used as an example in Fig. 44, a similar trend is observed at other inlet velocities.

When swirl is introduced in the flow field by canting the inlets (Fig. 43), the pressure at the axis of the burner at the dump plane is reduced. The degree of reduction in the pressure depends upon the swirl angle (more precisely on the swirl number). This local low pressure region at the axis tends to induce an

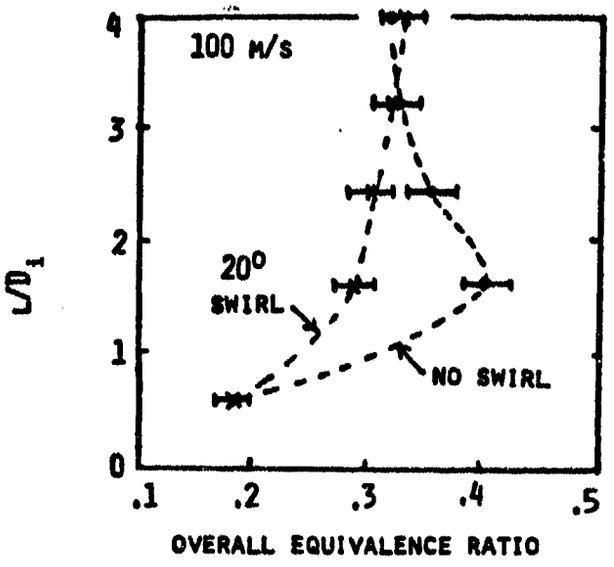

Figure 44. Rich blowoff limits as a function of the length to head L with and without swirl. Inlet velocity = 100 m/s.

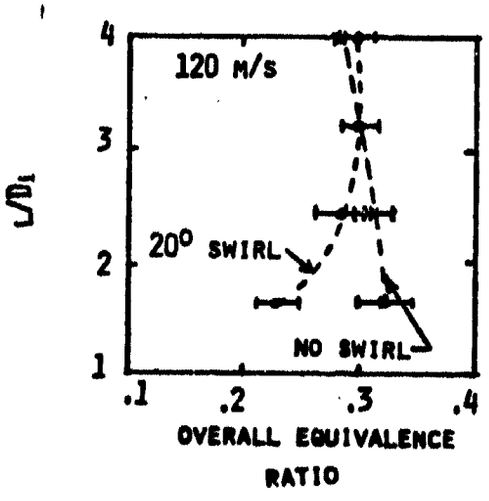

Figure 45. Rich blowoff limits as a function of the length to head L with and without swirl. Inlet velocity = 120 m/s.

opposing flow from the head toward the dump plane thereby weakening the system of vortices at the head. The net effect of the weakened system of vortices for a 20 degree swirl is shown in Fig. 44. The adverse effect of the swirl can be overcome by increasing the length L. Unlike many other combustors, introduction of swirl by canting the inlets of a side dump combustor will require a burner of larger characteristic length for wider flame blowoff limits. The characteristic length of the system can be reduced effectively by eliminating swirl. When the swirl angle was increased to 45 degrees, it was not possible to stabilize any flame until an L/D_i value of 3.2 was reached. Even then the flame could not be stabilized beyond an inlet velocity of around 30 m/s. Figure 45 shows the effect of swirl on L at an inlet velocity of 120 m/s. For satisfactory operation of a side dump burner with swirl a larger characteristic length is required. Therefore, for small, compact burners, introduction of swirl by canting the inlets is completely unnecessary. Figure 46 shows a typical rich flame blowoff data with and without swirl by canted inlets.

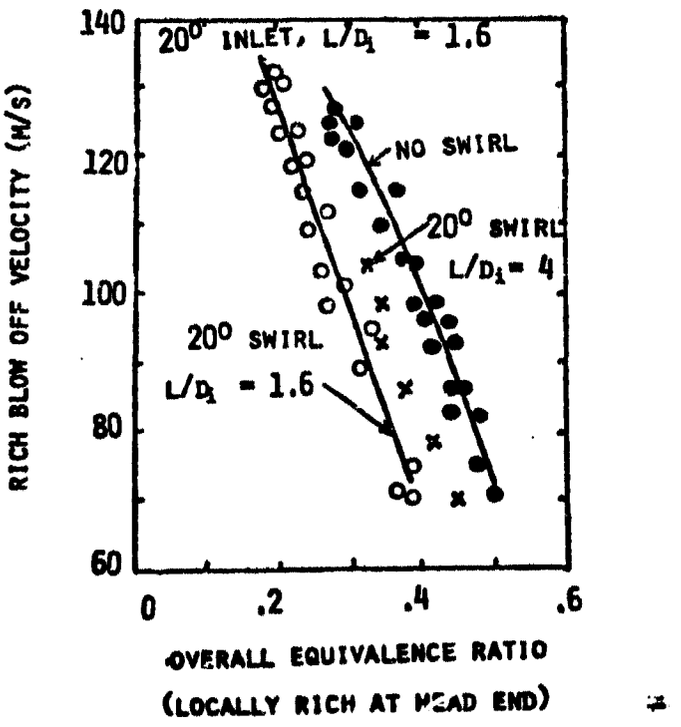

Figure 46. Typical rich blowoff velocities. Injection pressure 2 to 4.5 atm. Injection equivalence ratio 12 to 28. Stabilization is not possible for 45° swirl at $L/D_i = 1.6$.

As indicated earlier, the vortex system at the head and not the secondary vortices at the dump plane is primarily responsible for flame holding. Therefore, only a small amount of fuel is necessary for stable operation of the burner. This is evidenced by the rich flame blowoff at rather low values of the overall equivalence ratios of Figs. 44, 45, and 46. Earlier work on the effect of gas injection in the recirculation zone corroborates the present observation.[29] Because of the low overall equivalence ratio, the exhaust gases are relatively cool and no flame is visible. Analysis of the exhaust gases at various positions showed that the combustion was complete and no unburned fuel or CO left in the exhaust. Depending upon the operating equivalence ratio, the measured exhaust temperatures range from 500 to 900°C. These values for most cases, were within 5% of the calculated values. The deviation between the measured and calculated value for the worst case was within 10%. The exhaust temperature and composition were not affected significantly either by swirl or the change in length L. The variations were well within the scatter of the experimental data. Satisfactory operation at low temperatures and consequent absence of unburned hydrocarbons and visible signature in the exhaust can have important military application.

Rich flame blowoff at low values of overall equivalence ratios indicates that only a small amount of energy can be added to the system with fuel injection at the head. In order to make the burner more versatile, fuel should also be injected in the inlets. Experiments with fuel injection at multiple points in the inlet show that the recirculation zones immediately downstream of the inlets (Fig. 43) are rather weak. It was not possible to operate the burner by only injecting fuel directly in these zones. As long as the head vortex acted as a pilot flame, multiple injection in the inlets was very effective. However,

flame blowoff resulted as soon as the fuel injection at the head was discontinued. Therefore, for a versatile system it will be necessary to keep the "pilot" flame at the head operating all the time and additional fuel can be injected in the inlets when needed.

A streamlined ring (Fig. 43) was inserted in the burner to perturb the secondary vortices and determine their influence on the system of vortices at the head. Size of the secondary vortices had no perceptible influence on the blowoff limits of the burner in all cases except when the ring acted as a flame holder downstream of the dump plane. With the ring acting as a flame holder, fuel injection at the head (i.e., the "pilot" flame at the head) was no longer necessary. Perturbation of the secondary vortices did not result into rough burning in a side dump burner. Also a simulated angle of attack flight by decreasing the flow rates through two inlets did not have any perceptible effect on the stable behavior of the system vortices at the head.

The important observations from the study of a side dump combustor can be summarized in the following manner:

1. The system of vortices at the head is crucial to the stable operation of the burner,

2. Anything that tends to weaken the recirculation zone at the head (e.g., swirl and axial fuel injection) should be avoided.

3. Radial fuel injection with swirl at the head plane will give rise to a region of low pressure at the head and will help strengthen the recirculation zone there.

4. The "pilot flame" at the head is very stable and operates satisfactorily independently of the perturbation of the vortex system downstream of the dump plane.

5. The low temperature exhaust without any CO, unburned hydrocarbons and visible signature can have important implications in a variety of applications.

6. A side dump burner of small characteristic length without the use of swirl is possible.

Although the stagnation pressure and temperature of the burner used in this study are near atmospheric and the flow is not choked in the exhaust nozzle, the behavior of the system of vortices is not expected to change significantly in an actual operating system with a choked nozzle.[30]

5 COMBUSTION INSTABILITY

5.1 Introduction

Dump combustors have been plagued with unwanted pressure oscillations which are induced by the pressure fluctuations in the inlet. In order to understand the coupling between the inlet pressure perturbation and combustor pressure oscillations a JANNAF workshop had been proposed (Ref. 31) to look for avenues of understanding and the possibility of eliminating the problem.

The flow transients in the inlets of dump combustors which are responsible for pressure oscillation and rough burning are being investigated. Special emphasis is placed upon the spectral character and amplitude of the input disturbance which induces combustion instability in a dump combustor. Pressure oscillation in the inlet of a dump combustor has been introduced by mechanical means. This allows one to study the conditions under which the inlet pressure oscillations are amplified by the chemical reaction in the combustion chamber. Once the combination of frequency, amplitude phase angle and waveform leading to combustion pressure oscillation has been identified, the method of vortex control will be applied to smooth out rough burning. Preliminary study with pulsing pressure in the inlet shows the feasibility of drastically reducing rough burning in a combustor by this technique. A novel concept of a feedback loop is presently under investigation which could, in principle, significantly reduce the possibility of combustion instability induced by the pressure fluctuation in the inlet.

5.2 Preliminary observation and results:

In order to try to understand the coupling between the inlet pressure pulsation and combustion instability, a flow pulsing device has been designed and incorporated with a two-dimensional channel burner (Figure 47). The channel burner with glass sides allows visual observation of the dump plane and the behavior of the shear layer under pulsing conditions. Air jets are incorporated upstream of the dump plane to change the characteristics of the shear layer which is about to become unstable. The flow pulsing device consists of a rotating cap with holes. When the holes of the cap line up with the holes in the bypass line the pressure drops. When the holes are covered up the pressure rises. The frequency of oscillation can be changed by changing the speed of rotation and the number of holes in the cap. The amplitude of pressure oscillation is changed by the valve upstream of the cap (Figure 47). The amplitude and frequency of pressure pulsation are measured by means of a pressure transducer and a single channel Hewlett-Packard frequency analyzer.

Figure 48 shows the amplitude-frequency characteristics in the combustion chamber under cold flow conditions when a cap with 4 holes are used. Figure 49 shows a similar plot when a cap with 8 holes are used. Resonances for the chamber under cold flow conditions are clearly seen in these two plots. Resonance allows a larger pressure amplitude to be imposed on the system and the corresponding frequency can be changed simply by changing the characteristic length of the bypass section shown in Fig. 47. Figure 50 is a composite plot of Figures 48 and 49. It also shows the possible threshold where the combustion oscillation is so severe that flame actually blows off. The spectral content of the pressure oscillations are shown in the figure. One can expect a much higher amplitude due to magnification caused by a coupling between the inlet oscillation

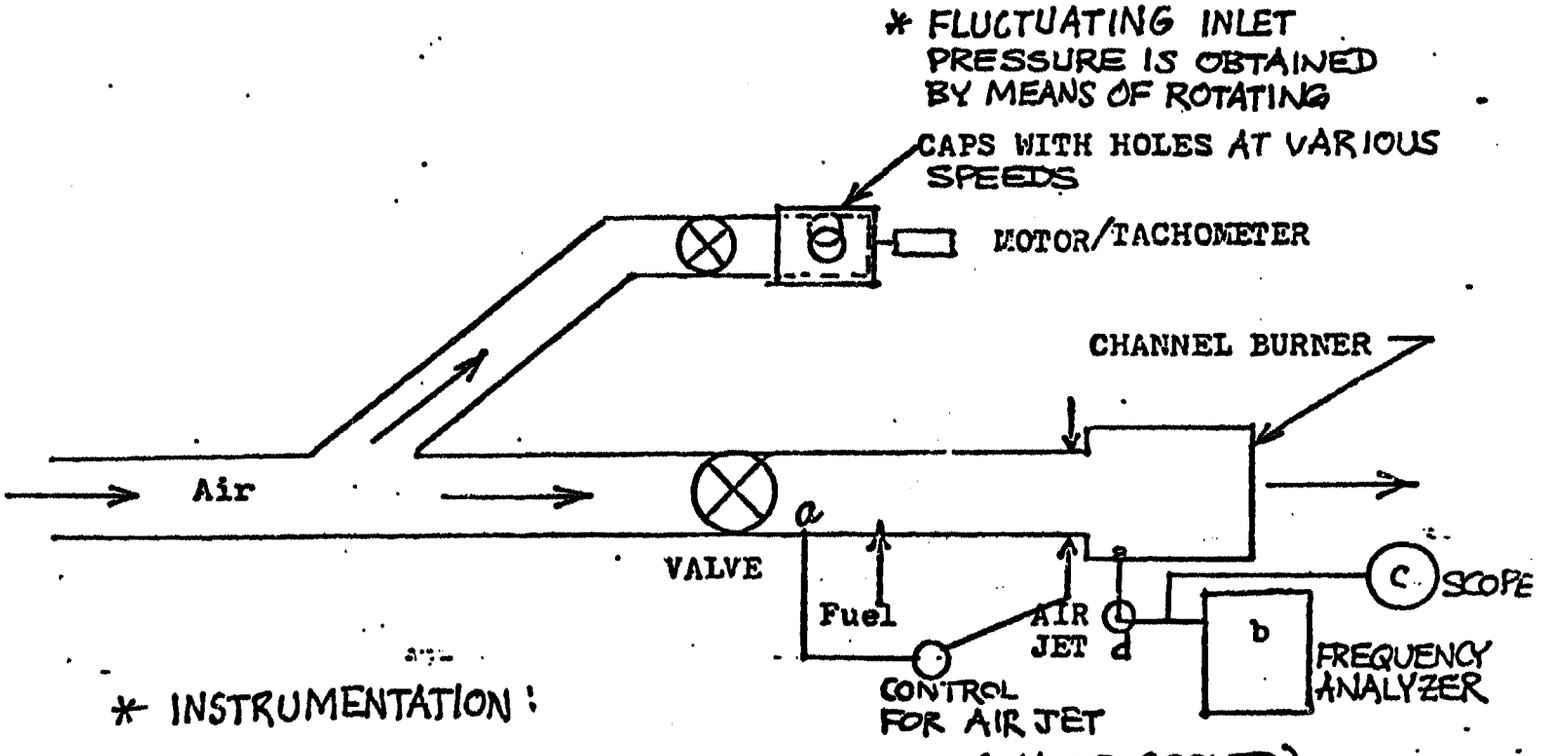

Figure 47. Sketch of flow pulsing device in a channel burner.

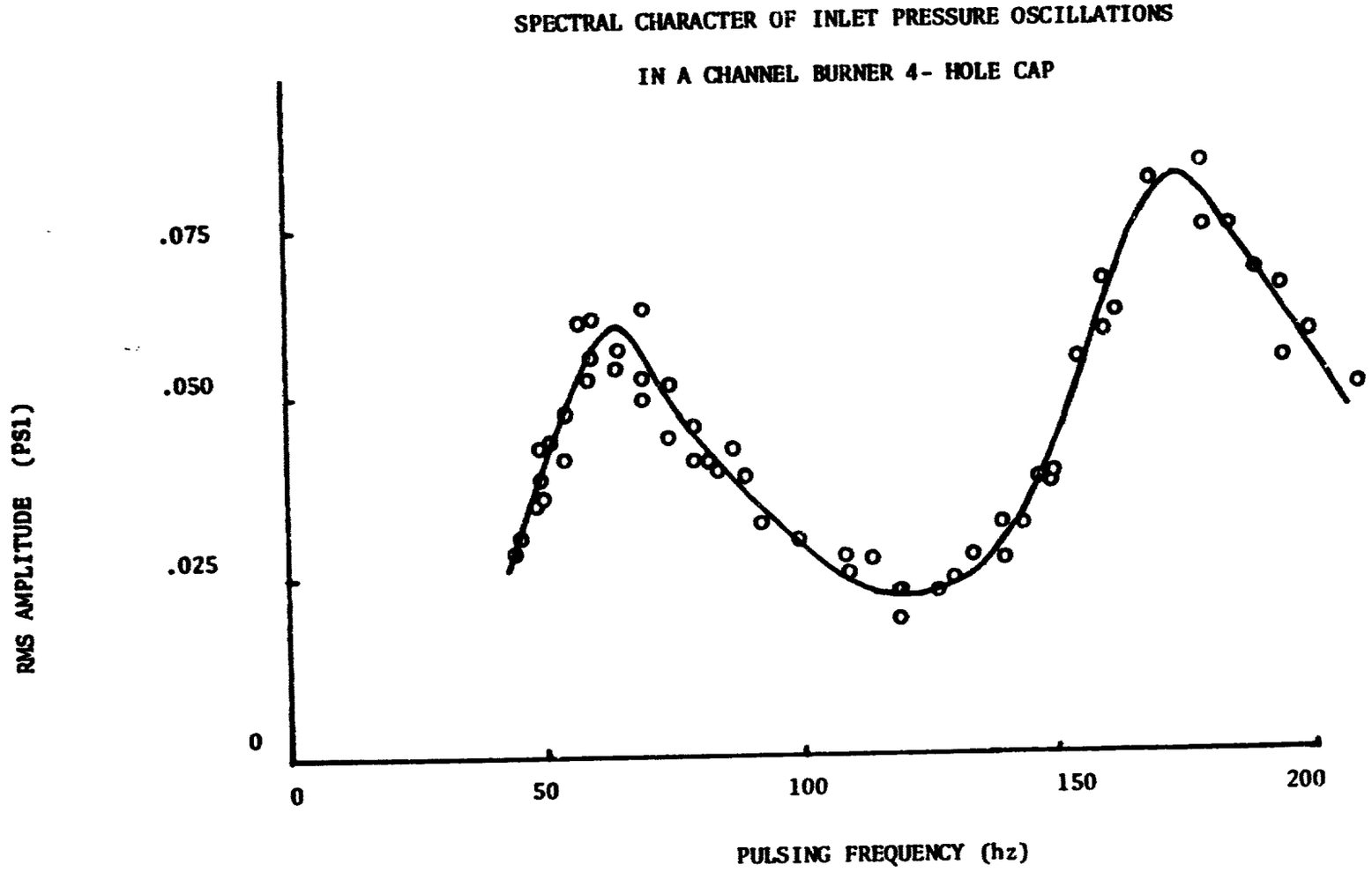

Figure 48. Amplitude-frequency characteristics with a 4-hole cap.

SPECTRAL CHARACTER OF INLET PRESSURE OSCILLATIONS IN A CHANNEL BURNER 8-HOLE CAP

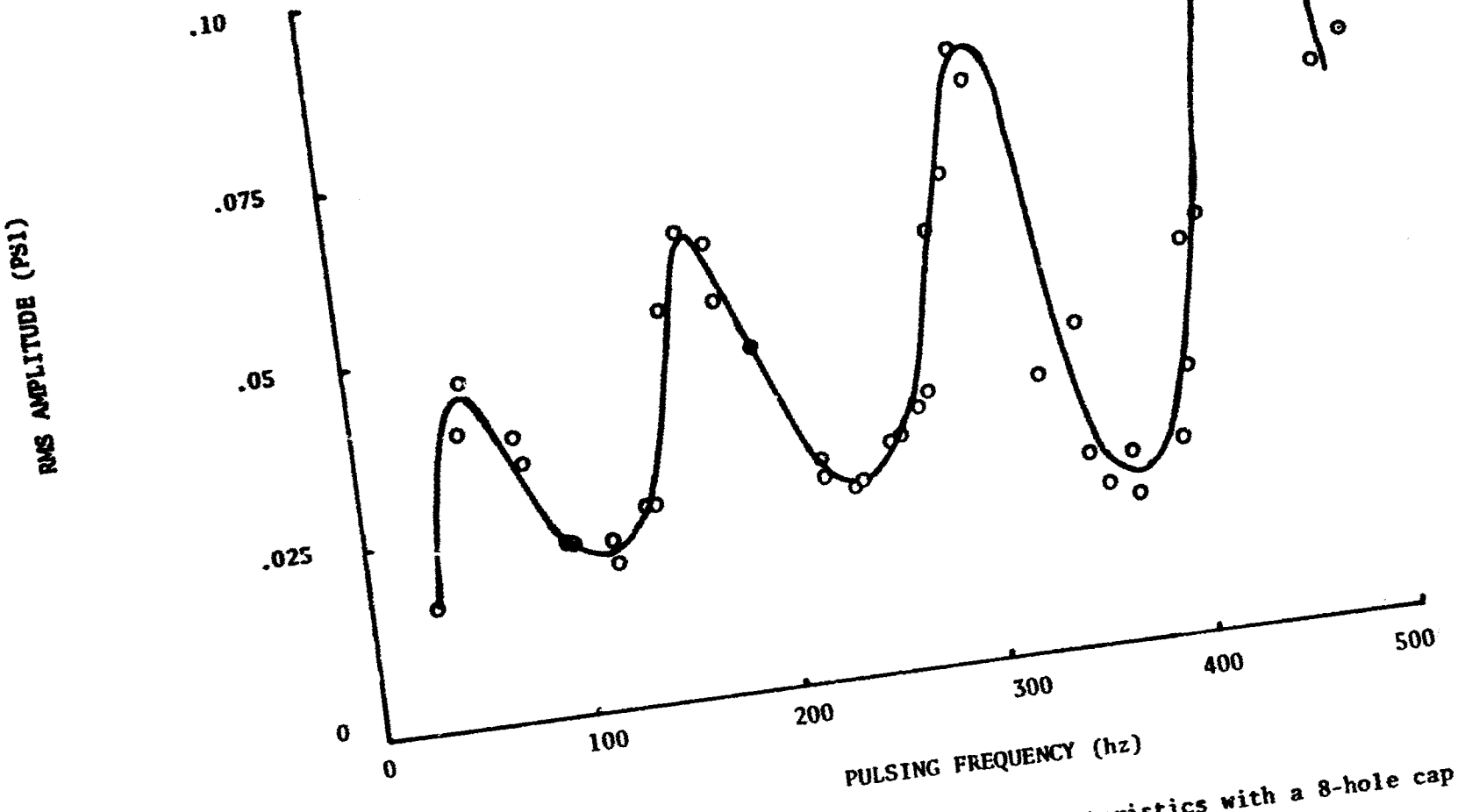

Figure 49. Amplitude-frequency characteristics with a 8-hole cap.

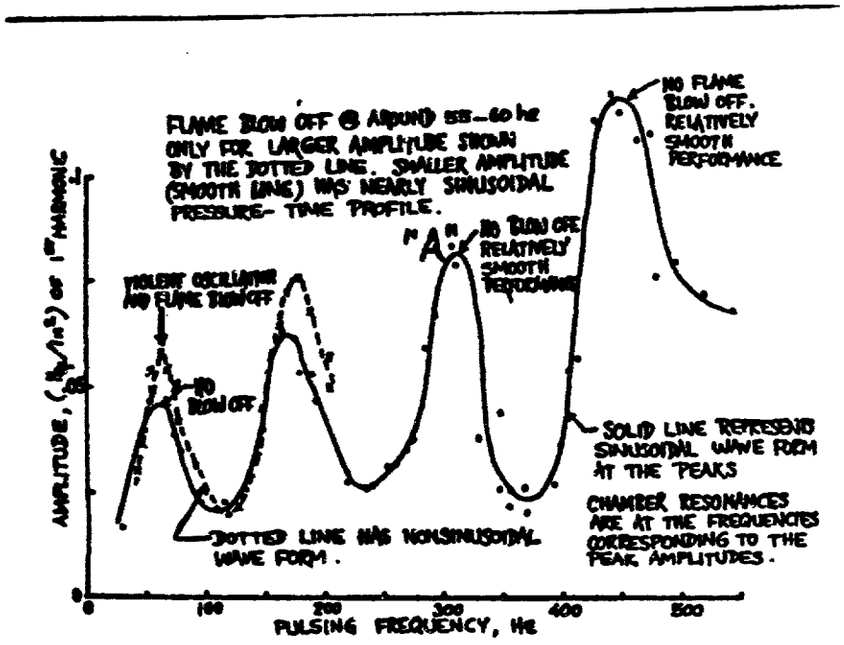

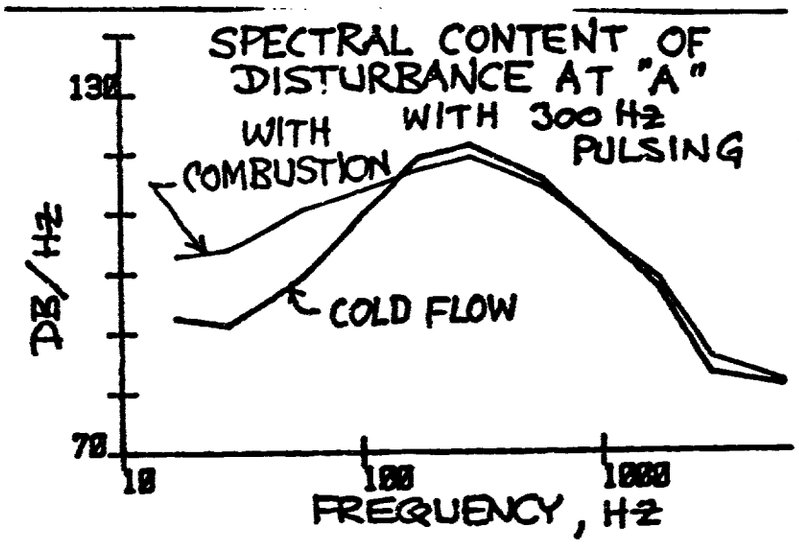

- DISTURBANCE IS NOT AMPLIFIED BY THE FLAME TO INDUCE COMBUSTION INSTABILITY

Figure 50. Amplitude-Frequency Characteristics and Spectral Distribution of Pressure Oscillation

and combustion. Preliminary observation indicates that a combination of frequency, amplitude phase angle and wave form is responsible for combustion instability. Once the cause-effect relationship including the phase angles are known, it will be possible to suggest a feedback loop to negate the effect of inlet pressure oscillation on the combustion chamber. In the case of a channel burner the control system will actuate the air jets and pulse them with a proper combination of phase, frequency and momentum flex to negate the effect of inlet pressure oscillations. Experiments have shown that the air jets are able to change the shear layer characteristics and smooth out rough burning (Ref.19). The air jets seem to smooth out rough burning even with pressure oscillation in the inlet. Figure 51 shows the concept for a side dump combustor. As soon as the sensor in the inlet detects the critical combination of wave form, frequency and amplitude, the control system will pulse the gas generator flow to counteract the induced oscillation of the recirculation zone at the head.

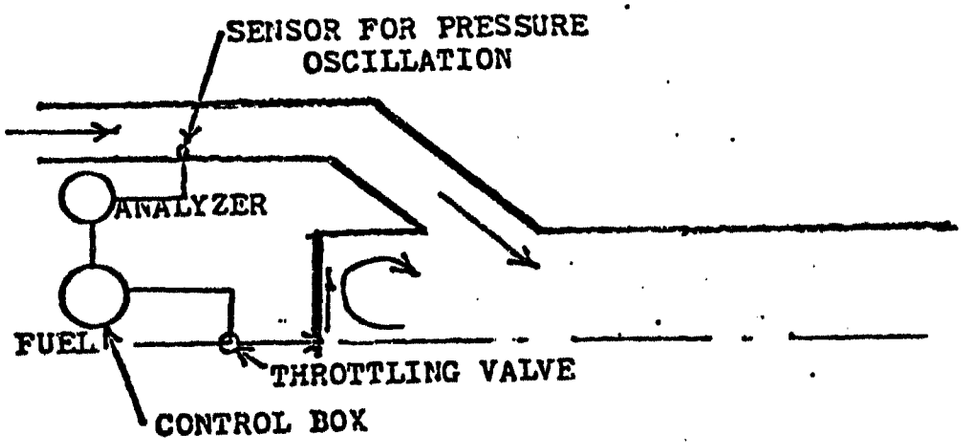

Figure 51 . Sketch of a Feedback System for Decreating Combustion Oscillations in a Side Dump Combustor.

Since the flow field and the problem of vortex interaction are more complex in a side dump burner (Ref. 32), experiments with inlet pressure perturbation will continue with such a burner immediately after the experiments with channel burner are concluded. Unlike the case of a channel burner the feedback control system here will pulse the recirculation zone at the head.

5.3 Future work on combustion instability

Experiments will be continued to understand the coupling between the input amplitude, frequency and the waveform leading to combustion oscillation. Attempts will be made to determine the phase relationship between the input pressure pulse and the combustion pressure oscillation. Pressure transducers will be placed at several points in the combustion chamber and the inlet duct to determine the correlation between the input disturbance and the chamber pressure oscillations. A DEC LSI 11/23 computer system will facilitate data acquisition and reduction. Also a D to A converter will be used for the control system described earlier.

A one-dimensional unsteady model of the combustor with a pulsing reacting flow is being developed to explain the mechanism by which the input pressure oscillations are damped (or magnified) in the combustion zone. Also a computer program is developed for predicting the flow field so that the effect of the combustor variables on the head vortex can be predicted.

REFERENCES

1. Farhangi, Shahram, "Evaporation of Fuel Drops on a Hot Surface Considering Liquid Phase Decomposition," Ph.D. Dissertation, June 1979, Mechanical Engineering Department, University of Southern California, Los Angeles.

2. Shapiro, A.H. and Erickson, A.J., "On the Changing Size Spectrum of Particle Clouds Undergoing Evaporation, Combustion or Acceleration". Transactions of ASME, Vol. 79, 1957, pp. 775-788.

3. Hildebrand, F.B., "Advanced Calculus for Engineers", Prentice-Hall, Inc., New York.

4. Hottel, H.C., Williams, G.C., and Simpson, H.C., "Combustion of Droplets of Heavy Liquid Fuels," 5th Symposium on Combustion, Reinhold Publishing Co., New York, pp. 101-129 (1955).

5. Benson, S. and Nangia, P., "Some Unresolved Problems in Oxidation and Combustion," Accts. Chem. Res. 12, 223 (1977)

6. Wasserman, A., "Diels-Alder Reactions," Elsevier Publishing Co., (1965).

7. Kanury, A.M., "Introduction to Combustion Phenomena," Gordon and Breach Science Publishers, New York, p. 209 (1975).

8. Lefebvre, Arthur H., "Airblast Atomization," Prog. Energy Combst. Sci, Vol. 6 pp. 233-261, (Fig. 34). Pergamon Press, 1980.

9. Carnahan, B., Luther, H.A., and Wilkes, J., "Applied Numerical Methods," John Wiley and Sons, 1969,

10. Obert, E.F., "Internal Combustion Engines and Air Pollution," Intext Educational Publishers, New York, 1968.

11. Mansour, M., "The Vaporization Behavior of a Fuel Drop on a Hot Surface," Ph.D. Dissertation, University of Southern California, Los Angeles, June 1977.

12. Gerstein, M. and Choudhury, P.Roy, "Liquid Phase Decomposition: A Possible Problem with Fuels in High Pressure Systems," Proceedings of the 1980 Heat Transfer and Fluid Mechanics Institute, Stanford University Press, pp. 79-91.

13. Blazowski, W.S., and Rigano, D.C., "Carbon Slurry Fuel Combustion," Abstract of the 1979 AFOSR Contractors Meeting on Air-Breathing Combustion Dynamics and Kinetics, Alexandria, Va, 28 January 1980 - 1 February 1980, AFOSR TR 12 1173, pp. 94-102.

14. Bopp, A.F., and McCoy, J.R., "Combustion Phenomena Associated with Advanced Fuels for Volume Limited Propulsion Systems", Abstract of the 1979 AFOSR Contractors Meeting, p 113.

15. Reese, B.A., and Carbone, H.M., "General Results of Combustion of Slurry Fuels in a Sudden Dump Ramjet Combustor", Air Breathing Missile Fuels Specialists Session Papers, Chemical Propulsion Information Agency Publication 254, August 1974.

16. Clewell, H.J., and Martone, J.A., "Air Force Supported Research Program and Needs Associated with Gas Turbine Engine Emissions and other Combustion Related Problems", Abstract of the 1979 AFOSR Contractors Meeting, pp. 94-102.

17. Miyasaka, K. and Law, C.K., "Combustion and Agglomeration of Coal-Oil Mixtures in Furnace Environments, Combustion Science and Technology, Vol. 24, 1980, pp 71-82.

18. Stull, F.D., Craig, R.R., and Hojnacki, J.T., "Dump Combustor Parametric Investigation," Fluid Mechanics of Combustion, Joint Fluids Engineering and CSME Conference, Montreal, Quebec, May 13-15, 1974, pp. 135-154.

19. Choudhury, P.R. and Lobell, M., "Experimental Investigation of Rough Burning in a Dump Combustor of a Small Volume," Progress in Aeronautics and Astronautics: Turbulent Combustion, Vol. 58, edited by L.A. Kennedy, AIAA, New York, 1978, pp. 471-483.

20. Choudhury, P.R. Lobell, M., Yep, F., and Chunn, T. "Feasibility of a Smooth Burning, Volume Limited Dump Combustor," Chemical Propulsion Information Agency Publ. 281, Vol III, Dec. 1976.

21. Choudhury, P.R. and Lobell, M., "Status of the Modified Dump Combustor - A Variable Strength Flame Holder," Chemical Propulsion Information Agency Publ. 280, Oct. 1976, pp. 423-433.

22. Choudhury, P.R. and Negarestani, M., "Novel Combustor Concept with Variable Strength Swirl Induced by Gas Jets," Chemical Propulsion Information Agency Publ. 297, Vol. III, Feb. 1979, pp. 367-380.

23. Choudhury, P.R. and Reeves, R.L., "Geometric Scaling of Sudden Expansion Burners with Air Jets Upstream of the Dump Plane," Chemical Propulsion Information Agency Publ. 292, Vol. II, Dec. 1977, pp. 421-432.

24. Longwell, J.P. Frost, E.E., and Weiss, M.A., "Flame Stability in Bluff Body Recirculation Zones," Industrial and Engineering Chemistry, Vol. 45, Aug. 1953, pp. 1629-1633.

25. Kramer, P.A., and Benkmann, P., "Design Considerations and Analytical Comparison of Different Types of Ramjets and Ramrockets", 58th AGARD Symposium on Propulsion and Energetics Panel, London, October 1981.

26. Krohn, E.O., and Triesch, K., "Multiple Intakes for Ramrockets", 58th AGARD Symposium on Propulsion and Energetics Panel, London, October 1981.

27. Choudhury, P.Roy, "Experiments on Multiple Vortices in a Side Dump gas Generator Ramjet", 17th JANNAF Combustion Meeting, NASA Langley, VA, Sept. 1980. Chemical Propulsion Information Agency Publication 329, Vol. 1, Nov. 1980.

28. Boray, R.S., "Flow Field Studies of Ducted Rockets", 17th JANNAF Combustion Meeting, NASA Langley, VA, Sept. 1980. Chemical Propulsion Information Agency Publication 329, Vol. 1, Vol. III, Nov. 1980, pp. 585-604.

29. Fetting, F., Choudhury, A.P.R., and Wilhelm, R.H., "Turbulent Flame Blowoff Stability, Effect of Auxilliary Gas Addition into Separation Zone", Seventh International Symposium on Combustion, Explosion, etc. Buttersworth Scientific Publications, 1959, pp. 621-635.

30. Choudhury, P.Roy, "Scaling and Performance of Dump Combustors with Transverse Gas Jets", AIAA Journal, Vol. 18, April 1980, pp. 450-454.

31. Culick, F.E.C., "Report of the JANNAF Workshop on Pressure Oscillations in Ramjets", 17th JANNAF Combustion Meeting, NASA Langley, Hampton, Va, September 1980.

32. Choudhury, P.Roy, "Characteristics of a Side Dump Gas Generator Ramjet" AIAA-82-1258, AIAA/SAE/ASME 19th Joint Propulsion Conference, Cleveland, June 21-23, 1982.